2008-09-02

Fibrin Microthreads Promote Stem Cell Growth for Localized Delivery in Regenerative Therapy

Megan K. Murphy
Worcester Polytechnic Institute

Fibrin Microthreads Promote Stem Cell Growth for Localized Delivery in Regenerative Therapy

Megan Kay Murphy

A thesis to be submitted to the faculty of Worcester Polytechnic Institute in partial fulfillment of the requirements for the Degree of Master of Science

Submitted by:

Megan Murphy
Department of Biomedical Engineering

_____

Approved by:

George Pins, PhD
Associate Professor
Department of Biomedical Engineering

_____

Glenn Gaudette, PhD
Assistant Professor
Department of Biomedical Engineering

_____

Marsha Rolle, PhD
Assistant Professor
Department of Biomedical Engineering

_____

September 3, 2008

Acknowledgments

Many thanks to my advisors: George Pins, Glenn Gaudette, and Marsha Rolle for their countless hours of feedback and their continued guidance in my education.

Much appreciation to the following individuals whose assistance was vital to the completion of this project:

Sharon Shaw

Ray Page, PhD

Tanja Dominko, PhD, DVM

Dan Filipe

Jacques Guyette

Tracy Gwyther

Katie Bush

Shawn Carey

Craig Jones

Lisa DiTroia

Robert Orr

Thank you to the American Heart Association for the stipend I received through their Scholarship in Cardiovascular Disease and Stroke.

And finally, special thanks to my parents and Scott Proulx for their encouragement and unwavering support when it was most needed.

Abstract

Recent evidence suggests that delivering human mesenchymal stem cells (hMSCs) to the infarcted heart reduces infarct size and improves ventricular performance. However, cell delivery systems have critical limitations such as inefficient cell retention, poor survival, and lack targeted localization. Our laboratories have recently developed a method to produce discrete fibrin microthreads that can be attached to a needle and delivered to a precise location within the heart wall. We hypothesize that fibrin microthreads will support hMSC proliferation, survival and retention of multipotency, and may therefore facilitate targeted hMSC delivery to injured tissues such as infarcted myocardium. To test this hypothesis, we bundled 100 μm diameter microthreads to provide grooves to encourage initial cell attachment. We seeded hMSCs onto the microthread bundles by applying 50,000 cells in 100 μL of media. The number of cells adhered to the microthreads was determined up to 5 days in culture. Cell density on the fibrin microthreads increased over time in culture, achieving an average density of 730 ± 101 cells/mm^2. A LIVE/DEAD assay confirmed that the cells were viable and Ki-67 staining verified the increase in cell number over time was due to proliferation. Additionally, functional differentiation assays suggested the hMSCs cultured on microthreads retained their ability to differentiate into adipocytes and osteocytes. The results of this study suggest that delivering 1 to 4 cell seeded microthreads to the infarcted rat myocardium will provide a quantity of cells that has been shown to produce positive improvement in mechanical function. Additionally these findings suggest that cell-seeded microthreads may serve a platform technology to improve localized delivery of viable cells to infarcted myocardium to promote functional tissue regeneration.

Table of Contents

Table of Figures

Table of Tables

Chapter 1: Introduction

The heart is the central pump vital to the function of the circulatory system. It is responsible for pumping oxygen and nutrient rich blood through the blood vessels to feed all the body's organs and tissues. With such a crucial role, the health of the heart is of utmost importance to maintaining an individual's overall well being. This overall well being can be severely compromised if blood supply to a region of heart tissue is blocked, producing an infarction. This results in cardiac myocyte death which ultimately forms a scarred region of non contractile tissue, diminishing the volume of blood pumped per minute (cardiac output) by the heart [1, 28, 30].

The heart is unable to repair itself after infarction. If left untreated, the scarred region of dead tissue will thin and resulting in remodeling of left ventricular chamber dimensions [1]. The ejection fraction, defined as the fraction of blood within the ventricle that is ejected with each stroke of the heart, declines with infarct size. However, compensatory responses work to maintain a normal stroke volume. The extra pressure and volume generated by the compensatory response causes stress in the ventricular wall to increase. This puts the ventricle at risk of aneurysm and rupture [1]. Current medical interventions only treat the effects of infarction by reshaping the heart from the dilated, spherical shape, back to the original, efficient elliptical shape. Procedures such as direct linear closure and endocardial patch plasty remove the area of infarcted myocardium and either suture the sides of the heart wall back together or insert a synthetic patch in place of the excised myocardium [2-4]. While these procedures restore ventricular geometry and pressures, they do not address the basic issue of regenerating the lost myocardium. Instead, the area continues to be a region of scarred tissue, not contributing to the overall work of the heart.

Cellular therapy has emerged as a technique to facilitate the regeneration of new, contractile tissue to replace the infarcted region and prevent pathological ventricular remodeling. Recent evidence suggests that the delivery of human mesenchymal stem cells (hMSCs) to the infarcted heart reduces infarct size and improves ventricular performance [5-10]. However, current cell delivery systems have critical limitations such as inefficient cell retention and lack of targeted localization that lead to cell death, thus limiting the effectiveness of the delivered cells [11-15].

Recent research efforts have attempted to overcome these limitations by utilizing biomaterial for more efficient delivery of cells to the heart. Materials such as collagen, fibrin, gelatin, alginate, and Matrigel have been studied in this application in the form of injectable gels or three dimensional biomaterial scaffolds [16-22]. Many of these materials have shown potential for success; however they are not without their limitations. The issue of cell and material retention in injectable gels, as well as vascularization and nutrient diffusion through three-dimensional biomaterial scaffolds, remains a challenge [6, 16]. This illustrates the need for a biomaterial scaffold that will allow targeted, controlled delivery of stem cells to treat the patient, while maintaining cell viability. Here, we propose a novel scaffold and delivery method that will provide a matrix for cell attachment and growth, while anchoring cells during delivery.

Recent work by Cornwell et al. has resulted in the formation of discrete fibrin microthreads [23]. Fibrin is a natural provisional matrix for cell attachment and migration during wound healing and has been used in the form of gels for cell delivery to infarcted myocardium [16, 17, 24]. These microthreads were developed for use as a scaffold leading to organized, aligned tissues and have been shown to support fibroblast attachment, proliferation and alignment [23]. Fibrin microthreads have the potential to overcome many of the limitations that

other scaffolds have encountered in cell delivery by providing a matrix for cell attachment and alleviating the potential for cells to wash out of the implant site. Their ability to be used in a manner similar to a suture is also advantageous, presenting a novel approach to scaffold delivery. By attaching the microthreads to a needle, the surgeon now possesses the ability to deliver stem cells to a precise location within the heart wall.

In summary, we hypothesize that fibrin microthreads will support hMSC proliferation, survival and retention of differentiation capability, and may therefore facilitate targeted cell delivery to injured tissues such as infarcted myocardium. In this way, we can directly treat the cause of the decline in cardiac function and restore contractile tissue within the infarcted area.

Chapter 2: Background

This project investigates a novel method for stem cell delivery to infarcted myocardium. There are numerous aspects that need to be considered when researching a novel regenerative approach for any application. This work is a critical first step in exploring several fundamental questions regarding the overall feasibility of delivering human mesenchymal stem cells via a fibrin microthread scaffold. This section will present a brief review of cardiac anatomy and the implications of infarction as well as a summary of the current approaches to cardiac cell therapy and an overview of their limitations.

2.1 Myocardial Infarction

As the central pump for the circulatory system, the heart's four chambers are repetitively filling with and expelling blood to deliver oxygen and nutrients to the rest of the body. The walls of the heart are principally muscular and thickest in the left ventricle where the highest pressures are reached. The heart muscle, or myocardium, is lined on either side by the endocardium and epicardium [25]. Gap junctions, coupling myocardial cells electrically, allow action potentials to propagate through the cell membranes and cause rhythmic contraction of all myocytes. Upon contraction, blood is forced out of the ventricle and into the aorta and coronary arteries, feeding the rest of the body and the heart muscle itself [26, 27].

When a portion of the coronary circulation is blocked, blood supply to the myocardium is compromised and myocytes are starved of oxygen and nutrients. Within seconds, physiological and metabolic changes occur [28, 29]. Shortly after occlusion, adenosine triphosphate (ATP) production in the myocardium switches from an aerobic mechanism to an anaerobic mechanism. This happens as a result of oxygen and glucose deficiency in the tissue and causes the production of ATP to fall rapidly. Since the myocytes have less ATP to use for energy, the muscle

begins to lose its ability to contract. A short time later, the supply of creatine phosphate, which is used as an energy reserve for ATP production, is largely depleted. As anaerobic glycolysis continues, hydrogen ions accumulate as a byproduct and after several minutes the intracellular pH of the myocytes decreases [28]. This causes osmotic flooding of water into the myocytes. Edema occurs as the heart tissue continues to swell and irreversible damage and cell death occurs in the myocardium. Within weeks to months, scar formation takes place as fibroblasts infiltrate the infarct area and deposit fibrous collagen. Macrophages, monocytes, and neutrophils migrate to the infarcted area as part of the inflammatory response and matrix metalloproteinases (MMPs) released from the neutrophils causes further infarct expansion and myocyte collagen degradation [30].

This process has been estimated to affect a billion cells in the heart, rendering them unable to contribute to the daily workload of the heart [11]. The American Heart Association estimates the economic cost of myocardial infarction and coronary heart diseases to be $156.4 billion. Myocardial infarction alone affects an estimated 920,000 people annually, and increases the chance of sudden death by four to six times that of the general population. Additionally, after an infarction, 22% of men and 46% of women are disabled by heart failure within six years. In this stage, the heart cannot pump enough blood to the body's organs so patients are constantly tired and short of breath and thus cannot exert themselves in daily activities [31].

2.2 Clinical Treatment for Myocardial Infarction

Since the heart is unable to repair itself after infarction, medical intervention is necessary. If left untreated, the scarred region of dead tissue will thin and resulting in remodeling of left ventricular chamber dimensions [1]. The

ejection fraction, defined as the fraction of blood within the ventricle that is ejected with each stroke of the heart, declines with infarct size. However, compensatory responses work to maintain a normal stroke volume. Stroke volume is defined as the volume of blood ejected from the ventricle with each beat. This extra pressure and volume generated by the compensatory response causes stress in the ventricular wall to increase. This puts the ventricle at risk of aneurysm and rupture [1].

Current medical interventions only treat the effects of infarction either by performing bypass surgery or reshaping the heart from the dilated, spherical shape, back to the original, efficient elliptical shape. Coronary artery bypass grafting (or CABG) is typically done first to restore blood flow however this procedure does nothing to treat the infarct [32]. Alternatively, the use of surgical ventricular restoration has increased over the past 2.5 years in the United States as widespread clinical trials begin to prove its efficiency [33]. This is done using one of two procedures, direct linear closure or endocardial patch plasty [3].

In direct linear closure, the infarcted myocardium is removed and the remaining heart tissue is sutured back together. This provides a method for restructuring the shape and size of the heart. However, there is not always enough myocardial tissue available to achieve the proper dimensions [4]. If the opening is larger than 3 cm an alternate surgery, called endoventricular patch plasty, is used which employs the use of a patch that is sutured in place of the excised infarct [2]. Specifically, the Dor procedure has been used since 1984 and requires the heart to be completely arrested. Coronary revascularization is performed to restore blood flow to the epicardial layer and preserve infarct thickness [32]. The infarcted region is cut out and a balloon is inflated within the left ventricle as a guide to restore the appropriate volume and shape for more

efficient heart function. A suture placed around the incision is used to tighten the ventricle to the shape of the balloon. Once the suture is tightened, a synthetic patch of polyethylene terephthalate (PET, also known as Dacron™) or polytetrafluoroethylene (PTFE) is used to close any remaining gap in the ventricular wall. The patch functions to restore the volume of the ventricle and prevent further distortion [2, 4].

While this surgical technique restores ventricular dimensions and maintains pressures within the heart, it does not facilitate the regeneration of new contractile tissue. The materials used in these procedures are inert, form large regions of fibrosis, and are typically 4 orders of magnitude stronger than native myocardium which produces a severe mismatch in mechanical properties [34]. Thus, the area continues to be a region of scarred tissue, not contributing to the overall work of the heart.

2.3 Cellular Therapy: Cellular Cardiomyoplasty and Systemic Delivery

Recent research efforts have focused on replacing dead myocardium with functional tissue in prevention of pathological ventricular remodeling. One method, cellular cardiomyoplasty also known as intramuscular injection, is defined as direct injection of cells into the myocardial wall, and aims to entrap a bolus of therapeutic cells within the vicinity of the infarct zone. Another method is systemic delivery which utilizes the circulatory system for a non-invasive method to repeatedly administer therapeutic cells via blood vessels. Both of these approaches focus on replacing the scarred, dead myocardium with viable cells [35, 36].

Many different cell types have been utilized in these approaches including skeletal myoblasts, bone marrow stem cells, embryonic stem cells, resident cardiac stem cells and fetal cardiomyocytes [14, 36]. Skeletal myoblasts do not

electrically couple with the native myocardium and embryonic stem cells raise several political and ethical issues, as well as the potential for tumor formation. Much controversy still surrounds the existence of cardiac stem cells and fetal cardiomyocytes cannot be obtained in sufficient numbers to be an effective clinical treatment [14, 15, 36]. Thus, bone marrow stem cells, specifically human mesenchymal stem cells (hMSCs), have emerged as a promising cell type for cardiac repair.

2.2.1 Human Mesenchymal Stem Cells in Cardiac Applications

Isolated from adult bone marrow, hMSCs are a rare population of cells which represent only 0.001% to 0.01% of nucleated cells within the bone marrow [9, 37]. These cells are an adherent, multipotent population which possesses the ability to differentiate into tissues such as bone, cartilage and fat. They are particularly attractive for use in regenerative therapy due to their relative ease of isolation, high expansion potential in-vitro, and genetic stability [9, 37, 38]. Specifically for myocardial regeneration, hMSCs have the unique characteristics to be used allogeneically without immune suppression, home to areas of injured tissue, induce increased angiogenesis, and have been shown to differentiate into a cardiomyocyte-like phenotype within the myocardium [8, 9, 14, 39, 40].

Several research groups have investigated the effects of hMSCs on the post-infarcted heart and have reported many functional improvements as outlined in Table 1. This includes reduction of infarct size and improvements in ventricular performance [5-8, 40-44]. They have also demonstrated potential for myocyte differentiation and release of cytokines or growth factors that may stimulate repair mechanisms native to the myocardium [5-8, 41, 43, 44]. It is important to note that the mechanism by which cellular cardiomyoplasty and systemic delivery aid in functional cardiac improvements is highly controversial. Several different mechanisms have been proposed, including differentiation of

transplanted cells, passive presence of additional cells within the myocardial wall, cell fusion, and paracrine signaling [35, 44]. While the mechanism remains unknown, researchers agree that cellular therapy using hMSCs restores a significant portion of myocardial function and thus it remains a promising treatment.

Table 1: Outcomes of MSC use in cellular therapy

Species	# Cells Delivered	Method of Delivery	Functional Outcome	Source
Rat	$1x10^7$	Intramuscular injection	-Decrease infarct size -Greater left ventricular wall thickness -Capillary density significantly higher -Cardiomyocyte-like differentiation of hMSCs	[41]
Rat	$3x10^6$	Intramuscular injection	-LV systolic dysfunction attenuated -hMSCs expressed cardiac muscle proteins in the infarct -scar thinning was attenuated and microvessel formation increased	[5]
Rat	$2x10^6$	Intramuscular injection	-Enhanced neovascularization -Increase in collagen and thickness preventing the scar thinning and expansion -Engrafted hMSCs stained positive for desmin -No evidence of synchronous contraction with native myocardium	[6]
Rat	$2.5x10^6$ or $5x10^6$	Intramuscular injection	-Effects are dose dependant, $5x10^6$ MSCs nearly abolished the infarct area -Systolic performance improved to a level indistinguishable from sham animals -Improvement in diastolic function -Transplanted MSCs developed into cardiac myocyte-like cells	[7]
Rat	$4x10^6$	Systemic (femoral vein, left ventricular infusion or right ventricular infusion)	-All animals in right ventricular infusion group died of massive pulmonary emboli -Intravenous delivery is limited by entrapment of donor cells in the lungs -MSCs are preferentially attracted to and retained in ischemic tissue -Fewer than 1% of MSCs migrated to the myocardium after 4 hours	[40]

Species	# Cells Delivered	Method of Delivery	Functional Outcome	Source
Pig	$1x10^3$ to $1x10^6$per kg body weight	Systemic (ear vein)	-Stem cell treated animals had higher increase in body weight and heart weight -MSCs homed to areas of ischemia and showed dose dependant reduction of infarct size, improvement of ejection fraction, and hemodynamics at $1x10^5$ and $1x10^6$ cells per kg body weight -MSCs were not detected in lung, liver or spleen, contrary to other similar studies	[42]
Pig	$2x10^8$	Intramuscular injection	-Less than half of the implanted MSCs engrafted within the first 8 weeks -Decrease in infarct size and significant improvement in cardiac function -Myocardial efficiency increased to a normal level by 4 weeks -Transplanted cells expressed proteins normally restricted to cardiac myocytes, vascular endothelium, and smooth muscle	[44]
Mouse	$5x10^5$ or $1x10^6$	Intramuscular injection	-Majority of delivered cells identified in the spleen, liver, and lungs -0.44% engraftment rate after 4 days -transplanted cells became morphologically indistinguishable from native myocardium and expressed desmin, β-myosin heavy chain, α-actinin, cardiac troponin T, and phospholamban -Observed sarcomeric organization of contractile proteins	[8]
Mouse	$3x10^4$ to $2x10^5$	Intramuscular injection	-New myocytes occupied more than half of the infarcted region, confirmed by cardiac specific staining (myocyte enhancer factor 2, cardiac specific transcription factor GATA-4, and the early marker of myocyte development Csx/Nkx2.5) -Transplanted cells appeared to differentiate to endothelial cells and smooth muscle cells -Reduction of infarct size and improvement in hemodynamics	[10]

2.2.2 Limitations of Cellular Therapy

While the literature outlined in Table 1 demonstrates the positive outcomes of cellular therapy, severe limitations exist. These limitations are inherent in the mode of delivery and include a lack of cell retention, localization, cell survival, and matrix for cell attachment leading to cell death [11, 13-15, 45].

The injection of a bolus of cells into a muscular wall which is constantly contracting results in a large percentage of the freshly transplanted cells leaking back out the needle track and escaping the myocardial wall [11, 45]. Systemic delivery lacks targeted localization as well since a multitude of cells become entrapped in other major organs such as the lungs, liver, and spleen [40, 46]. Additionally since all cells were suspended in either phosphate buffered saline (PBS) or media, these cells lacked a matrix for cell attachment during delivery which also plays a role in their death [13, 15].

As a result of these limitations, less than 1 to 10% of cells actually engraft and survive within the myocardial wall [11, 36, 47]. With such significant losses in cell numbers, this brings forth the following question: how many cells ultimately need to be delivered to the myocardium to have a beneficial effect? Table 2 highlights key literature detailing the number of cells delivered and the respective engraftment rates that were observed. Current approaches deliver between $0.5x10^6$ to $50x10^6$ cells per heart [8, 13, 39, 40, 42, 43, 48]. Since the percent engraftment is reported, the actual number of cells that engraft in each study can be calculated from the total number of cells delivered. Also, this number of engrafted cells can be normalized to the rat heart since there are a variety of different species present and this is the animal model of concern for this project. Based on published weight measurements, the rat heart is about 1% the size of a pig heart and 8 times the size of a mouse heart [49-53]. Thus, 400 to 40,000 cells must be delivered to the rat myocardium in order to observe reductions in infarct size and improvements in ventricular performance.

Table 2: Engraftment rates for cellular therapy

Species	Number of Cells Delivered	Engraftment	Number of Cells Engrafted	# Cells Engrafted Normalized to Rat	Source
Mouse	$5x10^5$	0.44%	2,200	17,600	Toma, 2002
Mouse	$5x10^5$	0.2%	1,000	8,000	Zhang, 2008
Rat	$4x10^6$	< 1%	<40,000	<40,000	Barbash, 2003
Pig	$50x10^6$	0-6%	$<3x10^6$	<36,900	Freyman, 2006
Pig	$1x10^5$ to $1x10^6$ per kg bodyweight	1-3%	1,000-30,000 per kg bodyweight	400-12,000	Wolf, 2008

2.3 Biomaterials for Cardiac Regeneration

The use of biomaterials presents an opportunity to overcome the limitations of cellular cardiomyoplasty and systemic delivery for more efficient delivery of cells to the heart. Biomaterials allow researchers to control the cellular microenvironment, and thus enable direction of cellular behavior [54]. Many factors must be taken into consideration when selecting and designing a biomaterial scaffold including properties such as scaffold degradation, porosity, compliance, size, and cell adhesion [15, 54, 55]. Materials such as collagen, gelatin, fibrin, and alginate, and Matrigel have been studied in cardiac applications as either injectable gels or three dimensional biomaterial constructs [16-22, 48, 56-61].

Alginate is a naturally derived polysaccharide from brown seaweed and has been used in the form of gels or three dimensional sponges for delivery of cells to infarcted myocardium [62]. Leor et at. used a cell seeded alginate sponge to create a bioengineered cardiac graft. This and other studies have demonstrated that alginate is favorable for tissue engineering constructs due to its hydrophilic nature, tunable porosity, extensive neovascularization in vivo, and biocompatibility [20, 62-64].

However alginate is unable to specifically interact with mammalian cells due to its lack of arginine-glycine-aspartic acid (RGD) cell adhesion ligands, thus alginate is frequently covalently modified with this ligand [62]. Also, alginate is known to be mechanically unstable in vivo due to its ionic cross-linking and it undergoes slow uncontrolled dissolution [15, 65]

Gelatin sponges are commercially available biomaterials made of purified porcine skin gelatin [66]. Studies by Akhyari et al. and Li et al. used gelatin sponges for culture and delivery of cells to the myocardium. This material is biodegradable and supports the attachment and spontaneous contraction of cultured cells. However, this scaffold is too porous and naturally thrombogenic to be used in blood contacting applications [61, 66, 67].

Matrigel is a liquid basement membrane extract of collagen, proteoglycans, and laminins that consolidates to gel consistency after a few hours at 37°C [22]. Studies have shown that it is angiogenic largely due to its growth factor contents, it can assume the geometry of the host environment, and in combination with collagen gel, it supports injection of cells for improvements in cardiac function [19, 21, 22, 57]. However, due to its consistency, it is not ideal for use alone or as a scaffold that promotes in situ regeneration [15].

Collagen is the main component of connective tissues and is the most abundant protein in mammals. Its use in cardiac applications, either as a three dimensional sponge or as a gel, has shown its support of cells for delivery and spontaneous contraction [60, 68, 69]. Collagen is hydrophilic, degradable and an excellent substrate for cell attachment and infiltration. However it can have poor mechanical properties, lack structural stability, exhibit a large degree of swelling in culture medium, and is weakly immunogenic and thrombogenic [58, 70].

Christman et al. were the first to demonstrate the improvement in cell survival when using an injectable fibrin scaffold as compared to intramuscular injection of a cell

suspension [15]. Fibrin is a natural provisional matrix for cell attachment and migration during wound healing. A complex series of coagulation reactions, triggered by platelet adherence after injury, leads to the production of thrombin. This enzyme cleaves fibrinogen, which is naturally circulating in the blood, and forms a complex, interwoven, fibrin clot to stop bleeding and encourage healing [71, 72]. These two components, fibrinogen and thrombin, are used commercially to mimic this final stage in the coagulation cascade as surgical fibrin sealants and fibrin gels for tissue engineering [24]. The natural presence of RGD binding motifs to facilitate cell adhesion, the possibility of using autologous fibrinogen and thrombin, the natural presence of growth factors, its Food and Drug Administration (FDA) approval for clinical use, and its angiogenic characteristics make fibrin attractive for cardiac applications [16, 56, 73].

While all these materials have shown potential for increasing cell survival, the issue of cell and material retention in injectable gels continues to remain a challenge [16, 24, 48]. Additionally, the three-dimensional biomaterial constructs meant to be full thickness patches for infarct regeneration are plagued by problems with vascularization and nutrient diffusion [6, 16]. These patches are typically on the order of several millimeters in thickness while diffusion can only supply nutrients to a depth of 150μm [11]. This is not suitable for keeping the entire construct viable while vascularization is taking place in vivo. This illustrates the need for design of a biomaterial scaffold to facilitate targeted, controlled delivery of stem cells to the myocardial wall, while allowing stem cell growth and maintaining cell viability. This scaffold should induce angiogenesis for new blood vessel formation and persist long enough to guide the integration of cells, but not so long as to interfere with cell coupling essential to myocardial function [54]. The ability to deliver growth factors via this scaffold is a desirable capability as well, since growth factors can be used to direct many cellular processes.

2.3.1 Fibrin Microthreads

Discrete fibrin microthreads have recently been developed by Cornwell et al. as a novel scaffold to direct cell orientation and migration for tissue regeneration. These microthreads are attractive as tissue engineering scaffolds due to their combination of cell signaling and structural properties [23]. Evaluation by Cornwell et al. demonstrated that fibrin microthreads were significantly higher in tensile strength than fibrin gels and proved their support of fibroblast viability, alignment, growth, and migration for 7 days in culture. These fibrin microthreads are able to be crosslinked for increased tensile strength and stiffness, and can be loaded with growth factors to influence cellular processes [23, 74].

Here, we propose to use fibrin microthreads as a matrix for cell attachment to anchor cells during delivery. Fibrin has been shown to support hMSC viability and growth in the form of a gel [16, 17, 24]. Fibrin is angiogenic, biodegradable and the microthreads are capable of being loaded with growth factors. Also their structural properties present the opportunity for the microthreads to be used in a manner similar to a suture is also advantageous, presenting a novel approach to scaffold delivery. By attaching the microthreads to a needle, the surgeon now possesses the ability to deliver the stem cells to a precise location within the heart wall.

Chapter 3: Hypothesis and Specific Aims

We hypothesize that fibrin microthreads will support hMSC proliferation, survival, and retention of differentiation capability and may therefore facilitate targeted hMSC delivery to injured tissues such as infarcted myocardium. Specifically, quantification of the number of cells will verify that the microthreads are capable of delivering between 400 and 40,000 hMSCs and immunohistochemistry and functional differentiation assays will confirm cell viability, proliferation, and retention of multipotency.

Specific Aim 1: Quantify cell number on fibrin microthreads

Here we hypothesize that fibrin microthreads are capable of supporting between 400 and 40,000 hMSCs. To test this we bundled individual fibrin microthreads in groups of 4 and seeded them with hMSCs. After 1, 3, and 5 days in culture, microthreads were analyzed by two methods. For the first method, microthreads were removed from culture and stained with Hoechst dye to visualize nuclei. The number of nuclei per area of microthread was counted using ImageJ software. For the second method we sought to develop a reproducible, time efficient assay for cell quantification to improve upon the limitations of counting Hoechst dye stained nuclei. Microthreads were digested in trypsin and hMSCs were re-plated in a standard tissue culture plate. The CyQuant Cellular Proliferation Assay was used to quantify cell number by converting fluorescence intensity, produced by a cyanine dye binding to cellular DNA, to cell number via a standard curve.

Specific Aim 2: Confirm hMSC viability and proliferation on fibrin microthreads

Here we hypothesize that fibrin microthreads support the viability and proliferation of hMSCs. Human mesenchymal stem cells seeded on fibrin microthread bundles for 1, 3, and 5 days were stained with Ki-67, a protein present in the nuclei of

proliferating cells. The number of Ki-67 positive cells was counted and a percentage of Ki-67 expression was calculated relative to the total number of cells present. To investigate the effect of fibrin on hMSC proliferation Ki-67 expression on microthreads was also compared to Ki-67 expression of hMSCs cultured on standard and fibrin coated chamber slides. Cell viability was determined using the LIVE/DEAD assay.

Specific Aim 3: Demonstrate hMSC retention of multipotency

Finally, we hypothesize that hMSCs will retain their ability to differentiate after being cultured on fibrin microthreads. Fibrin microthread bundles seeded with hMSCs were cultured for 5 days. At the conclusion of culture time the bundles were digested with trypsin, re-plated in a standard tissue culture plate, and exposed to standard differentiation protocols for adipogenesis and osteogenesis. Adipogenic cultures were stained for the presence of lipid vacuoles using Oil Red O and osteogenic cultures were evaluated for calcium deposition via Alizarin Red S staining.

Chapter 4: Materials and Methods

This section details the procedures used to achieve our specific aims. Fibrin microthread production and seeding of hMSCs will be described, as well as our methods of analysis for quantification of cell number, proliferation, viability, and differentiation.

4.1 Fibrin Microthread Production and Seeding

Fibrin microthreads were produced according to a previously published protocol [23]. Briefly, fibrinogen and thrombin from bovine plasma (Sigma Aldrich, St. Louis, MO) were placed into separate 1 mL syringes. The solutions were combined by a blending applicator tip (Micromedics, St. Paul, MN) and extruded through polyethlyene tubing (0.38mm inner diameter, Beckton Dickinson, Franklin Lakes, NJ) into a bath of 10mM HEPES, pH 7.4 at room temperature (Figure 1). After 15 minutes, the microthreads were removed from the bath and hung to dry overnight. This process produced individual fibrin microthreads with an average hydrated diameter of 100 um [23].

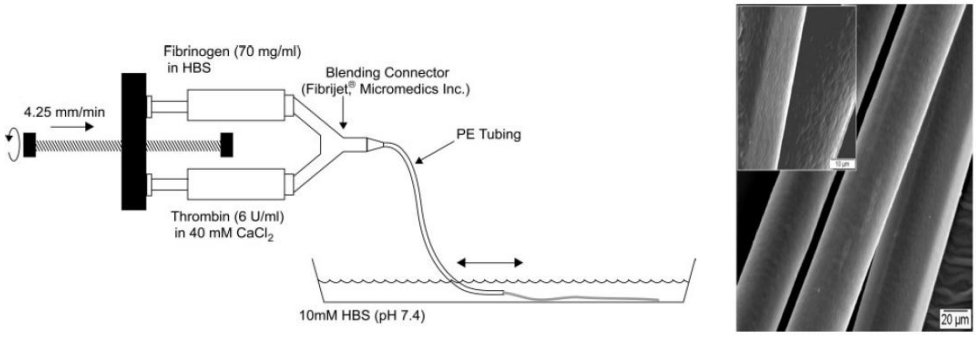

Figure 1: Fibrin microthread extrusion process [23]

In order to facilitate cell attachment, the individual microthreads were grouped together to form a bundle of fibrin microthreads. Specifically, bundles of microthreads were formed by placing four microthreads adjacent to each other and dragging a droplet of phosphate buffered saline (PBS) along the length of the microthreads until

they adhered to each other (Figure 2). This provided grooves for initial cell attachment and increased surface area for cell growth as compared to a single large diameter microthread.

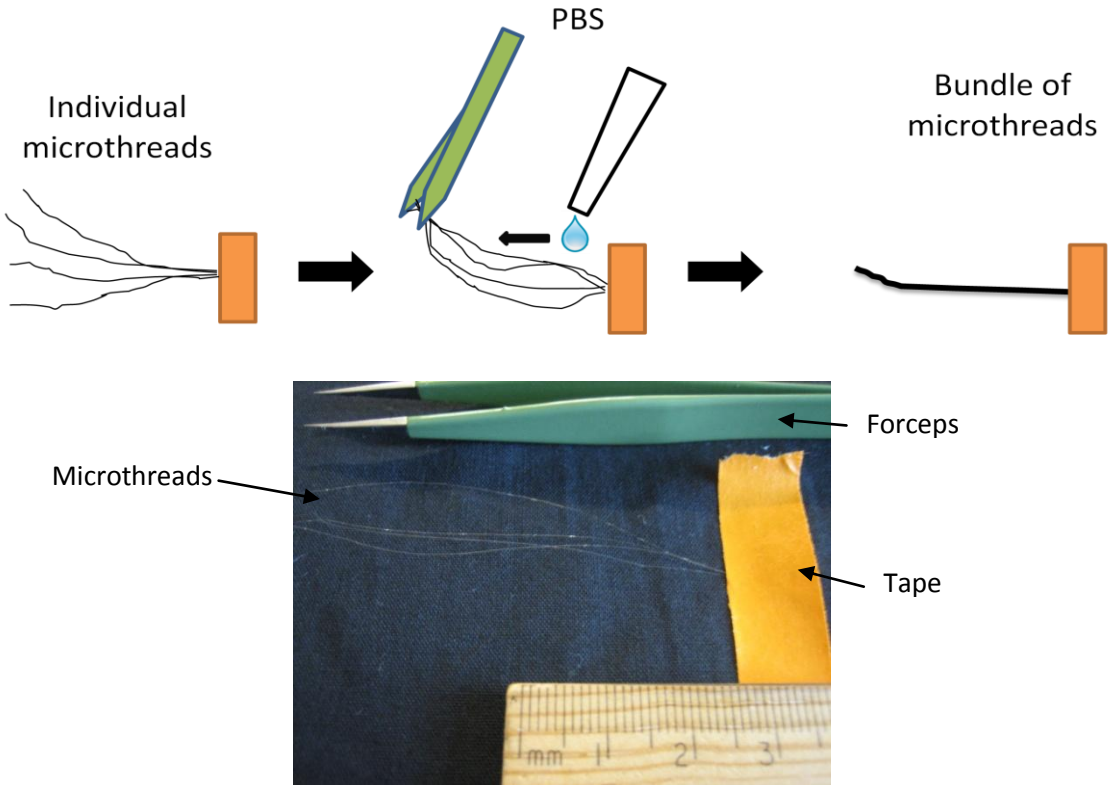

Figure 2: Microthread bundling procedure

To prepare microthreads for seeding, bundles were glued to 3.0 cm outer diameter stainless steel washers (Seastrom Manufacturing, Twin Falls, ID) with Silastic Silicone Medical Adhesive Type A (Dow Corning, Midland, MI). Individual washers were placed in wells of a standard 6-well plate over a 13 mm diameter circular Thermanox™ coverslip (Nalge Nunc International, Rochester, NY) as seen in Figure 3. Prior to seeding, the washers with attached bundles were rehydrated with PBS for 15 minutes, then sterilized using 70% isopropyl alcohol for 1 hour, rinsed with three washes in sterile PBS for 15 minutes, and air dried in a laminar flow hood overnight.

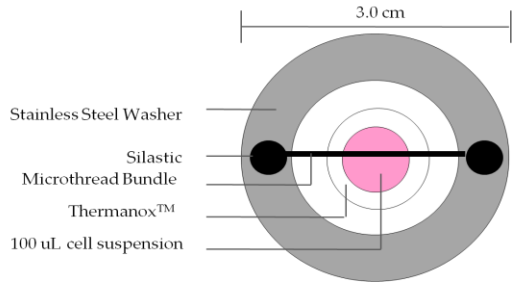

Figure 3: Microthread/washer diagram

Microthread bundles were seeded with hMSCs according to standard cell culture procedures. Human mesenchymal stem cells (Lonza, Walkersville, MD) in culture were trypsinized, centrifuged, and re-suspended at a concentration of 500,000 cells/mL in Mesenchymal Stem Cell Growth Medium (MSCGM: 10% mesenchymal stem cell growth supplement, 2% L-glutamine, 0.1% gentamicin sulfate/amphotericin-B in mesenchymal stem cell basal medium, Lonza, Walkersville, MD). Passage 4-9 hMSCs were used for all experiments. A 100 μL drop of cell suspension was placed in the center of the coverslip and the plate was placed in a 37^0 C, 5% CO_2 incubator. After 2 hours of incubation, the washers with attached microthreads were rinsed with PBS to remove unattached cells and transferred to new 6-well plates containing 2 mL of fresh media, changed every three days (Figure 4).

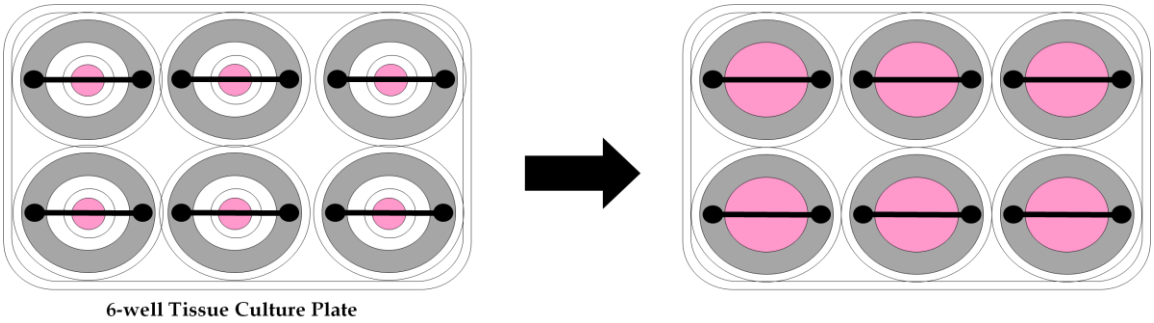

Figure 4: Microthread/washer culture

4.2 Quantification of Cell Number

The procedures described here focus on quantifying the number of cells that can be delivered to the target location using fibrin microthread bundles. Initially, microthreads were seeded with hMSCs and counterstained with Hoechst dye to determine cell density by counting. While this method allows quantification of cell number it has several limitations that restrict the efficacy of the results. Thus we sought to develop a quantitative assay for assessment of cell number to overcome these limitations.

4.2.1 Estimation of Cell Attachment

An approximation of cell attachment on fibrin microthreads can be obtained by calculating the surface area available for cell attachment on a microthread bundle and dividing it by the average area of an hMSC. In this way, we can obtain an estimate of how many hMSCs can theoretically be cultured on a bundle of fibrin microthreads.

The surface area of a bundle of four microthreads was calculated by first approximating the circumference of the microthread bundle and multiplying it by the microthread length. Based on Figure 5, about 75% of an individual microthread circumference is exposed for cell attachment. Therefore, the circumference of a bundle of 4 microthreads is as follows:

$$\text{Bundle Circumference} = \alpha(\pi d_1)\beta$$

Where d_1 is the diameter of a single microthread (100 um), α is the approximate percentage of individual microthread exposed for cell attachment in the bundle (0.75), and β is the number of microthreads in the bundle (4). The total surface area was then determined by multiplying the bundle circumference by the length of the microthread bundle.

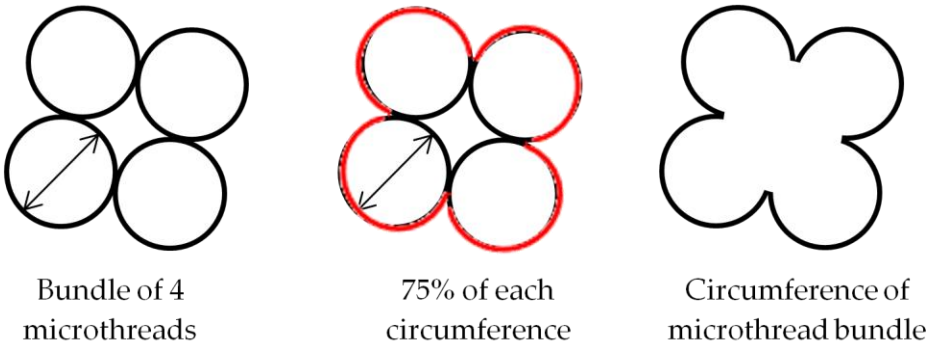

Figure 5: Microthread bundle circumference

Average hMSC area was calculated based on a phalloidin stained image of hMSCs cultured on an 8-well chamber slide (Nalge Nunc International, Rochester, NY). Using ImageJ software (National Institutes of Health, Bethesda, MD), the freehand sections tool was used to trace the perimeter of twenty cells and the measure function was used to determine the area within the trace. The number of cells per microthread was calculated by dividing the total surface area of the microthread bundle by the average area of an hMSC (1,255 $\pm$ 911 um^2).

4.2.2 Quantification of Cell Number via Hoechst Dye Staining

Microthread bundles were seeded as previously described. After 5h, 1, 2, 3, 4, and 5 days in culture, washers with attached microthread bundles were removed from the 6-well plate and rinsed with PBS. The microthreads were cut from the washers, placed on glass slides, fixed in 4% paraformaldehyde in PBS (Boston Bioproducts, Worcester, MA) for 10 minutes, rinsed with two washes of PBS for 5 minutes each, and then permeabilized with 0.25% Triton-X100 in PBS for 10 minutes. Then microthreads were blocked with 1% bovine serum albumin in PBS for 10 minutes and stained with Alexa Fluor 488 conjugated phalloidin (5µL stock solution in 200µL PBS, Invitrogen A12379, Carlsbad, CA) for 30 minutes to illuminate the f-actin filaments in the cytoskeleton. Microthreads were then rinsed with three washes of 1% bovine serum albumin in PBS for 10 minutes each and counterstained with Hoechst dye (Cambrex Bio

Science, Charles City, IO) at a concentration of 1:6000 for 5 minutes to visualize cell nuclei.

Cell density was determined by counting the number of cells per square millimeter of microthread from fluorescent images taken with a Leica DM LB2 microscope. A total of six microthread bundles from two separate experiments were imaged per time point under 10x magnification. Images were taken successively along the cell populated region of the microthreads until the entire length was viewed, this required anywhere from 5 to 13 images. Counts and area measurements were performed using Image J software with the Cell Counter plug-in. Raw data was reported as the number of cells per square millimeter of microthread bundle.

In order to compare the results from this quantification method to alternate quantification methods and results from literature, the total number of cells per microthread bundle needed to be calculated. The total number of cells per microthread bundle can be extrapolated from the raw data by using the bundle surface area calculation from Section 4.2.1 and multiplying by the number of cells/mm^2 counted. Adjustments for the unseeded ends of the microthread bundle, as seen in Figure 6, were made by measuring the unseeded area of three microthreads at each time point. The average unseeded area was then subtracted from the total surface area of the microthread bundle, to yield the average cell populated area of microthread. This adjustment was necessary in order to account for the tail portions of the microthread that were not populated by cells, otherwise simple multiplication of the entire surface area of the microthread bundle by cell density would overestimate cell number. This type of data manipulation is by no means an ideal method for determining total cell number on the microthread bundle since it calculates the surface area of a three dimensional sample based on a two dimensional image. It is meant only to serve an approximation of total cell number for comparative purposes.

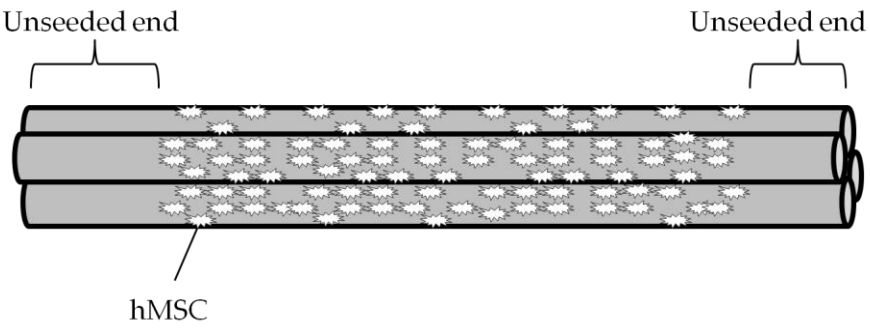

Figure 6: Diagram of hMSCs on microthread bundle

4.2.3 CyQuant Cellular Proliferation Assay

While counting Hoechst dye stained nuclei allows quantification of cell number it has several limitations. First, it is very time consuming to count individual nuclei on microthread bundles which effectively limits sample size. Second, since we are limited to imaging this three dimensional scaffold in a single plane, not all the cells on the microthread are able to be counted. Finally, the amount of microthread area visible in images varies due to the placement of the microthread on the slide and flattening by the coverslip. Thus, all counts of nuclei must be normalized to the viewable surface area.

To overcome these limitations we sought to develop an automated assay for more reproducible, quantitative, and high throughput analysis. Based on the cell count from the Hoechst dye protocol, we determined that the assay must detect as few as 1,000 cells and up to 20,000 cells. Product research revealed that the CyQuant Cellular Proliferation Assay (Invitrogen, Carlsbad, CA) had the appropriate sensitivity. This assay employs a cyanine dye that fluoresces upon binding to double stranded DNA and can detect as few as 50 cells [75, 76]. This dye has been proven to correlate well with measurements made using [3H]-thymidine, which in turn has been shown to be equivalent to the Hoechst 33342 fluorochrome [75, 77].

First, to determine dye incubation time, hMSCs were passaged according to standard cell culture protocols and plated in a 96-well plate (Beckton Dickinson, Franklin Lakes, NJ) at concentrations of 100 to 50,000 cells per well in 100 μL of

CyQuant dye prepared as per kit protocol. The dye was allowed to incubate with the cells in a 37^0 C, 5% CO_2 incubator and a reading was taken with a Victor^3 1420 Multilabel Counter every ten minutes from 30 minutes to 80 minutes. Wells with dye alone served as controls for background fluorescence subtraction. Fluorescent intensity was plotted versus time for each cell concentration. The appropriate dye incubation time was determined as the time after which fluorescence intensity does not statistically change with time.

Cell attachment to microthreads was quantified using the CyQuant assay at 1, 3, and 5 days in culture. The diagram in Figure 7 depicts the procedure. Microthreads were cut from the stainless steel washers and digested in 0.5 mL of 0.25% trypsin in Hank's Balanced Salt Solution (Invitrogen, Carlsbad, CA) at 37^0 C for 5 minutes. An equivalent amount of MSCGM was added to inactivate the trypsin and the suspension was centrifuged for 5 minutes at 1,000 RPM. The supernatant was removed by pipetting and the pellet was re-suspended in 200 μL of fresh media and transferred to wells of a 96-well plate. The plate was placed in a 37^0 C, 5% CO_2 incubator for 4 hours to allow complete cell attachment. Each well was then rinsed with 200 μL of sterile PBS twice to remove residual thread debris. CyQuant dye (100 μL per well) was added to the plate and it was returned to incubation. After one hour, a reading was taken with the Victor^3 1420 Multilabel Counter to measure fluorescence intensity and cell number was calculated based via a standard curve. Unseeded threads and hMSCs plated at 1,000 cells per well served as controls. Background fluorescence was measured by way of wells with CyQuant dye alone.

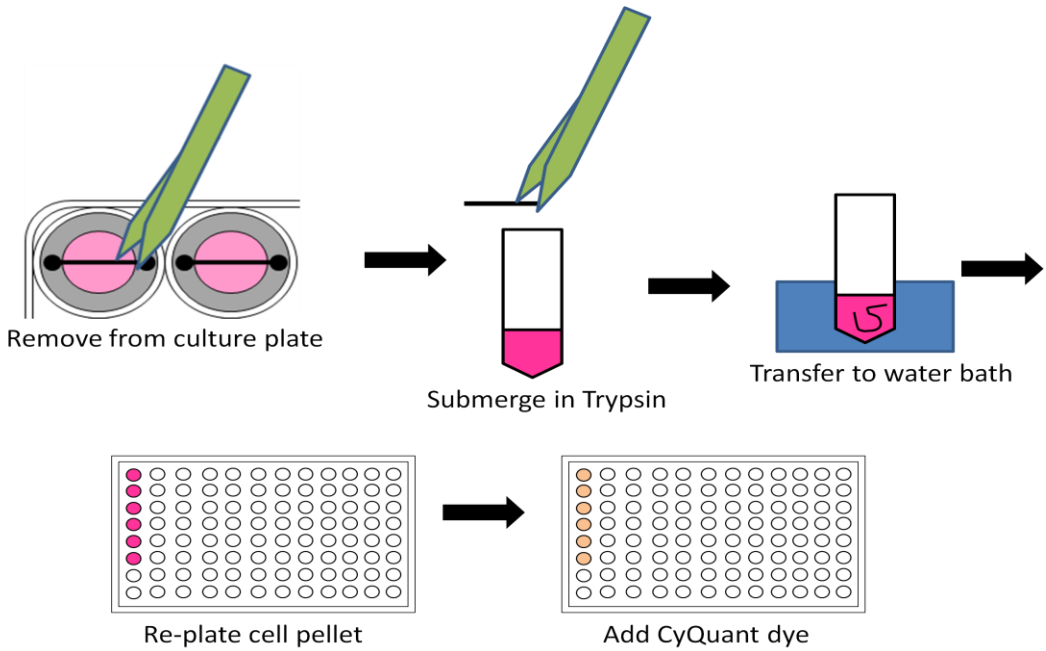

Figure 7: CyQuant procedure

To correlate fluorescence intensity with cell number, a standard curve was created. Human mesenchymal stem cells were passaged and seeded at 100 to 50,000 cells per well in a 96-well plate. Cells were allowed to attach overnight and then were processed in the same manner as the microthreads. By creating the standard curve in this way, we ensured that the cells were exposed to the same conditions and thus accounted for any loss of cells due to the assay procedure. Wells with CyQuant dye alone were used to measure background fluorescence of the dye. The standard curve was created by subtracting the background fluorescence from the fluorescence intensity of each cell concentration and plotting known cell number versus fluorescence. A linear trend line was fit to the graph and R-squared value and slope were determined.

4.3 Cell Proliferation

To confirm that the increase in cell number over time in culture on fibrin microthreads is due to cellular proliferation, microthreads were fixed and stained with an antibody against Ki-67. Ki-67 is a protein expressed during G1, S, G2, and M phases

of the cell cycle. The white arrows in Figure 8 show Ki-67 positive nuclei. Microthread bundles were seeded with hMSCs as described previously. At 1, 3, and 5 days bundles were removed from the washers, rinsed in PBS and placed on glass slides. Microthreads were fixed with 4% paraformaldehyde in PBS for 15 minutes, rinsed in PBS for 5 minutes, and permeabilized with 0.25% Triton-X100 in PBS for 10 minutes. Following two rinses in PBS for 5 minutes each, microthreads were exposed to epitope retrieval for 40 minutes in 10% Dako Cytomation Target Retrieval Solution, pH 9 (S2367, Dako, Carpinteria, CA) in diH_2O and allowed to cool for 20 minutes. Microthreads were then rinsed twice with PBS for 5 minutes each and then blocked with 5% normal rabbit serum in PBS for 30 minutes. Next microthreads were incubated in a 1:100 dilution of Ki-67 mouse IgG1 (sc-23900 Santa Cruz Biotechnology Inc, Santa Cruz, CA) in 5% normal rabbit serum for 1 hour, rinsed with three washes of PBS for 5 minutes each, and then incubated with a 1:200 dilution of Alexa 488 rabbit anti mouse IgG (A11059 Invitrogen, Carlsbad, CA) in 5% rabbit serum for 1 hour. Following three rinses in PBS for 5 minutes, microthreads were counterstained with Hoechst dye at a concentration of 1:6000 for 5 minutes (Cambrex Bio Science, Charles City, IO) to visualize cell nuclei. Seeded microthreads incubated in a 1:100 dilution of mouse IgG (I-2000 Vector Labs, Burlingame, CA) in place of the Ki-67 primary and unseeded threads stained with both the Ki-67 primary and secondary served as negative controls. Fluorescent images were captured with Leica DM LB2 microscope from four bundles stained in two separate experiments. Images were taken randomly along the cell populated region of microthread. From these, ten images were randomly selected and the percentage of cells in the cell cycle was calculated by counting the number of Ki-67 positive cells and dividing that by the total number of cells per image.

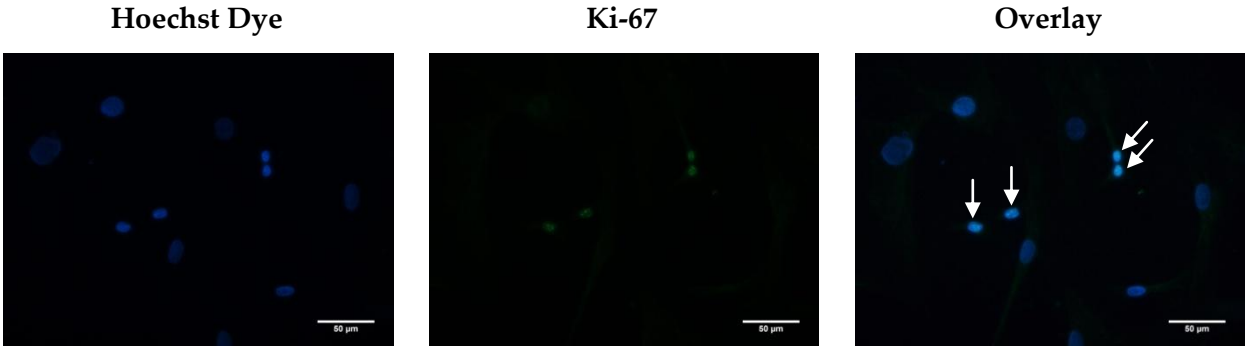

Figure 8: hMSCs labeled with Ki-67

Typical doubling time for low passage (P2-10) hMSCs in culture is 5 to 7 days [78]. Looking at the data from Hoechst dye counts, hMSCs appear to be proliferating much faster, increasing 7-fold over 5 days. To investigate if fibrin had an effect on hMSC proliferation we compared hMSC proliferation on normal tissue culture surface to hMSC proliferation on a fibrin coated surface. Fibrin gels, consisting of the same components as the microthreads, were formed by spreading 48.6 μL of 35 mg/mL fibrinogen in the bottom of an 8-well chamber slide (Nalge Nunc International, Rochester, NY) using a shaker plate [79, 80]. After 5 minutes the shaker plate was turned off, 48.6 μL of 6 U/mL thrombin was added to each well, and the shaker plate turned back on. After 15 minutes, the slides were transferred 4^0 C and left overnight to allow gel formation. To form a thin fibrin coating, the slides were removed from 4^0 C and allowed to dry overnight in a desiccator. Each well was then rinsed two times in 10mM HEPES buffer for 5 minutes, sterilized in the same manner as the fibrin microthreads, and allowed to dry overnight in a laminar flow hood. Presence of a fibrin coating was assessed by trypan blue staining and light microscopy.

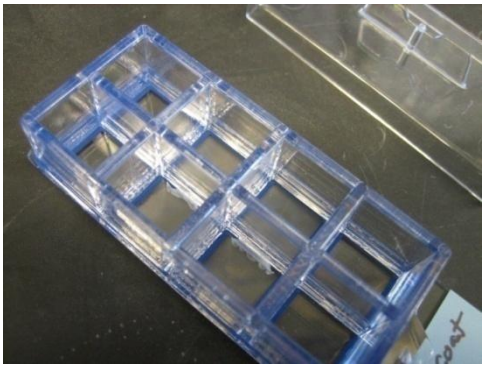

Figure 9: Fibrin coated chamber slide

Human mesenchymal stem cells were seeded in fibrin coated 8-well chamber slides (200μL of 10,000 cells/mL) following standard cell culture practices. After 1, 3, and 5 days, the 8-well chamber slides were stained with Ki-67 as described previously. Human mesenchymal stem cells cultured on normal tissue culture treated 8-well chamber slides at the same density served as a comparison. Percentage of cells in the cell cycle was calculated by counting the number of Ki-67 positive cells and dividing that by the total number of cells per image. Ten images (20x magnification) were randomly selected from four chambers of two slides stained in two separate experiments.

4.4 Cell Viability

In order to confirm viability of hMSCs cultured on microthreads, the hMSC seeded bundles were exposed to LIVE/DEAD Viability/Cytoxicity Kit for mammalian cells (Invitrogen L-3244, Carlsbad, CA). This is a dual component stain, calcein enters the cytoplasm of live cells and upon conversion by intracellular esterase activity, fluoresces green. Ethidium enters the nuclei of dead cells and fluoresces red upon binding to nucleic acids. This experiment was done by preparing and seeding microthread bundles as described previously. After 5 days in culture, the microthread bundles were cut from the washers, rinsed in PBS, and placed on a glass slide to incubate in 8 μM ethidum, 4 μM calcein in PBS for 30 minutes. Fluorescent images were

captured with a Leica DM LB2 microscope at 20x magnification of two slides stained in two separate experiments. Controls were prepared by incubating hMSCs in 30% methanol for 30 minutes to prove that any green fluorescence seen was a result of live cells and not autofluorescence of the microthread bundle.

4.5 Differentiation

As with all multipotent stem cells, hMSCs are able to differentiate into a variety of cell types. To confirm that hMSCs maintain their multipotency after culture on fibrin microthreads, cells were exposed to standard differentiation protocols using an adipogenic kit available from Lonza (Adipogenic Differentiation Medium, PT-3004) and an osteogenic kit from Invitrogen (StemPro Osteogenesis Differentiation Kit, A10072-01). Mesenchymal stem cells that had not been cultured on threads served as positive and negative controls.

Microthreads were bundled, sterilized, seeded, and cultured for 5 days. At the conclusion of time in culture microthread bundles were digested in 0.5 mL of 0.25% trypsin in Hank's Balanced Salt Solution (Invitrogen, Carlsbad, CA) at 37^0 C for 5 minutes. An equivalent amount of MSCGM was added to inactivate the trypsin and the suspension was centrifuged for 5 minutes at 1,000 RPM. For adipogenic differentiation, cells were re-suspended and re-plated at 2.1×10^4 cells per cm^2 tissue culture surface area and fed every 2–3 days with MSCGM until cultures reached 100% confluence, approximately 5–13 days. Cells were then fed for three cycles of 3 days with Adipogenic Induction Medium followed by 1–3 days with Adipogenic Maintenance Medium. Negative control hMSCs were fed with Adipogenic Maintenance Medium only. After the three cycles, all cells were cultured for an additional week in Adipogenic Maintenance Medium. At the end of each week cells were analyzed using light microscopy for characteristic lipid vacuole formation as seen in Figure 10. At the conclusion of the feeding cycle adipogenic cultures were stained with Oil Red O to

assess lipid vacuole formation. Cultures were fixed in 4% paraformaldehyde in PBS for 15 minutes, rinsed in distilled water for 5 minutes and dehydrated in 60% isopropanol for 5 minutes. An Oil Red O stock solution was made by dissolving 300 mg of Oil Red powder (MP Biomedical, Solon, OH) in 100 mL of 100% isopropanol. Oil Red O working solution was made by combining 3 parts stock solution with 2 parts distilled water in distilled water and then passed through a syringe filter (0.80μm membrane, Corning Incorporated, Corning, NY). Cultures were stained with Oil Red O working solution for 10 minutes and then rinsed in 60% isopropanol for 5 minutes, and distilled water for 5 minutes. Cells were counterstained with Mayer's hematoxylin (Sigma Aldrich, St. Louis, MO) for 1 minute, rinsed with distilled water, and viewed under a light microscope.

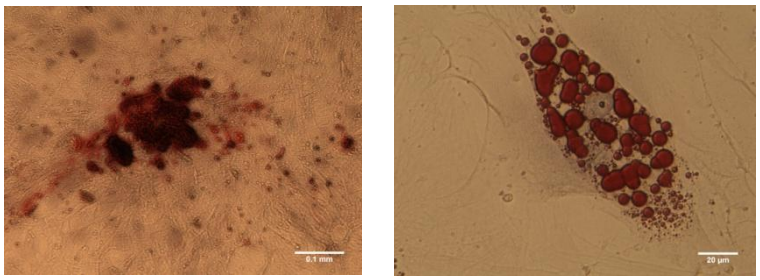

Figure 10: Osteogenic (left) and adipogenic (right) cultures

For osteogenic differentiation, cells were re-suspended and re-plated at 5 x 10^3 cells per cm^2 tissue culture surface area and cultured overnight in MSCGM. Cells were then fed with Complete Osteogenesis Differentiation Medium which was replaced every 3–4 days for 2–3 weeks. Negative control cells were fed with MSCGM on the same schedule. At the end of each week cells were analyzed using light microscopy for characteristic cobblestone appearance. At the conclusion of the feeding schedule, cells were stained with Alizarin Red S to assess calcium deposition, as seen in Figure 10. Cells were removed from culture, rinsed in PBS containing calcium and magnesium (Invitrogen, Carlsbad, CA) for 1 minute and fixed in 4% paraformaldehyde in PBS for 15 minutes. Cultures were then rinsed with one wash of PBS containing calcium and

magnesium for 5 minutes followed by one wash of distilled water 5 minutes. Alizarin Red S stock solution was made by dissolving 2 grams of Alizarin Red powder in 100 mL distilled water and adjusting pH to 4.1-4.3 with 10% ammonium hydroxide. Cells were stained with Alizarin Red S working solution for 5 minutes, then rinsed three times with distilled water for 5 minutes each, and viewed under a light microscope.

4.6 Statistics

Statistical comparisons were carried out using SigmaStat 3.1 (Systat Software, Inc., Point Richmond, CA). Statistical difference between two groups was analyzed using Student's T-test or the Mann Whitney Rank Sum test for cases of unequal variance. Statistical difference between groups was analyzed using ANOVA with Holm-Sidak post hoc testing. In cases where data failed the normality test an ANOVA on Ranks followed by a Tukey post hoc test was used since data was not transformed to accommodate the non normality. Significance was established for $p < 0.05$. All experiments were repeated to a minimum of $n = 2$.

Chapter 5: Results

5.1 Quantification of Cell Number

The estimated number of cells that we hypothesize could feasibly attach to a fibrin microthread bundle is shown in Table 3. Detailed measurements for hMSC area can be found in Appendix A. The grooves created by bundling 4 individual 100 um microthreads together increases surface area for cell attachment by about 50% as compared to a single, 200 um diameter microthread. The number of cells expected to attach to a bundle of 4 microthreads is approximately 15,000 cells per 2 cm length of thread.

Table 3: Theoretical cell attachment calculations

Parameter	Bundle of 4	Large diameter thread
Microthread Diameter (um)	100	200
Microthread Circumference (um)	314	628
Circumference Available	0.75	1
Number of Microthreads	4	1
Microthread Length (cm)	2	2
Microthread Surface Area (mm^2)	**18.8**	**12.6**
hMSC Area (um^2)	1,255	1,255
hMSC/2cm Microthread	**15,008**	**10,005**

5.1.1 Quantification of Cell Number via Hoechst Dye Staining

Hoechst dye and phalloidin stained images are shown in Figure 11. The Hoechst dye images show a clear increase in cell number from day 1 through day 5. Cells appear to settle in the grooves of the thread bundle at day 1, then proceed to spread out and cover the entire surface of the microthreads by day 5. Phalloidin staining shows that the hMSCs appear to align with the long axis of the microthread as compared to their random orientation on a chamber slide, however this was not quantitatively evaluated.

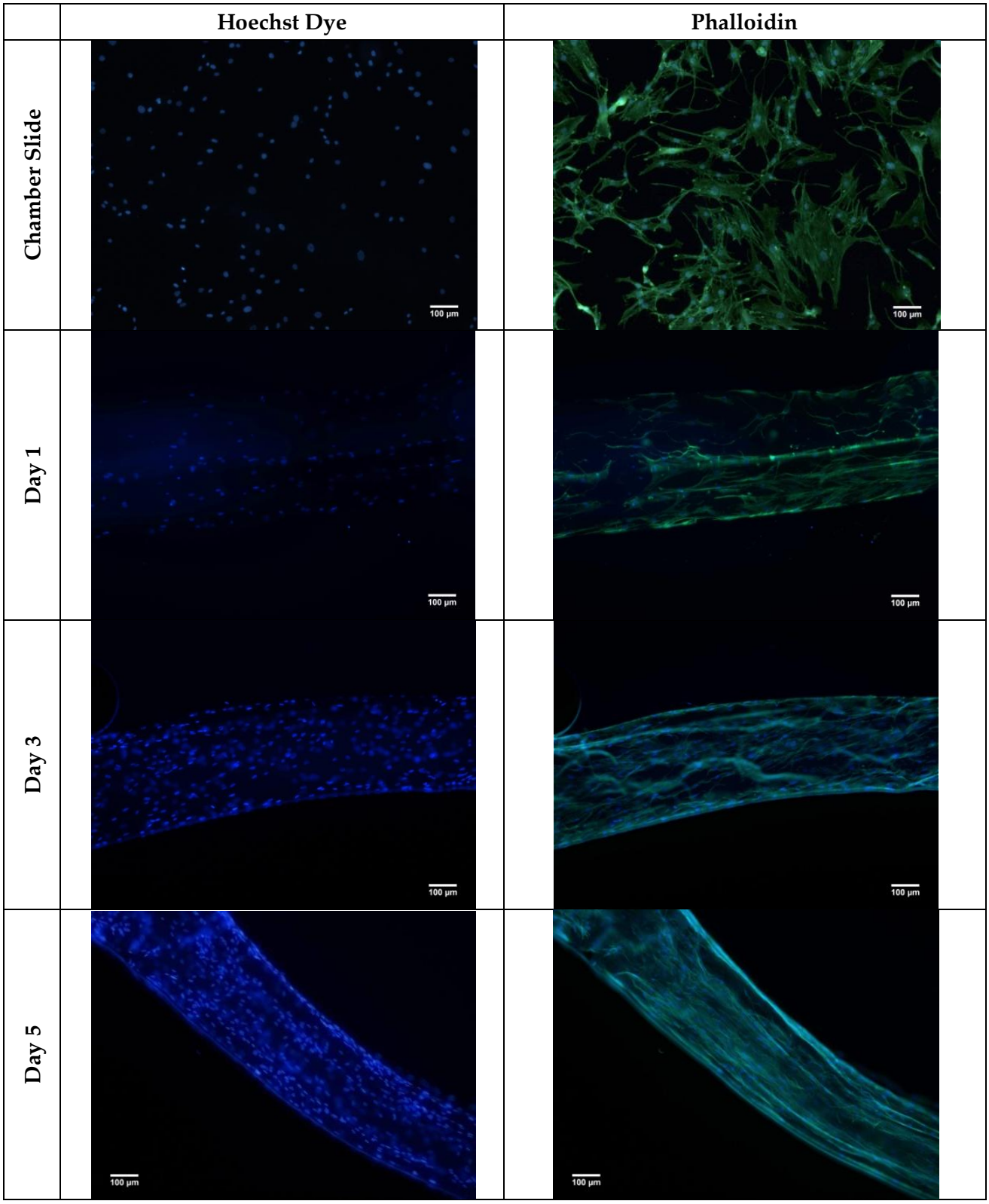

Figure 11: Hoechst dye and phalloidin images of microthread bundles

The density of cells attached to a bundle of 4 microthreads as determined by visual counting is shown in Figure 12 and Table 4. There was a statistically significant increase in cell number by days 4 and 5, reaching 731 ± 101 cells/mm^2 after 5 days (the latest time point evaluated). Raw data including counts, area measurements, and statistics can be found in Appendix B.

Table 4: Average number of cells/mm^2 on microthread bundles (n = 6)

Time Point	Average #cells/mm^2 ± SEM
5 hours	93 ± 21
1 day	253 ± 57
2 day	315 ± 84
3 day	555 ± 49
4 day	616 ± 83
5 day	731 ± 101

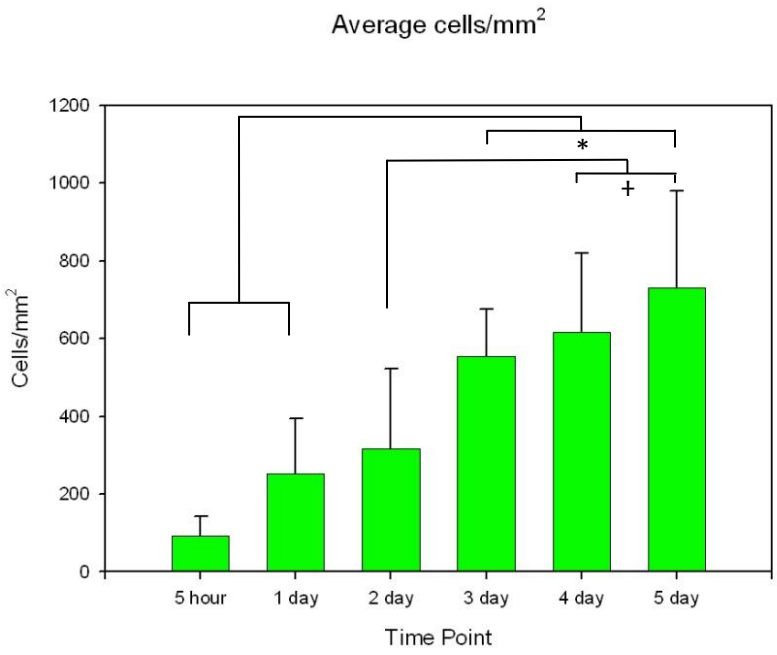

(* indicates statistically significant difference between 5 hour, 1 day and 3, 4, 5 day for $p<0.05$, there is no statistical difference between 5 hour and 1 day as well as between 3, 4, and 5 days; † between 2 day and 4, 5 day for $p<0.05$, there is no statistical difference between 4 day and 5 day)

Figure 12: Cells/mm^2 of microthread bundle (n = 6)

In order to compare the results from this quantification method to alternate quantification methods and results from literature the total number of cells per microthread bundle was calculated. From the calculations in Table 3, the surface area of a microthread bundle is 18.8 mm^2. Since the tail ends of the microthread bundle are not populated with cells, the average unpopulated area (5.6 $\pm$ 1.1 mm^2) was subtracted from the surface area of the bundle (18.8 mm^2) before multiplying by the cell density from Table 4. This adjustment was necessary in order to account for the tail portions of the microthread that were not populated by cells, otherwise simple multiplication of the entire surface area of the microthread bundle by cell density would overestimate cell number. The data in Table 5 and Figure 13 shows the total number of cells on the microthread bundle. Based on these calculations the microthread bundles support approximately 10,000 hMSCs at 5 days in culture. Raw data from these calculations can be found in Appendix C.

Table 5: Total number of cells per microthread bundle

Time Point	Average #cells/bundle $\pm$ SEM
5 hours	1,225 $\pm$ 272
1 day	3,344 $\pm$ 755
2 day	4,169 $\pm$ 1,109
3 day	7,320 $\pm$ 652
4 day	8,125 $\pm$ 1,097
5 day	9,644 $\pm$ 1,339

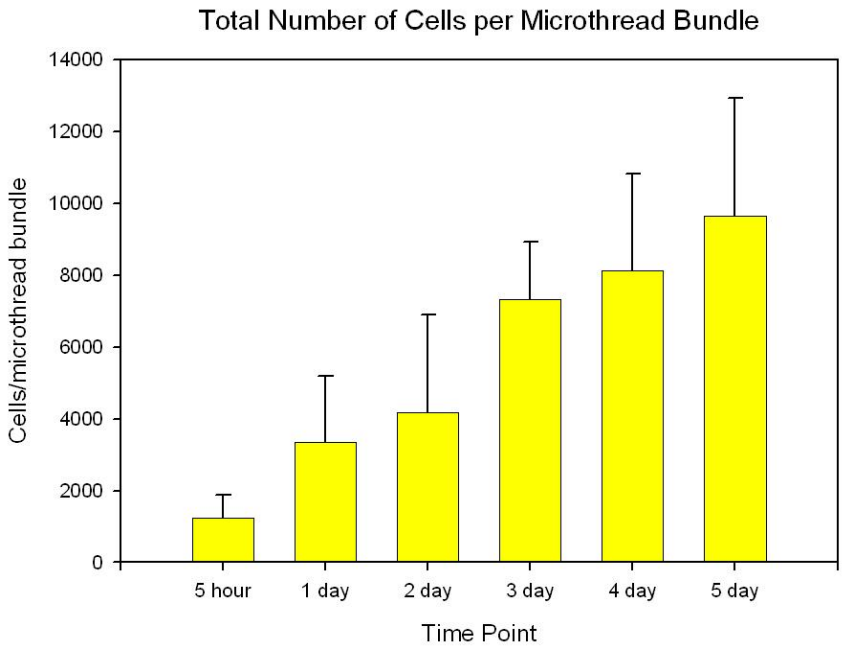

Figure 13: Cells per microthread bundle

5.1.2 CyQuant Cellular Proliferation Assay

To overcome the limitations encountered by quantifying cell number on microthreads via Hoechst dye counts, we attempted to develop an assay for more reproducible, high throughput analysis. The standard curve for the CyQuant assay is shown in Figure 15. It can be fit with a linear trend line with R^2 value approaching 1 (R^2 = 0.9845). Statistics indicate the curve is sensitive enough to detect as few as 100 cells. Graphing fluorescence intensity versus time shows that after 50 minutes of dye incubation there is no statistical change in intensity with time. Thus, all CyQuant experiments were allowed to incubate for 60 minutes. Raw data and statistics can be found in Appendix E.

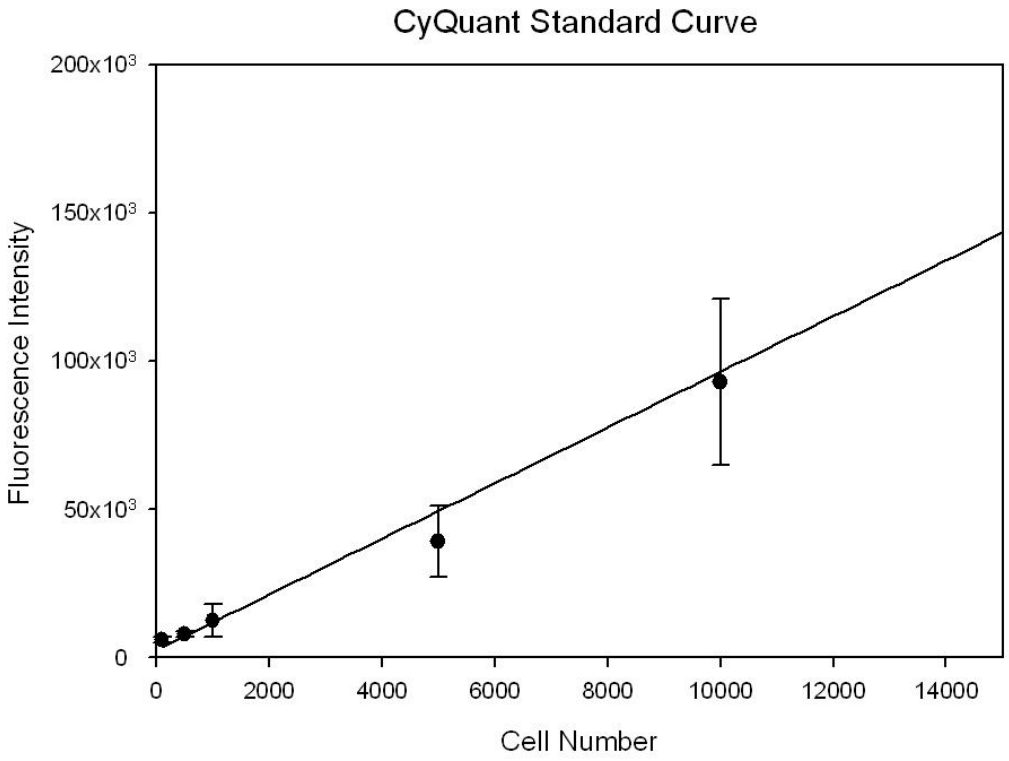

Figure 14: CyQuant standard curve, microthreads (n = 5)

Analysis of the supernatant from centrifugation and the PBS from rinses showed minimal cell loss. This indicates that neither of these steps is causing significant numbers of cells to be lost from the assay. Additionally, statistics indicate that there was no difference between the thread control group and the blank wells (Figure 17). Figure 15 shows a representative image of thread debris in a thread control well before rinsing. Figure 16 shows a thread control well after rinsing, largely free of any debris. This indicates that any fluorescent intensity measured after background subtraction is a result of cells and not remnants of microthread left after digestion. Raw data can be found in Appendix F.

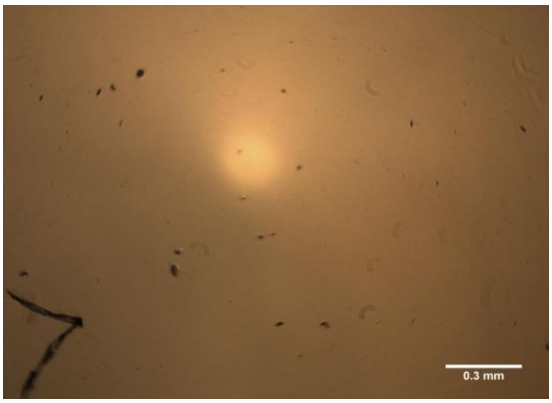

Figure 15: Thread control well before rinsing

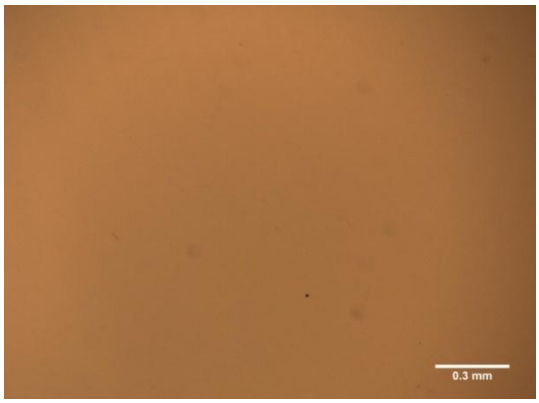

Figure 16: Thread control well after rinsing

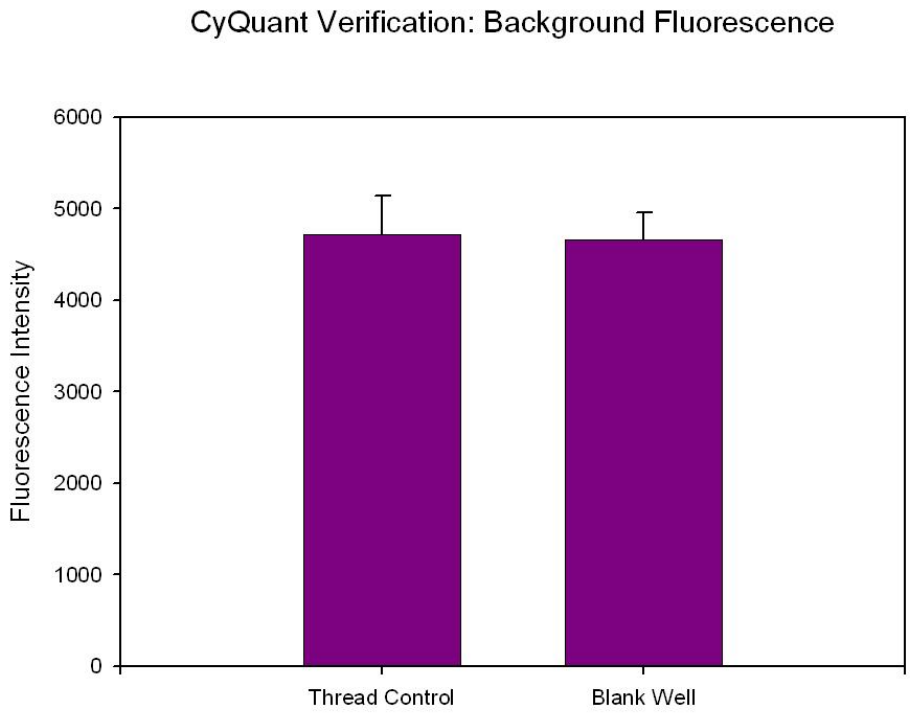

Figure 17: Comparison of thread control well to blank well (n = 24)

The number of hMSCs per microthread bundle measured by the CyQuant assay is summarized in Figure 18 and Table 6. Only microthread bundles at 5 days showed a statistically significant increase in cell number ($p < 0.05$), reaching an average of 4,000 cells per bundle. This is significantly less than the number of cells found by Hoechst dye counts (Figure 13 and Table 5). Raw data can be found in Appendix G.

Table 6: CyQuant - number of cells per bundle (n = 12)

Time Point	Average # cells/bundle± standard deviation
1 Day	1,588 ± 608
3 Day	1,652 ± 704
5 Day	4,016 ± 3,346

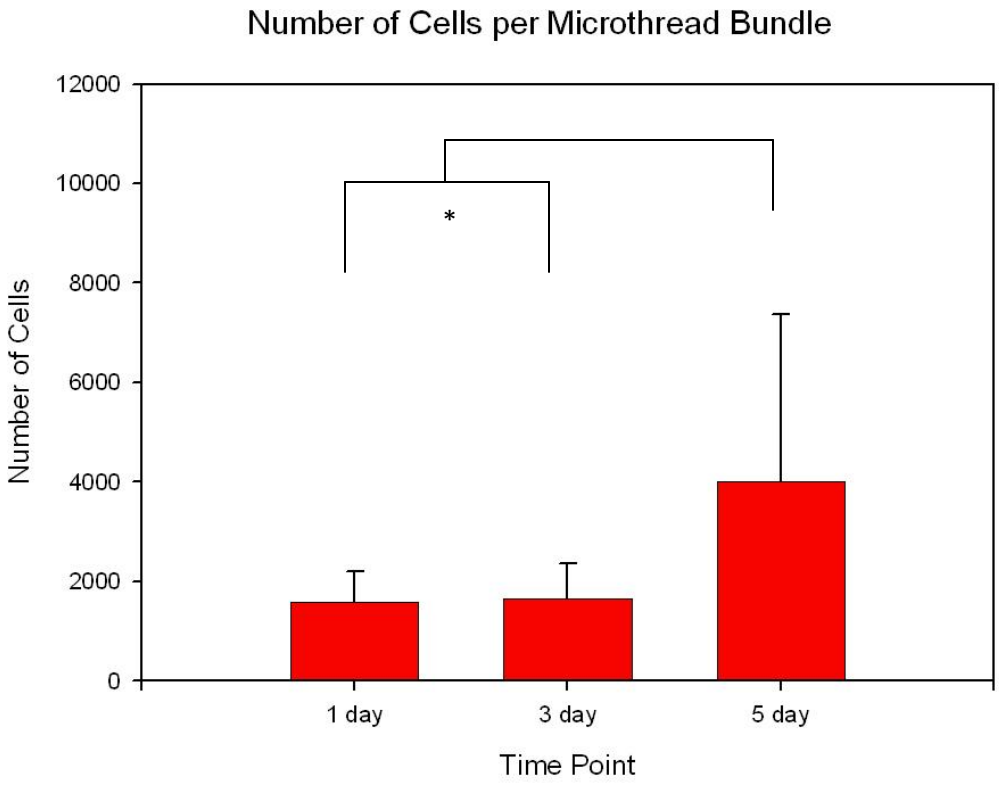

(* indicate statistically significant difference between 1, 3 days and 5 days for $p<0.05$, there is no statistical difference between 1 and 3 days)

Figure 18: CyQuant - number of cells per bundle (n = 12)

5.2 Cellular Viability and Proliferation

The results of the LIVE/DEAD assay are shown in Figure 19. The first column depicts the calcein which turns the cytoplasm of live cells green. The second column depicts the ethidium which turns the nuclei of dead cells red. The third column is the overlay of the previous two images. This demonstrates that cells were viable after 5 days in culture on microthread bundles with minimal cell death (dead cells indicated by

white arrows). The control (hMSCs fixed in 30% methanol) proved that all green fluorescence seen on the microthread bundle was due to live hMSCs.

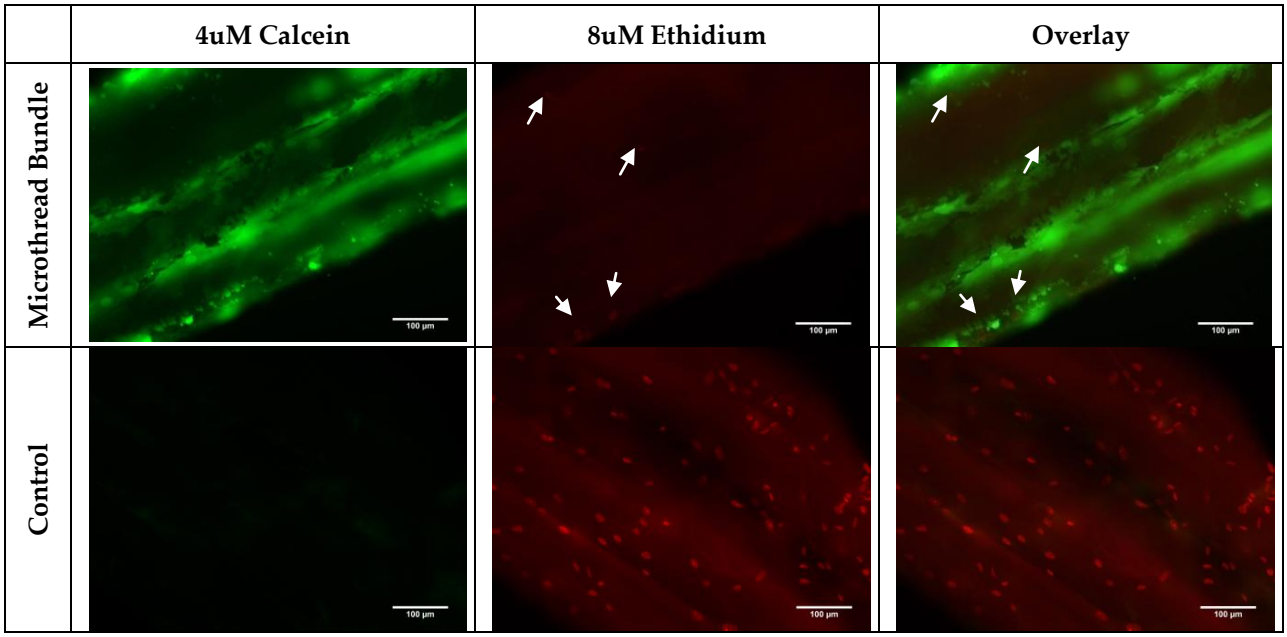

Figure 19: LIVE/DEAD staining of hMSCs on microthreads

Ki-67 staining of bundles showed that hMSCs are entering the cell cycle over 5 days in culture on microthreads. Figure 20 shows Hoechst dye, Ki-67, and overlay images at 1, 3, and 5 days in culture. Few cells enter the cell cycle after 1 day, however by day 3 there is a statistical increase in the number of Ki-67+ hMSCs. Staining is still present at day 5 however there is a statistically significant decrease in percentage of positive cells from day 3. Table 7 shows a summary of the percentage of Ki-67 expression at each time point. Data was taken from 10 randomly selected images of 4 bundles stained in two separate experiments. An average of 69 cells was examined per image (~ 690 cells per time point).

Table 7: Percent of Ki-67 positive hMSCs on microthreads (Average ± Stdev)

Time Point	% hMSCs in cell cycle
1 Day	4.9 ± 5.4
3 Day	22.6 ± 5.9*
5 Day	6.8 ± 5.7†

(* indicates statistically significant differences between day 1 and day 3 $p<0.05$, † indicates statistically significant difference between day 3 and day 5)

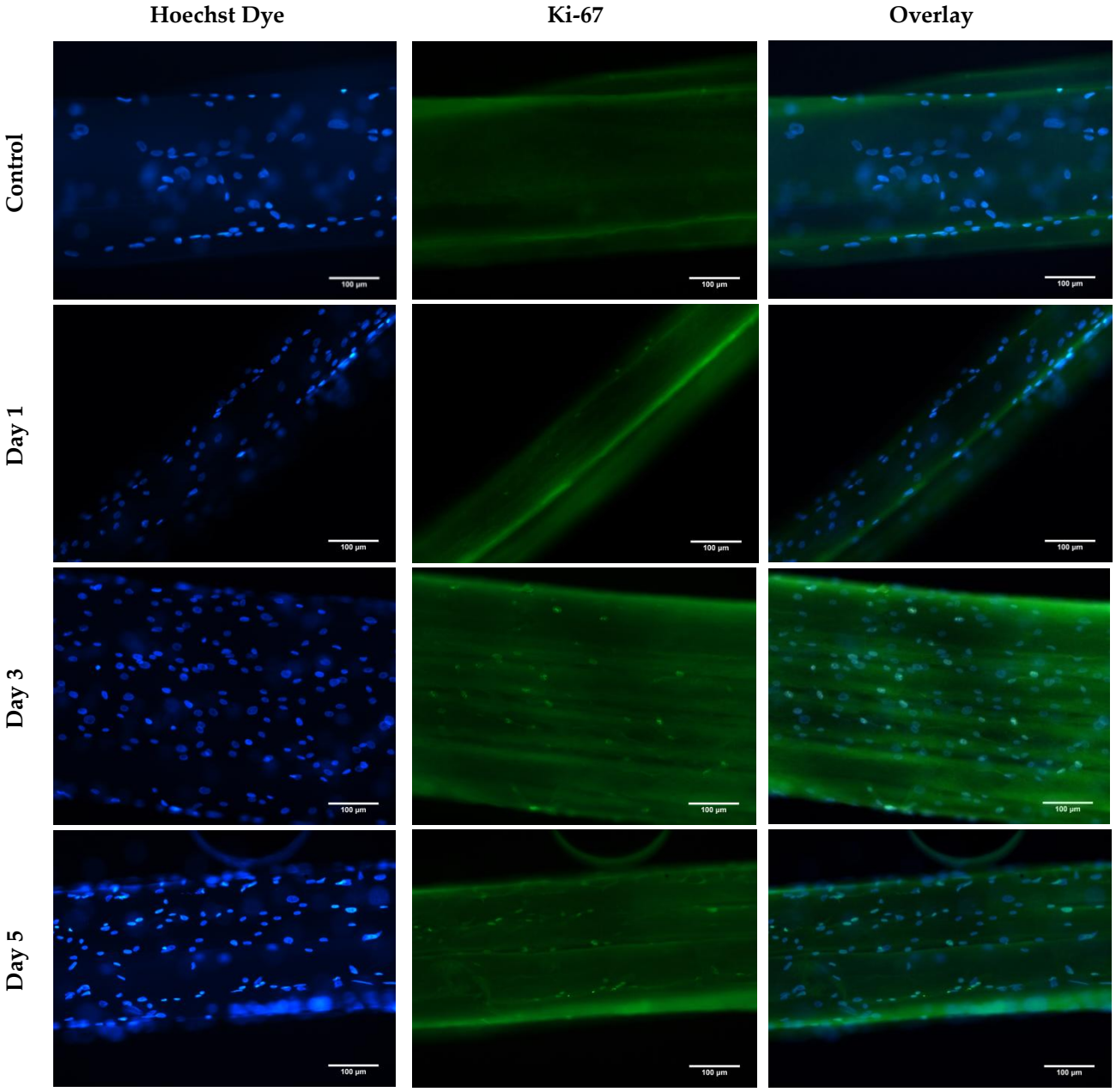

Figure 20: Ki-67 of hMSCs on microthreads

Our Hoechst dye counts indicated hMSCs seemed to be proliferating faster than commonly observed in culture. Therefore we coated chamber slides with a thin layer of fibrin to investigate its effect on proliferation rates. Drying fibrin gels in 8-well chamber slides resulted in adherence of a thin film of fibrin to the bottom of the wells. Trypan blue staining in Figure 21 shows the presence of this coating. The non trypan blue stained wells indicate the presence of crystals in the fibrin layer. After rinsing with 10mM HEPES and sterilizing, the crystals were eliminated and a uniform coating of fibrin remained.

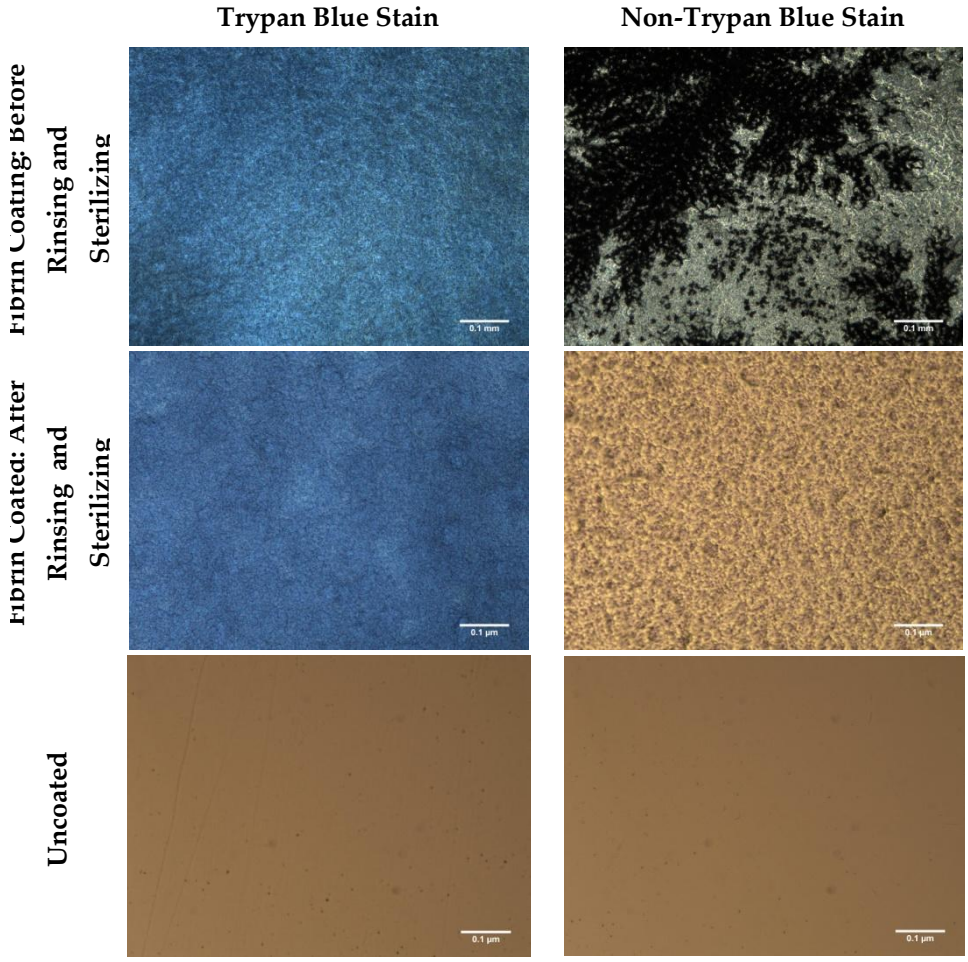

Figure 21: Trypan Blue staining of fibrin coatings

Ki-67 staining of hMSCs seeded on standard 8-well chamber slides is shown in Figure 22 and fibrin coated 8-well chamber slides is shown in Figure 23. The percentage

of cells in the cell cycle at each time point is shown in Table 8. Data is taken from 10 randomly selected images of 4 wells of 2 chamber slides stained in two separate experiments. An average of 30 and 18 cells was examined per image for standard and fibrin coated slides respectively (~300 and ~180 cells per time point).

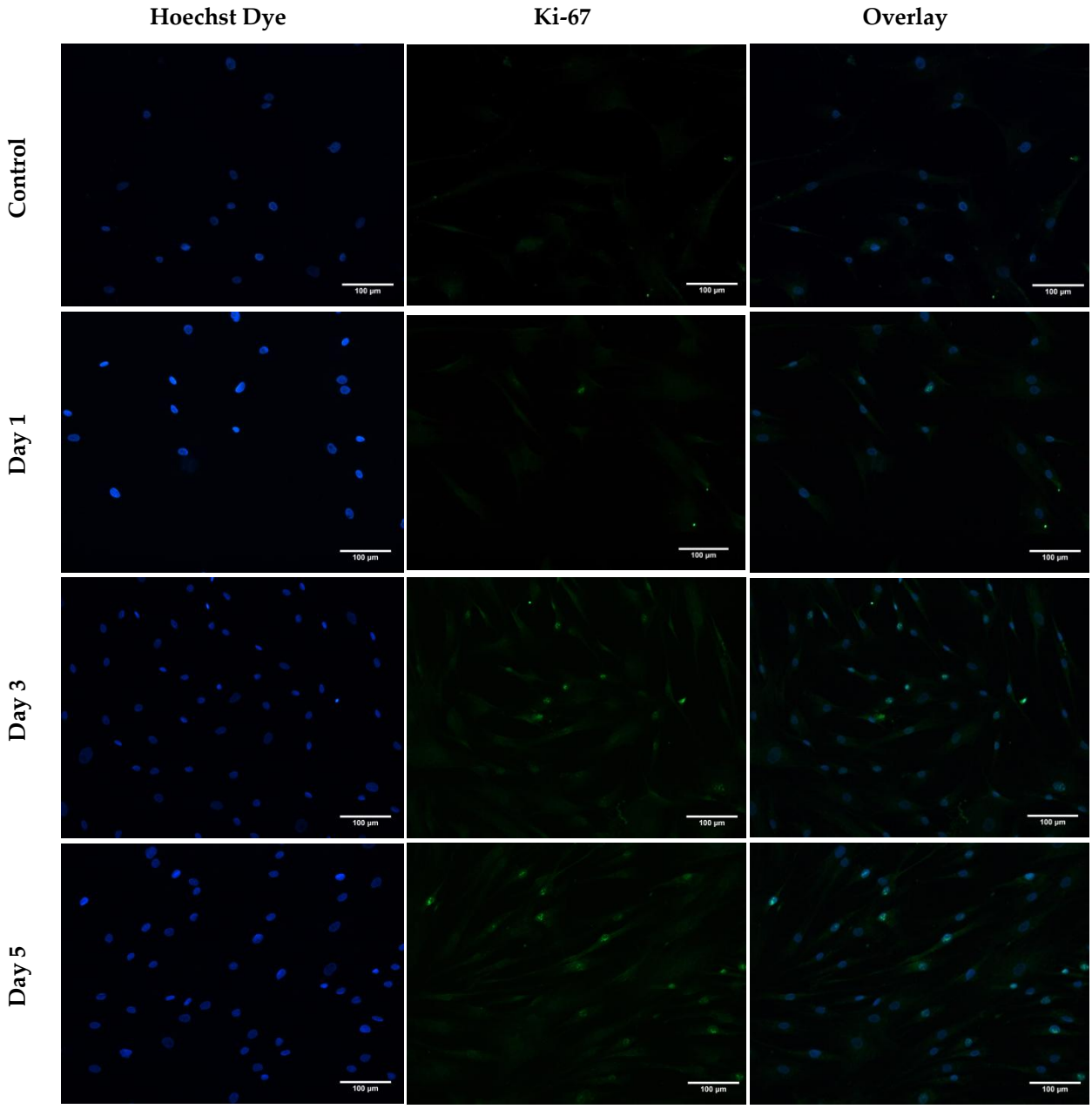

Figure 22: Ki-67 on non-coated chamber slides

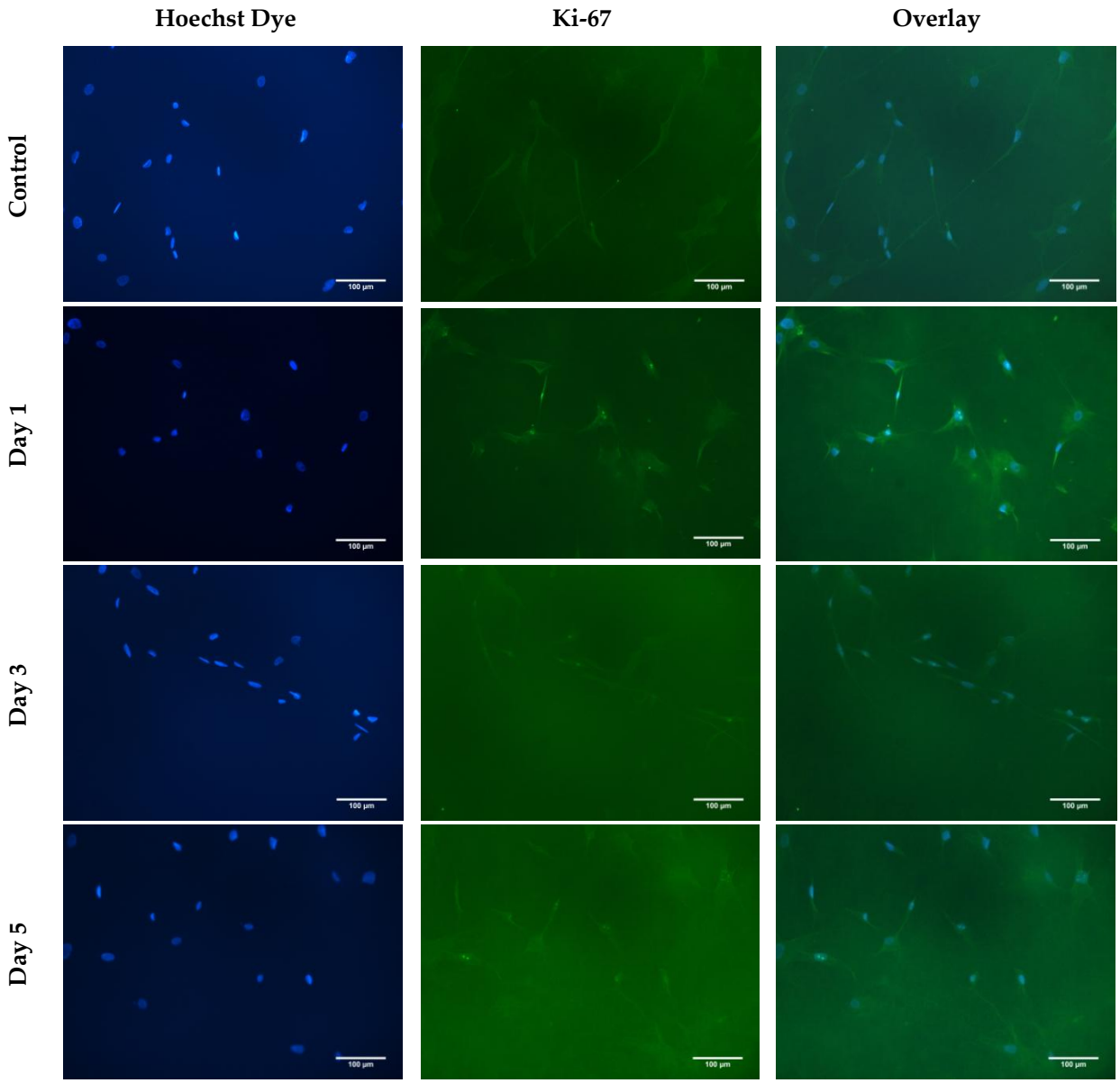

Figure 23: Ki-67 on fibrin coated chamber slides

The percentage of Ki-67 positive hMSCs on standard, uncoated chamber slides showed a statistical increase after 1 day in culture. Between 3 days and 5 days in culture there was no statistically significant difference in the percentage of Ki-67 positive hMSCs. Data from fibrin coated chamber slides showed no statistical increases in percent expression over 5 days in culture.

Table 8: Percent of Ki-67 positive hMSCs on chamber slides (Average ± Stdev)

Time Point	% hMSCs in cell cycle: uncoated	% hMSCs in cell cycle: fibrin coated
1 Day	10.3 ± 10.4	20.1 ± 19.0
3 Day	26.2 ± 12.7*	33.3 ± 18.3
5 Day	29.0 ± 12.3*	20.8 ± 8.1

(* indicate statistically significant difference from 1 day for $p<0.05$)

The graph in Figure 24 compares the percentage of Ki-67+ cells on microthreads, standard chamber slides, and fibrin coated chamber slides. Ki-67 expression by hMSCs at 5 days on microthreads was statistically lower than expression on uncoated or fibrin coated slides. All other combinations showed no statistical difference.

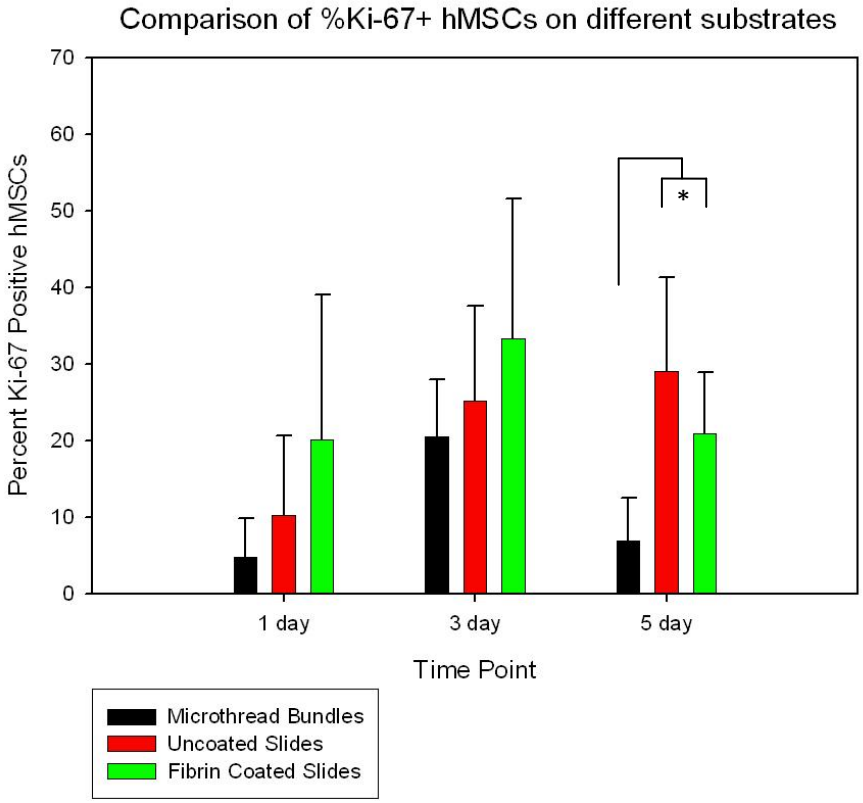

(* indicates statistically significant difference between 5 day microthreads and uncoated, coated slides for $p<0.05$, there is no statistical difference between uncoated and coated slides)

Figure 24: Comparison of Ki-67 expression on different substrates

5.3 Differentiation

Functional differentiation assays proved that hMSCs retained their ability to differentiate into adipocytes and osteocytes after being cultured on microthread bundles for 5 days. Both experiments were repeated to n = 2 with treated control (n = 6), untreated control (n = 6), and hMSCs from threads (n = 4) for each experiment. After 3 weeks in culture, treated hMSCs began to form lipid vacuoles as seen in Figure 25. Oil Red O staining after 5 weeks of culture confirmed the presence of lipid vacuoles as seen in Figure 26.

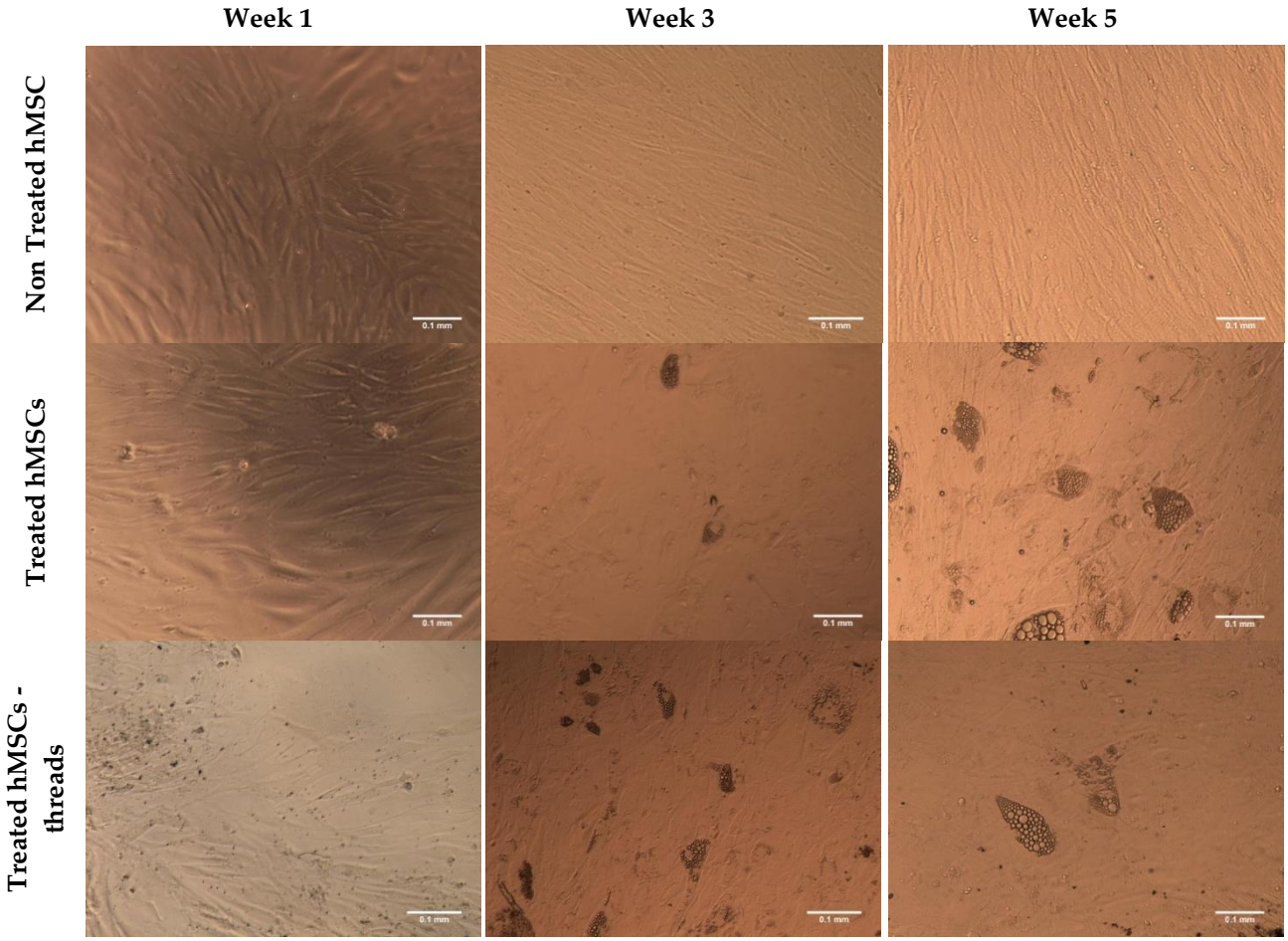

Figure 25: Adipogenic differentiation

Figure 26: Oil Red O staining of lipid vacuoles

After 4 weeks in culture, Alizarin Red S staining of osteogenic cultures showed extensive calcium deposition by treated hMSCs, indicating their differentiation into osteocytes (Figure 27).

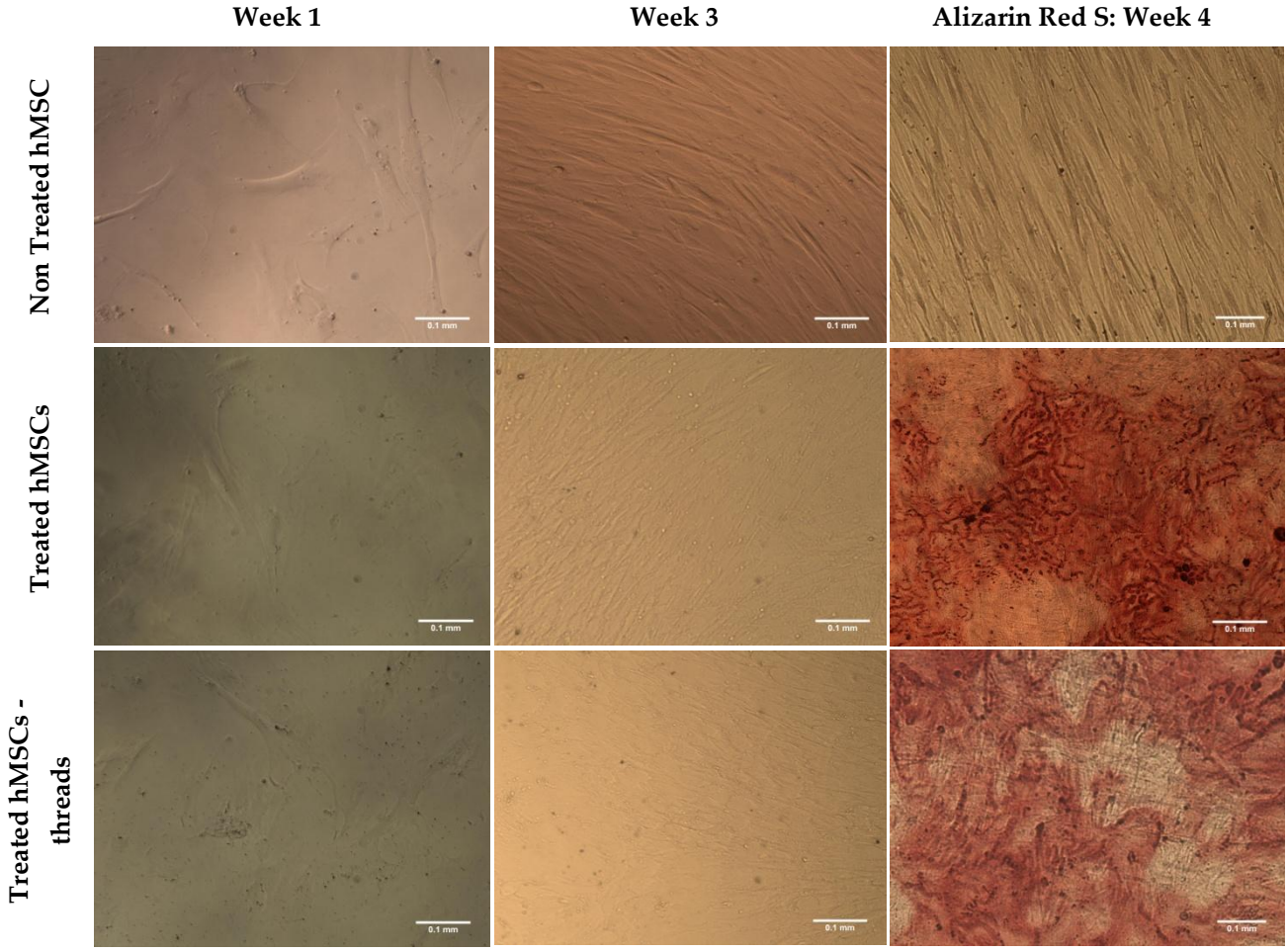

Figure 27: Osteogenic differentiation

Within the osteogenic cultures were small clusters of adipocytes, as seen in Figure 28. This only occurred in wells with hMSCs that had been trypsinized from threads, with less than 10 adipocytes present per well. All other treated controls contained no adipocytes. The red staining is Alizarin Red S for calcium deposition.

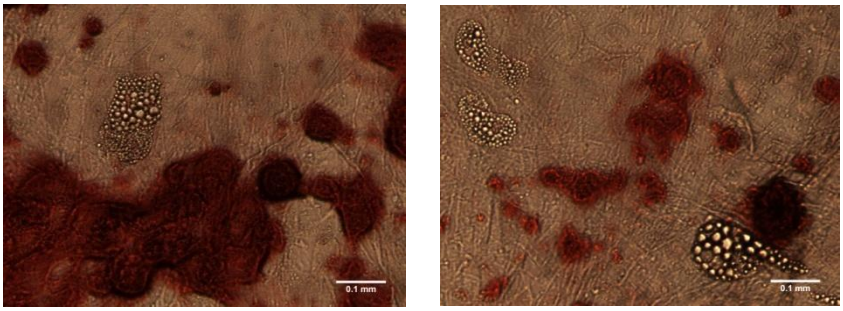

Figure 28: Adipocytes present in osteogenic cultures

Chapter 6: Discussion

This project has succeeded in quantifying the number of hMSCs attached to a bundle of four fibrin microthreads, confirmed they enter the cell cycle and remain viable, as well as verified their ability to maintain multipotency. This section discusses the significance of these results in terms of the goal of this project.

6.1 Quantification of Cell Number: Hoechst dye

Counts of Hoechst dye stained nuclei indicated that we can achieve an average density of 731 $\pm$ 101 cells/mm^2 of microthread. By extrapolating this data to calculate the total number of cells per microthread bundle, we find that it is theoretically possible to deliver approximately 10,000 cells with one 2 cm long bundle. This coincides well with our predicted hMSC attachment of 15,000 cells on a bundle of microthreads and falls within the range of 400 to 40,000 cells that must be delivered to the rat heart to see functional improvements (refer to Table 2 for data and references).

While a single microthread bundle will deliver 10,000 cells, 4 bundles will deliver approximately 40,000 cells which is the upper end of the desired delivery range. Delivering 1 to 4 microthread bundles to the rat heart is feasible, as their diameter is only a fraction of the wall thickness of infarcted rat hearts (1.5 to 2mm) [81]. Delivering the entire 2 cm length of microthread in one pass may difficult. However with multiple passes, either in parallel or around the infarct zone, the necessary length of microthread bundle could be implanted. The length of microthread needed could also be shortened if the number of microthreads per bundle were increased, providing a larger circumferential surface area for cell attachment and growth.

These calculations assume that the engraftment rate of hMSCs delivered by suturing the microthread bundle into the heart wall is 90 to 100%. However, this has not been evaluated as of yet. Since the hMSCs are cultured on the exterior of the microthread bundle, shear stress will be exerted on them during delivery. There is a distinct possibility that the shear stress these cells encounter while the microthread

bundle is being sutured into the myocardium could detrimentally impact cell viability and adhesion. While this work shows microthread bundles support hMSC attachment and growth, it is unknown how much shear stress hMSCs can handle before becoming unattached from the bundle. Should this be identified as a problem, there are at least two approaches that could be implemented to try and protect the hMSCs from shear stress.

One is to utilize a sheath of silicone tubing or similar material to protect hMSCs during delivery. This protective sheath would then be removed once the microthread is implanted. The protective sheath could also serve as a bioreactor for culture of hMSCs on microthreads pre-implantation. However, this approach may limit the surgeon's ability to freely suture the microthreads in curved or circular patterns based on the flexibility of the sheath. Also, it will still expose hMSCs to shear stress while the sheath is being removed. If the material used is rigid and there is enough clearance space between the inner wall and the microthread this may not pose a problem. However since fibrin microthreads have a tendency to adhere to anything in their proximity, it is inevitable that the hMSCs would still be experiencing enough shear stress to decrease engraftment rates.

A second approach would be to develop an alternative method to bundling the fibrin microthreads to create a protective layer. If bundling were controlled so hMSCs were more concentrated in the grooves of the bundle rather than over the outer surface then they would be protected during implantation. Any shear stress experienced would be exerted on the outermost portions of the microthread bundle. This could also be achieved by coating the seeded microthread bundle in a fibrin gel to serve as a lubricant. Or alternatively, this could be achieved by co-extruding the hMSCs within the microthread bundles. While this could be a relatively simple solution, this presents issues with ensuring all cells remain viable and oxygen and nutrients are able to diffuse to the entrapped cells.

No matter the procedure for delivery, it is still vital to investigate how many cells are lost in the microthread implantation process and how this would affect the engraftment rate. We expect a much higher engraftment rate than systemic delivery because the cells are delivered locally and are attached to the microthread scaffold which should minimize, or even eliminate, the wash out phenomenon that has limited cell retention when direct intramyocardial injection is used as a delivery method.

6.2 Quantification of Cell Number: CyQuant Assay

We attempted to develop an automated, high throughput assay for cell quantification that would be more reproducible and time efficient than hand counting nuclei in images. While the Hoechst dye counting allows the researcher to analyze threads intact and provides more detailed analysis, it is time consuming and can be skewed by the different focal planes present when viewing with a standard upright microscope. Thus many nuclei are out of focus or not seen and as a result aren't included in the quantification. The use of confocal microscopy is highly recommended for any further quantification with Hoechst dye staining. Confocal microscopy allows images to be taken in one plane at a time, thus eliminating out of focus objects and building a three dimensional image of the sample. Viewing the microthreads in this way would allow all the nuclei present on any plane to be counted and included in quantification.

The CyQuant assay reported less than half of the total number of cells counted in the Hoechst dye analysis. A comparison between two standard curves (Figure 29) illustrates this loss of cells. The standard curve labeled 'plated' was made by incubation of CyQuant dye on known numbers of hMSCs cultured in a standard tissue culture plate. The standard curve labeled 'digestion/re-plate' was made by taking known numbers hMSCs cultured in a standard tissue culture plate, and trypsinizing, centrifuging, re-plating, and then rinsing them before application of the CyQuant dye.

This is the same protocol that was used for quantification of hMSC attachment on microthreads. The discrepancy between the two slopes (31.0 as compared to 9.4) signifies that cells are being lost somewhere in the assay.

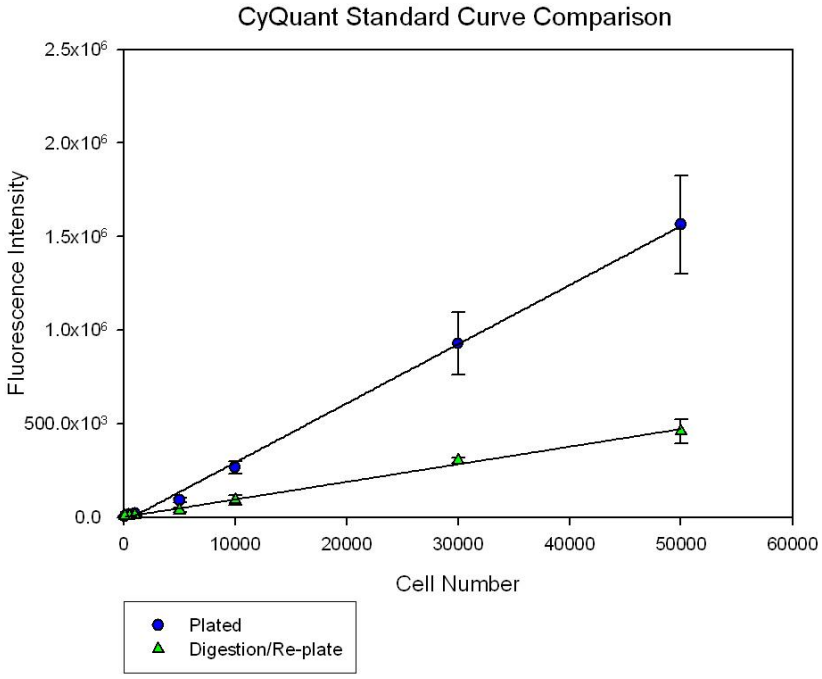

Figure 29: CyQuant standard curve comparison

One possible explanation is that the plate reader is not picking up the emitted fluorescence from all areas of the well. More often than not a significant number of re-plated cells are very close to the edge of the tissue culture well. Depending on the plate reader capabilities, it may not be able to gather signal from this part of the well. While verification steps proved minimal cell losses in centrifuge supernatant and PBS rinses, the trypsinization process could be digesting cells along with the fibrin microthread. Thus these cells would be lost before the assay process even began. Finally, it is possible that cells could remain attached to the thread debris and are rinsed away during the re-plating process. This was not investigated directly, however the amount of thread debris remaining after digestion would not easily lend itself to carrying half of the total number of cells present on the bundle.

Further refinement of the CyQuant assay is needed before we can be confident in its results. There are a variety of approaches that can be taken to attempt to narrow down the problem. First, to identify if the trypsinization process is killing the hMSCs, the cells can be subject to trypsinization, centrifuged, re-suspended and then counted via hemocytometer. Comparing this count to bundles of microthread digested and evaluated via the entire CyQuant assay procedure will illustrate whether or not trypsinization is the problem. For the seeding of the functional differentiation assays, we had to trypsinize the hMSCs from the microthreads and count them via hemocytometer in order to re-plate the cells at the appropriate concentration. This data provides a comparison technique for determining whether the discrepancy between the Hoechst dye results and the CyQuant results is due to the trypsinization process. Looking back at the cell counts shows there were a total of 37,440 cells digested from 36 microthread bundles. Thus, there were only just over 1,000 cells present per microthread bundle. This indicates that the hemocytometer counts and the CyQuant assay are in agreement with each other and thus there is a pretty good chance trypsinization is affecting the measurement of cell number. This verification process should be repeated to confirm these results.

Second, further verification should be performed by Hoechst dye staining the re-plated supernatant and PBS from rinsing. This will identify the presence of any cells still attached to the thread debris. This should be done by re-suspending these solutions in Hoechst dye, then centrifuging again and re-suspending in PBS to rinse the excess Hoechst dye. This is necessary because the thread debris will not adhere to the tissue culture plate when re-plated. Finally, if no previous verification reveals significant cell loss then this may indicate that reading of the emitted fluorescence by the plate reader is a problem. An alternative form of the CyQuant assay involves a freeze-thaw cycle to lyse cells and release the DNA into solution. This may alleviate problems due to cell

distribution within the well because it would allow the DNA to be in a homogenous solution when analyzed by the plate reader.

6.3 Cell Proliferation

Ki-67 staining of hMSCs cultured on microthread bundles illustrated that the increase in cell number over time is due to proliferation. It was necessary to confirm this because each sample in this experiment was taken individually. There was no carryover of samples from one time point to the next therefore it could be argued that any changes in cell number may be due to variation between samples. Since Ki-67 staining revealed that hMSCs are proliferating on microthreads, we know this increase is not sample variation but growth of hMSCs on the surface over time.

Typical doubling time for low passage (P2-10) hMSCs in culture is 5 to 7 days [78]. Looking at the data from Hoechst dye counts before analysis, hMSCs appear to be proliferating much faster, increasing 7-fold over 5 days. In order to determine if this increase is due to the substrate the hMSCs are being cultured on we compared proliferation rates on microthread bundles to that of standard chamber slides and fibrin coated chamber slides. The only significant difference in this comparison was the decrease in expression rate at 5 days on microthread bundles. Instructions from Lonza, the hMSC supplier, cite that hMSCs seeded at a concentration of 5,000 - 6,000 cells/cm^2 should reach confluence in 6 to 7 days. Quantification results show that hMSCs are initially seeded on microthreads at a concentration of 9,300 $\pm$ 2,100 cells/cm^2. Thus, we presume this decrease in Ki-67 expression may be due to the hMSCs beginning to reach confluence on the microthread bundle, thus their proliferation rates would be decreasing.

While this data suggests that hMSC proliferation on microthread bundles is no different from hMSC proliferation on a standard or fibrin coated culture surface, there are some limitations with this experiment. Both fibrin coated and uncoated chamber

slides were seeded at the same density, however there are statistically fewer cells present in the images counted for the fibrin coated chamber slides (18 $\pm$ 8 cells/image for fibrin coated compared to 30 $\pm$ 17 cells/image for uncoated). It is unknown why so few cells appear on the fibrin coated surface. Also, the initial purpose of this experiment was solely to demonstrate the presence of proliferation markers to support the claim that increases in cell number over time were due to cell growth. In order to make thorough comparisons of Ki-67 expression between chamber slides and microthreads, the chamber slides would have been seeded at a comparable density to what is observed on microthread bundles. Cells on chamber slides were seeded at what is equivalent to 28 cells/mm^2 while after 5 hours on microthreads the average cell density is just over 90 cells/mm^2. This renders comparison between the two in their current state somewhat futile because cells seeded at different densities will proliferate at different rates.

6.4 Differentiation

Functional differentiation assays demonstrated that hMSCs retain their ability to differentiate down adipogenic and osteogenic lineages after 5 days of culture on fibrin microthreads. This was expected as previous research has shown hMSCs can differentiate down both lineages when cultured in a fibrin gel [82, 83]. Catelas et al. investigated hMSC morphology, proliferation and osteogenesis in different formulations of fibrin gels. Cells entered into the early stages of osteogenic differentiation as measured by alkaline phosphatase assay, von Kossa staining, and real-time reverse transcriptase-polymerase chain reaction [82]. Additionally, Gerard et al. demonstrated adipogenic differentiation of hMSCs cultured in a fibrin gel as documented by Oil Red staining [83].

While our work shows that hMSCs retain their multipotency in terms of adipogenic and osteogenic lineages, we believe there is reason for further investigation. After 4 weeks of culture there were small pockets of adipocytes present in the Alizarin

Red S stained osteogenic wells of hMSCs that had been cultured on threads. This could indicate that hMSCs are predisposed to adipogenesis after culture on microthreads since adipocytes were not present in any other group. However, presence of adipocytes in these cultures was deduced solely by phenotype and was not confirmed by Oil Red staining. Also, this experiment did not include staining of non-induced hMSCs grown on fibrin microthreads. This important control would shed light on whether adipocytes spontaneously form in hMSC cultures from microthreads. Research in adipose tissue engineering cites the use of fibrin gels for supporting the growth of pre-adipocytes [84-86]. However, while Matrigel alone has been shown to produce spontaneous adipogenesis in murine models, research with fibrin gels to date shows no induction of adipogenesis [86, 87].

In order to do these experiments, the microthreads were removed from culture and digested in the same manner as the CyQuant assay. If the trypsinization process is killing some of the cells while it digests the microthread bundle as suspected, then we are potentially selecting for hMSCs that survive this process. If it is, then the digestion procedure will need to be eliminated in order to test the multipotency of all cells present. The microthread bundles could be cut from the washers, placed in the bottom of 12-well tissue culture plates and fed with the appropriate medium. In this way, no hMSCs are specifically selected for through any sort of digestion process and they are allowed to continue growing on the microthread during the feeding cycle. It is assumed that the cells would eventually break down the microthread and spread out to cover the bottom of the well during this cycle.

Adipogenesis and osteogenesis are only two of the many lineages hMSCs have been shown to differentiate into. Research suggests hMSCs are also capable of chondrogenic, myogenic, neurogenic and endothelial differentiation thus complete characterization of their multipotency would include these assays [37]. Barry et al.

demonstrated chondrogenic differentiation of MSCs when grown in a three dimensional culture format in a serum free medium with the presence of a member of the TGF-β family [88]. Endothelial differentiation was shown by Davani et al. after intramuscular injection of MSCs into a rat infarct model [89]. The MSCs differentiated into an endothelial phenotype and improved vascularization of the area. Deng et al. illustrated the neurogenic potential of MSCs when treated with isobutylmethlyxanthine and dibutyryl cyclic AMP after 6 days in culture. Finally, hMSCs injected into the myocardial wall of mice showed expression of desmin, β-myosin heavy chain, α-actinin, cardiac troponin T, and phospholamban at levels comparable to those of the host cardiomyocytes, indicating myogenic differentiation [8].

Chapter 7: Future Work and Implications

The use of fibrin microthreads as a biological scaffold for stem cell delivery to infarcted myocardium is a novel approach. This section describes some of the implications of these results and their significance for future investigations.

These fibrin microthreads are meant to be delivered to the heart in the same manner as a suture. This is highly advantageous because surgeons use suture as part of their daily routine, thus it would not require any special instructions or training for use. When used as a suture, the cell-seeded microthreads have the ability to be implanted to a precise location within the heart wall, thus localizing the therapeutic treatment where it is most needed. Some caution must be exercised with their use however, because the microthreads still need ready access to blood flow for the cells they are carrying to remain viable. The bundles could be sutured around the infarct at the border zone or within healthy myocardium and be in the presence of perfused tissue. If they are sutured directly through the center of the infarct zone it is likely that many of the cells with have difficulty surviving due to the diminished availability of nutrients within the harsh environment.

It is important to note that the mechanism by which the delivery of hMSCs aid in functional cardiac improvements is highly controversial. Several different mechanisms have been proposed, including passive presence of additional cells or materials within the myocardial wall, differentiation of transplanted cells, and paracrine signaling [35, 44]. Cell-seeded fibrin microthreads have the potential to function by all of these three mechanisms. Studies have shown that the delivery of passive material alone to the myocardium results in improved mechanical function [90] thus the presence of the fibrin microthread alone may help improve heart function. Other research, including Kajstura et al. and Toma et al., has demonstrated transdifferentiation of hMSCs upon implantation in murine myocardium [8, 91]. The latter study demonstrated that these

cells expressed levels of desmin, β-myosin heavy chain, α-actinin, cardiac troponin T, and phospholamban comparable to host cardiac myocytes with sarcomeric organization of contractile proteins [8]. Since fibrin microthreads are able to support the growth of undifferentiated hMSCs, these cells have the potential to differentiate in a similar manner once implanted into the myocardium. And finally, other groups have demonstrated improvements in cardiac mechanics attributed to paracrine effects initiated by introduction of MSCs [44, 91-93]. MSCs are known to secrete growth factors and cytokines such as vascular endothelial growth factor (VEGF), basic fibroblast growth factor (bFGF), insulin-like growth factor (IGF), and stromal cell derived factor (SDF) which may prevent apoptosis of cardiomyocytes, induce adipogenesis, and activate resident progenitor cells [91-93]. Thus delivery of hMSC-seeded microthreads to the infarct border zone would allow hMSCs to interact with the native myocytes in this way as well.

Another attractive feature of using fibrin microthreads is inherent in their combination of cell signaling and structural properties. Specifically, their cylindrical structure and small diameter facilitate orientation of cells based on the organization of the cell's actin microfilament bundles [94]. The structure of the heart consists of highly oriented muscle fibers strongly correlated to heart function. By guiding alignment of hMSCs on the fibrin microthreads, we may provide an aligned environment for regeneration. Our results hinted that hMSCs appear to align with the long axis of the fibrin microthread bundle. While this was not quantified, it may be an area for future development to characterize fibrin microthreads as a matrix for cell alignment as well.

An important consideration for any biomaterial delivery scaffold is persistence within the tissue. The fibrin microthreads should persist long enough to guide the integration of cells, but not so long as to interfere with cell coupling essential to myocardial function [54]. Fibrin is known for its rapid clearance upon implantation by

cellular mechanisms [48] thus it will be necessary to investigate their persistence in-vivo. Should the fibrin microthreads degrade too rapidly in their natural state, they can be crosslinked. However cross-linking of microthreads by ultraviolet light has shown a negative impact on cell proliferation when examined with fibroblasts [23]. Therefore an alternative form of cross-linking may need to be explored, such as those suggested by Cornwell et al. including cross-linking by aldehydes or use of enzymes from the transglutaminase family [23].

In summary, this study has begun to validate the use of fibrin microthreads as a platform technology for delivery of hMSCs to myocardial infarcts. While our work was done with a bundle of 4 fibrin microthreads, this technology has the capability for scale-up to accommodate increased number of cells to be applicable for the human heart. Either by increasing the number of threads per microthread bundle or by increasing the length of the bundles, the surface area for cell seeding and attachment can be increased. Fibrin microthreads can also be utilized as a platform for growth factor delivery. Previous studies have identified the growth factors that are up-regulated by hMSCs when transplanted into a myocardial infarct. By incorporation of these growth factors (such as VEGF, bFGF, IGF, SDF, or hepatocyte growth factor (HGF)) the microthreads can assist the hMSCs in controlling the microenvironment of the resident cardiac myocytes. Additionally, by combining the incorporation of growth factors with compounds such as 5-azacytdine or transcription factor Pax3, hMSCs grown on microthreads could be encouraged down a myogenic pathway [95]. This would control the fate of implanted hMSCs and potentially accelerate myocardial regeneration. Ultimately, this technology could further revolutionize surgical therapy for myocardial infarcts if it were adapted to be a semi or minimally invasive procedure. This would eliminate the need for open heart surgery, making this technology available to patients deemed too high risk for such invasive procedures.

Conclusions

The goal of this project was to explore several fundamental questions regarding the feasibility of culturing human mesenchymal stem cells on a fibrin microthread scaffold as a first step toward developing a microthread-mediated cell delivery system. Our results demonstrate that microthread bundles have the potential to deliver a physiologically relevant number of cells to the heart and that these hMSCs are viable, can proliferate on the microthread bundle, and retain their stemness after 5 days of culture. This study validates the feasibility of using cell-seeded microthreads as a platform technology to improve localized delivery of viable cells to infarcted myocardium for promotion of functional tissue regeneration.

References

1. Braunwald EPM. Ventricular remodeling after myocardial infarction: experimental observations and clinical implications. Circulation 1990;81:1161-1172.
2. Fang JC, Couper GS. Surgical Management of Congestive Heart Failure. Totowa NJ: Humana Press Inc, 2005.
3. Buckberg G. Ventricular Structure and Surgical History. Heart Failure Reviews 2004;9:255-268.
4. Tonnessen T, Knudsen CW. Surgical Left Ventricular Remodeling in Heart Failure. The European Journal of Heart Failure 2005;7:704-707.
5. Piao H, Youn T-J, Kwon J-S, Kim Y-H, Bae J-W, Bora-Sohn, et al. Effects of bone marrow derived mesenchymal stem cells transplantation in acutely infarcting myocardium. The European Journal of Heart Failure 2005;7:730-738.
6. Hou M, Yang K-m, Zhang H, Zhu W-Q, Duan F-j, Wang H, et al. Transplantation of mesenchymal stem cells from bone marrow improves damaged heart function in rats. International Journal of Cardiology 2007;115:220-228.
7. Mangi A. Mesenchymal stem cell modified with Akt prevent remodeling and restore performance in infarcted hearts. Nature Medicine 2003;9(9):1195-1201.
8. Toma C, Pittenger MF, Cahill KS, Byrne BJ, Kessler PD. Human Mesenchymal Stem Cells Differentiate to a Cardiomyocyte Phenotype in the Adult Murine Heart. Circulation 2002 January 1, 2002;105(1):93-98.
9. Pittenger MF. Mesenchymal stem cells and their potential as cardiac therapeutics. Circulation Research 2004;95:9-20.
10. Orlic D, Kajstura J, Chimenti S, Jakoniuk I, Anderson SM, Li B, et al. Bone marrow cells regenerate infarcted myocardium. Nature 2001;410(6829):701-705.
11. Laflamme M, Murry CE. Regenerating the Heart. Nature Biotechnology 2005;23(7):845-856.
12. Muller-Ehmsen J, Peterson KL, Kedes L, Whittaker P, Dow JS, Long TI, et al. Rebuilding a damaged heart: long-term survival of transplanted neonatal rat cardiomyocytes after myocardial infarction and effect on cardiac function. Circulation 2002;105:1720-1726.
13. Zhang M, Methot D, Poppa V, Fujio Y, Walsh K, Murry CE. Cardiomyocyte grafting for cardiac repair: graft cell death and anti-death strategies. J Mol Cell Cardiol 2001;33:907-921.
14. Reffelmann T, Kloner RA. Cellular cardiomyoplasty - cardiomyocytes, skeletal myoblasts, or stem cells for regenerating myocardium and treatment of heart failure? Cardiovascular Research 2003;58:358-368.
15. Christman KL, Lee RJ. Biomaterials for the Treatment of Myocardial Infarction. Journal of the American College of Cardiology 2006;48(5):907-913.

16. Christman KL, Vardanian AJ, Fang Q, Sievers RE, Fok HH, Lee RJ. Injectable Fibrin Scaffold Improves Cell Transplant Survival, Reduces Infarct Expansion, and Induces Neovasculature Formation in Ischemic Myocardium. Journal of the American College of Cardiology 2004;44(3):654-660.
17. Christman KL, Fok HH, Sievers RE, Fang Q, Lee RJ. Fibrin Glue Alone and Skeletal Myoblasts in a Fibrin Scaffold Preserve Cardiac Function after Myocardial Infarction. Tissue Engineering 2004;10(3-4):403-409.
18. Thompson CA, Nasseri BA, Makower J, Houser S, McGarry M, Lamson T, et al. Percutaneous transvenous cellular cardiomyoplasty: a novel nonsurgical approach for myocardial cell transplantation. Journal of the American College of Cardiology 2003;41(11):1964-1971.
19. Zhang P, Zhang H, Wang H, Wei Y-j, Hu S. Artificial matrix helps neonatal cardiomyocytes restore injured myocardium in rats. Artificial Organs 2006;30(2):86-93.
20. Leor J, Aboulafia-Etzion S, Dar A, Shapiro L, Barbash IM, Battler A, et al. Bioengineering Cardiac Grafts: A New Approach to Repair the Infarcted Myocardium. Circulation 2000;102(Suppl III):56-61.
21. Huang NF, Yu J, Sievers R, Li S, Lee RJ. Injectable Biopolymers Enhance Angiogenesis after Myocardial Infarction. Tissue Engineering 2005;11(11-12):1860-1866.
22. Kofidis T, Lebl DR, Martinez EC, Hoyt G, Tanaka M, Robbins RC. Novel injectable bioartificial tissue facilitates targeted, less invasive, large scale tissue restoration on the beating heart after myocardial injury. Circulation 2005;112:173-177.
23. Cornwell K, Pins G. Discrete crosslinked fibrin microthread scaffolds for tissue regeneration. Journal of Biomedical Materials Research 2007;82(1):104-112.
24. Ho W, Tawil B, Dunn JCY, Wu BM. The Behavior of Human Mesenchymal Stem Cells in 3D Fibrin Clots: Dependence on Fibrinogen Concentration and Clot Structure. Tissue Engineering 2006;12(6):1587-1595.
25. Humphrey J. Cardiovascular Solid Mechanics: Cells, Tissues and Organs. New York, New York: Springer-Verlag, 2001.
26. Sherwood L. Human Physiology: From cells to systems. Belmont, CA: Thomson Learning Inc, 2004.
27. Bers D. Cardiac excitation contraction coupling. Nature 2002;415:198-205.
28. Ferrero Jr JM. Wiley Encyclopedia of Biomedical Engineering: John Wiley & Sons, Inc, 2006.
29. Jennings RB. Consequences of Brief Ischemia: stunning, preconditioning, and their clinical implications Part 1. Circulation 2001;104:2981-2989.
30. Sutton MGSJ, Sharpe N. Left Ventricle Remodeling After Myocardial Infarction: Pathophysiology and Therapy. Circulation 2000;101:2981-2988.

31. American Heart Association. Heart and Stroke Facts; 2003.
32. Athanasuleas CL, Buckberg GD, Stanley AWH, Siler W, Dor V, Di Donato M, et al. Surgical ventricular restoration in the treatment of congestive heart failure due to post-infarction ventricular dilation. Journal of the American College of Cardiology 2004;44(7):1439-1445.
33. Hernandez AF, Velazquez EJ, Dullum MK, O'Brien SM, Ferguson TB, Peterson ED. Contemporary performance of surgical ventricular restoration procedures: data from the society of thoracic surgeons' national cardiac database. American Heart Journal 2006;152:494-499.
34. Kochupura P, Azeloglu E, Kelly D, Doronin S, Badylak S, Krukenkamp I, et al. Tissue Engineered Myocardial Patch Derived From Extracellular Matrix Provides Regional Mechanical Function. Circulation 2005;112:144-149.
35. Gaudette GR, Cohen IS. Cardiac Regeneration: Materials Can Improve the Passive Properties of Myocardium, but Cell Therapy Must Do More. Circulation 2006 December 12, 2006;114(24):2575-2577.
36. Schuldt AJ, Rosen MR, Gaudette GR, Cohen IS. Repairing damaged myocardium: evaluating cells used for cardiac regeneration. Current Treatment Options in Cardiovascular Medicine 2008;In Press.
37. Barry F, Murphy JM. Mesenchymal stem cells: clinical applications and biological characterization. The International Journal of Biochemistry and Cell Biology 2004;36:568-584.
38. Tae S-K, Lee S-H, Park J-S, Im G-I. Mesenchymal stem cells for tissue engineering and regenerative medicine. Biomed Mater 2006;1:63-71.
39. Freyman T, Polin G, Osman H, Crary J, Lu M, Cheng L, et al. A quantitative, randomized study evaluating three methods of mesenchymal stem cell delivery following myocardial infarction. European Heart Journal 2006;27:1114-1122.
40. Barbash IM, Chouraqui P, Baron J, Feinberg MS, Etzion S, Tessone A, et al. Systemic Delivery of Bone Marrow-Derived Mesenchymal Stem Cells to the Infarcted Myocardium: Feasibility, Cell Migration, and Body Distribution. Circulation 2003 August 19, 2003;108(7):863-868.
41. Tang J, Xie Q, Pan G, Wang J, Wang M. Mesenchymal stem cells participate in angiogenesis and improve heart function in rat model of myocardial ischemia with reperfusion. European Journal of Cardio-thoracic Surgery 2006;30:353-361.
42. Wolf D, Reinhard A, Katus H, Kuecherer H, Hansen A. Dose-dependent effects of intravenous allogeneic mesenchymal stem cells in the infarcted porcine heart. Stem Cells and Development 2008;In Press.
43. Orlic D, Kajstura J, Chimenti S, Limana F, Jakoniuk I, Quaini F, et al. Mobilized bone marrow cells repair the infarcted heart, improving function and survival. Proc Natl Acad Sci USA 2001;98(18):10344-10349.

44. Amando L. Cardiac repair with intramyocardial injection of allogenic mesenchymal stem cells after myocardial infarction. Proceedings of the National Academy of Sciences of the United States of America 2005;102(32):11474-11479.
45. Muller-Ehmsen J, Whittaker P, Kloner RA, Dow JS, Sakoda T, Long TI, et al. Survival and development of neonatal rat cardiomyocytes transplanted into adult myocardium. J Mol Cell Cardiol 2002;34:107-116.
46. Hou Dea. Radiolabeled Cell Distribution After Intramyocardial, Intracoronary, and Interstitial Retrograde Coronary Venous Delivery. Circulation 2005;112(suppl I):I-150-I-156
47. Widimsky P, Penicka M, Lang O, Kozak T, Motovska Z, Jirmar R, et al. Intracoronary transplatation of bone marrow stem cells: background, techniques, and limitations. European Heart Journal Supplements 2006;8(Supplement H):H16-H22.
48. Zhang G, Hu Q, Braunlin E, Suggs L, Zhang J. Enhancing efficacy of stem cell transplantation to the heart with a PEGylated fibrin biomatrix. Tissue Engineering 2008;14(6):1025-1036.
49. Guo Y, Li Q, Wu W-J, Tan W, Zhu X, Mu J, et al. Endothelial nitric oxide synthase is not necessary for the early phase of ischemic preconditioning in the mouse. Journal of Molecular and Cellular Cardiology 2008;44:496-501.
50. Iwatate M, Gu Y, Dieterle T, Iwanaga Y, Peterson K, Hoshijima M, et al. In vivo high efficiency transcoronary gene delivery and Cre-LoxP gene switching in the adult mouse heart. Gene Therapy 2003;10:1814-1820.
51. Ten Hove M, Chan S, Lygate C, Monfared M, Boehm E, Hulbert K, et al. Mechanisms of creatine depletion in chronically failing rat heart. Journal of Molecular and Cellular Cardiology 2005;38:309-313.
52. Schwartz LM, Lagranha CJ. Ischemic postconditioning during reperfusion activates Akt and ERK without protecting against lethal myocardial ischemia-reperfusion injury in pigs. Am J Physiol Heart Circ Physiol 2006;290:1011-1018.
53. Krause U, Harter C, Seckinger A, Wolf D, Reinhard A, Bea F, et al. Intravenous delivery of autologous mesenchymal stem cells limits infarct size and improves left ventricular function in the infarcted porcine heart. Stem Cells and Development 2007;16:31-37.
54. Davis M, Hsieh P, Grodzinsky A, Lee R. Custom Design of the Cardiac Microenvironment with Biomaterials. Circulation Research 2005;97:8-15.
55. Leor J, Cohen S. Myocardial Tissue Engineering: Creating a Muscle Patch for a Wounded Heart. Ann NY Acad Sci 2004;1015:312-319.
56. Ryu JH, Kim I-K, Cho S-W, Cho M-C, Hwang K-K, Piao H, et al. Implantation of bone marrow mononuclear cells using injectable fibrin matrix enhances neovascularization in infarcted myocardium. Biomaterials 2005;26:319-326.

57. Zimmermann W-H, Melnychenko I, Eschenhagen T. Engineered heart tissue for regeneration of diseased hearts. Biomaterials 2004;25:1639-1647.
58. Park H, Radisic M, Lim JO, Chang BH, Vunjak-Novakovic G. A Novel Composite Scaffold for Cardiac Tissue Engineering. In Vitro Cellular and Development Biology - Animal 2005;41:188-196.
59. Radisic M. Cardiac Tissue Engineering. J Serb Chem Soc 2005;70(3):541-556.
60. Simpson D, Liu H, Fan T-HM, Nerem R, Dudley Jr. SC. A tissue engineering approach to progenitor cell delivery results in significant cell engraftment and improved myocardial remodeling. Stem Cells 2007;25:2350-2357.
61. Akhyari P, Fedak PWM, Weisel RD, Lee T-YJ, Verma S, Mickle DAG, et al. Mechanical Stretch Regimen Enhances the Formation of Bioengineered Autologous Cardiac Muscle Grafts. Circulation 2002 September 24, 2002;106(90121):I-137-142.
62. Rowley JA, Madlambayan G, Mooney DJ. Alginate hydrogels as synthetic extracellular matrix materials. Biomaterials 1999;20(1):45-53.
63. Perets A, Baruch Y, Weisbuch F, Shoshany G, Neufeld G, Cohen S. Enhancing the vascularization of three dimensional porous alginate scaffolds by incorporating controlled release basic fibroblast growth factor microspheres. Journal of Biomedical Materials Research Part A 2002;65A(4):489-497.
64. Stevens M. A rapid-curing alginate gel system: utility in periosteum-derived cartilage tissue engineering. Biomaterials 2004;25:887-894.
65. Drury JL, Mooney DJ. Hydrogels for Tissue Engineering: Scaffold Design Variables and Applications. Biomaterials 2003;24:4337-4351.
66. Ponticiello M. Gelatin based resorbable sponge as a carrier matrix for human mesenchymal stem cells in cartilage regeneration therapy. Journal of Biomedical Materials Research 2000;52(2):246-255.
67. Li RK, Jia ZQ, Weisel RD, Mickle D, Choi A, Yau T. Survival and Function of Bioengineered Cardiac Grafts. Circulation 1999;100(II):63-69.
68. Eschenhagen T, Fink C, Remmers U, Scholz H, Wattchow J, Weil J, et al. Three dimensional reconsitution of embryonic cardiomyocytes in a collagen matrix: a new heart muscle model system. The Federation of American Societies for Experimental Biology Journal 1997;11:683-694.
69. Kofidis T, Akhyari P, Wachsmann B, Boublik J, Mueller-Stahl K, Leyh R, et al. A Novel Bioartificial Myocardial Tissue and its Prospective use in Cardiac Surgery. European Journal of Cardio-thoracic Surgery 2002;22:238-243.
70. Chevallay B. Collagen based biomaterials as 3-D scaffold for cell cultures: applications for tissue engineering and gene therapy. Med Biol Eng Comput 2000;38:211-218.
71. Cox S, Cole M, Tawil B. Fibrin Clots: Dependence on Fibrinogen and Thrombin Concentration. Tissue Engineering 2004;10(5/6):942-954.

72. Ratner BD, Hoffman AS, Schoen FJ, Lemons JE. Biomaterials science: an introduction to materials in medicine. 2nd ed. San Diego, CA: Elsevier Academic Press, 2004.
73. Mol A. Fibrin as a cell carrier in cardiovascular tissue engineering. Biomaterials 2005;26:3113-3121.
74. Cornwell K. Collagen and Fibrin Biopolymer Microthreads for Bioengineered Ligament Generation. Doctoral Dissertation, University of Massachusetts Medical School Graduate School of Biomedical Sciences 2007.
75. Jones LJ, Gray M, Yue ST, Haugland RP, Singer VL. Sensitive determination of cell number using the CyQuant cell proliferation assay. Journal of Immunological Methods 2001;254:85-98.
76. Myers MA. Direct measurement of cell numbers in microtitre plate cultures using the fluorescent dye SYBR green I. Journal of Immunological Methods 1998;212:99-103.
77. Blaheta R, Franz M, Auth M, HJC W, Markus B. A rapid non radioactive fluorescence assay for the measurement of both cell number and proliferation. Journal of Immunological Methods 1991;142:199-206.
78. Bruder SP, Jaiswal N, Haynesworth SE. Growth Kinetics, Self-Renewal, and the Osteogenic Potential of Purified Human Mesenchymal Stem Cells During Extensive Subcultivation and Following Cryopreservation. Journal of Cellular Biochemistry 1997;64:278-294.
79. Krasna M, Planinsek F, Knezevic M, Arnez ZM, Jeras M. Evaluation of a fibrin based skin substitute prepared in a defined keratinocyte medium. International Journal of Pharmaceutics 2005;291:31-37.
80. Krahn KN, Bouten CV, Tuijl Sv, van Zandvoort MA, Merkx M. Fluorescently labeled collagen binding proteins allow specific visualization of collagen in tissues and live cell culture. Analytical Biochemistry 2006;350:177-185.
81. Jayasankar V, Woo YJ, Pirolli TJ, Bish LT, Berry MF, Burdick J, et al. Induction of angiogenesis and inhibition of apoptosis by hepatocyte growth factor effectively treats postischemic heart failure. J Card Surg 2005;20:93-101.
82. Catelas I, Sese N, Wu B, Dunn J, Helgerson S, Tawil B. Human mesenchymal stem cell proliferation and osteogenic differentiation in fibrin gels in vitro. Tissue Engineering 2006;12(8).
83. Gerard C, Blouin K, Tchernof A, Doillon CJ. Adipogenesis in Nonadherent and Adherent Bone Marrow Stem Cells Grown in Fibrin Gel and in the Presence of Adult Plasma. Cells Tissues Organs 2008;187(3):186-198.
84. Kawaguchi N, Toriyama K, Nicodemou-Lena E, Inou K, Torii S, Kitagawa Y. De novo adipogenesis in mice at the site of injection of basement membrane and basic fibroblast growth factor. Proc Natl Acad Sci USA 1998;95:1062-1066.

85. Schoeller T, Lille S, Wechselberger G, Otto A, Mowlawi A, Piza-Katzer H. Histomorphologic and volumetric analysis of implanted autologous preadipocye cultures suspended in fibrin glue. Aesthetic Plastic Surgery 2001;25:57-63.
86. Patrick Jr CW. Tissue engineering strategies for adipose tissue repair. The Anatomical Record 2001;263:361-366.
87. Cronin KJ, Messina A, Thompson EW, Morrison WA, Stevens GW, Knight KR. The role of biological extracellular matrix scaffolds in vascularized three dimensional tissue growth in vivo. J Biomed Mater Res Part B: Appl Biomater 2007;82B:122-128.
88. Barry F, Boynton RE, Liu B, Murphy JM. Chondrogenic differentiation of mesenchymal stem cells from bone marrow: differentiation dependant gene expression of matrix components. Experimental Cell Research 2001;268:189-200.
89. Davani S, Marandin A, Mersin N, Royer B, Kantelip B, Herve P, et al. Mesenchymal progenitor cells differentiate into an endothelial phenotype, enhance vascular density, and improve heart function in a rat cellular cardiomyoplasty model. Circulation 2003;108:II-253-II-258.
90. Wall ST, Walker JC, Healy KE, Ratcliffe MB, Guccione J. Theoretical impact of the injection of material into the myocardium: a finite element model simulation. Circulation 2006;114(2627-2635).
91. Kajstura J, Rota M, Whang B, Cascapera S, Hosoda T, Bearzi C, et al. Bone marrow cells differentiate in cardiac cell lineages after infarction independently of cell fusion. Circulation Research 2005;96:127-137.
92. Uemura R, Xu M, Ahmand n, Ashraf M. Bone marrow stem cells prevent left ventricular remodeling of ischemic heart through paracrine signaling. Circulation Research 2006;98:1414-1421.
93. Wollert KC, Drexler H. Mesenchymal stem cells for myocardial infarction: promises and pitfalls. Circulation 2005;112:151-153.
94. Rovensky YA, Samoilov VI. Morphogenic response of cultured normal and transformed fibroblasts, and epitheliocytes to a cylindrical substratum surface. Journal of Cell Science 1994;107:1255-1263.
95. Gang EJ, Bosnakovski D, Simsek T, To K, Perlingeiro RC. Pax3 activation promotes the differentiation of mesenchymal stem cells toward the myogenic lineage. Experimental Cell Research 2008;314:1721-1733.

Appendix A: Measurement of Cell Area

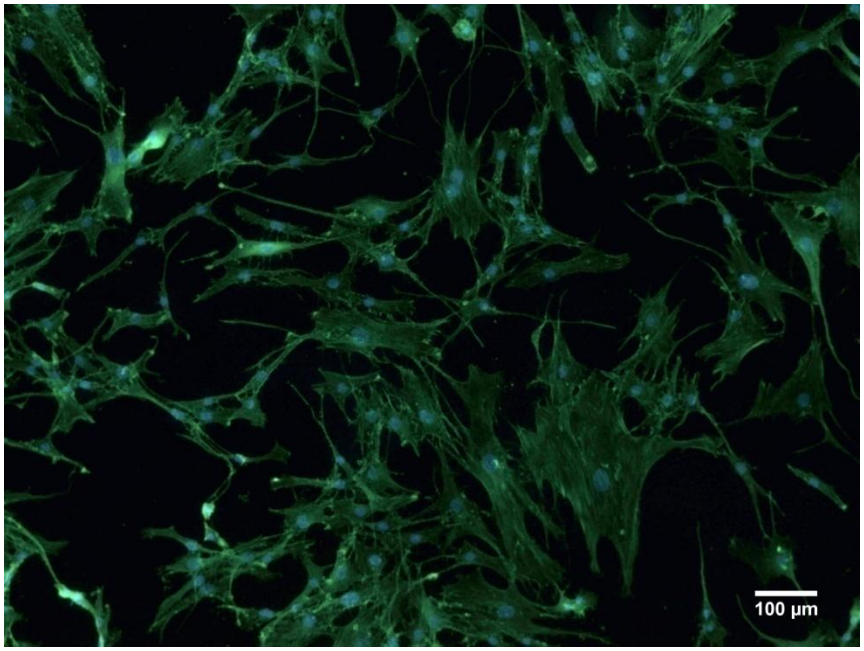

hMSC Area (pixels^2)
12189
24189
19732
6599
7809
11145
21380
19571
11115
5560
35002
12604
10428
54601
8569
42720
15486
18462
9171
8772

	Average	Stdev
hMSC Area (pixels^2)	17755	12887
Pixels^2/um^2	14.1	
Average hMSC Area (um^2)	1255	911

Appendix B: Cell Attachment Counts

Summary of counts: average and standard error of mean

Bundle of 4 EXP1				Bundles of 4 EXP2		
5h	Cells/mm	Cells/mm2		5h	Cells/mm	Cells/mm2
slide 1	38.47518	101.6026		slide 1	16.89665	54.07025
slide 2	30.56596	65.79344		slide 2	17.30985	40.40646
slide 3	48.18168	176.1056		slide 3	73.14241	118.6572
SEM	5.094034	32.49083		SEM	18.6801	24.13084
Avg	39.07427	114.5005		Avg	35.78297	71.04464
1 day	Cells/mm	Cells/mm2		1 day	Cells/mm	Cells/mm2
slide 1	57.57516	236.3595		slide 1	86.53155	217.9929
slide 2	127.1818	375.2458		slide 2	272.8309	455.0261
slide 3	54.73251	163.7388		slide 3	32.41627	71.52234
SEM	23.6902	62.04765		SEM	72.8145	111.7322
Avg	79.82982	258.4481		Avg	130.5929	248.1805
2 day	Cells/mm	Cells/mm2		2 day	Cells/mm	Cells/mm2
slide 1	88.85961	227.2843		slide 1	242.0238	569.2331
slide 2	56.56934	176.0828		slide 2	32.96182	85.92396
slide 3	86.52021	265.8301		slide 3	207.1453	570.776
SEM	10.39548	25.99353		SEM	64.66293	161.3608
Avg	72.71448	201.6835		Avg	137.4928	327.5785
3 day	Cells/mm	Cells/mm2		3 day	Cells/mm	Cells/mm2
slide 1	227.8468	658.5979		slide 1	197.5338	622.6984
slide 2	186.7754	700.3155		slide 2	147.5344	447.4031
slide 3	200.7821	486.0349		slide 3	196.5623	412.3011
SEM	12.05439	65.589		SEM	16.50695	65.07583
Avg	207.3111	679.4567		Avg	172.5341	535.0508
4 day	Cells/mm	Cells/mm2		4 day	Cells/mm	Cells/mm2
slide 1	369.1283	832.6093		slide 1	350.1025	752.9059
slide 2	144.1597	413.1605		slide 2	287.8568	657.5484
slide 3	254.6065	717.9605		slide 3	140.6223	319.0781
SEM	64.94638	125.1632		SEM	62.10857	131.627
Avg	256.644	622.8849		Avg	318.9797	705.2271
5 day	Cells/mm	Cells/mm2		5 day	Cells/mm	Cells/mm2
slide 1	262.5418	837.8298		slide 1	454.2129	783.4643
slide 2	110.8269	297.8002		slide 2	283.5794	602.7357
slide 3	300.6728	1002.742		slide 3	476.5664	858.9071
SEM	57.98127	212.8864		SEM	60.94598	76.00374
Avg	186.6843	567.815		Avg	368.8961	693.1

Bundle of 4 EXP1: P6 and 7 hMSCs								Total		
5h	Picture #	Mag	Area (um2)	Length (um)	# Cells	cells/mm	cells/mm2	Cells	Length	Cells/mm
slide 1	1	20x	294251.217	679	6	8.8	20.3907398	217	5640	38.47518
	2	20x	291347.541	679	19	28.0	65.214211			
	3	20x	311425.56	722	29	40.2	93.1201665			Cells/mm2
	4	20x	294709.286	714	55	77.0	186.624591			101.6026
	5	20x	258259.393	723	66	91.3	255.557017			
	6	20x	215465.85	748	13	17.4	60.3343871			
	7	20x	219882.017	695	27	38.8	122.793125			
	8	20x	227629.866	680	2	2.9	8.78619328			
								Total		
5h	Picture #	Mag	Area (um2)	Length	# Cells	cells/mm	cells/mm2	Cells	Length	Cells/mm
slide 2	1	20x	153745.19	514	1	1.9	6.50426852	155	5071	30.56596
	2	20x	199416.096	507	12	23.7	60.1756841			Cells/mm2
	3	20x	226963.841	509	5	9.8	22.0299409			65.79344
	4	20x	230863.937	508	15	29.5	64.9733354			
	5	20x	248514.175	511	25	48.9	100.597883			
	6	20x	243401.921	504	23	45.6	94.4939132			
	7	20x	246942.763	500	24	48.0	97.1885133			
	8	20x	246942.763	506	20	39.5	80.9904277			
	9	20x	222976.248	508	10	19.7	44.8478261			
	10	20x	232200.232	504	20	39.7	86.1325582			
								Total		
5h	Picture #	Mag	Area (um2)	Length	# Cells	cells/mm	cells/mm2	Cells	Length	Cells/mm
slide 3	1	20x	203367.05	644	32	49.7	157.350957	314	6517	48.18168
	2	20x	166392.669	678	35	51.6	210.345806			cells/mm2
	3	20x	189412.842	732	44	60.1	232.296815			176.1056
	4	20x	192417.171	730	54	74.0	280.640235			
	5	20x	170727.988	755	21	27.8	123.00268			
	6	20x	160431.474	760	29	38.2	180.762535			
	7	20x	213879.584	715	31	43.4	144.94137			
	8	20x	264218.043	750	38	50.7	143.82061			
	9	20x	268361.603	753	30	39.8	111.789465			
								Total		
1 Day	Picture #	Mag	Area (um2)	Length	# Cells	cells/mm	cells/mm2	Cells	Length	Cells/mm
slide 1	1	10x	254265.811	1455	45	30.9	176.980145	586	10178	57.57516
	2	10x	311823.91	1435	64	44.6	205.244043			
	3	10x	362271.361	1439	133	92.4	367.12811			cells/mm2
	4	10x	403143.427	1481	164	110.7	406.80311			236.3595
	5	10x	346049.832	1495	101	67.6	291.865479			
	6	10x	390712.221	1456	59	40.5	151.006282			
	7	10x	360428.084	1417	20	14.1	55.4895717			
								Total		
1 Day	Picture #	Mag	Area (um2)	Length	# Cells	cells/mm	cells/mm2	Cells	Length	Cells/mm
slide 2	1	10x	284804.891	1394	92	66.0	323.02816	1246	9797	127.1818
	2	10x	406217.482	1374	274	199.4	674.51553			cells/mm2
	3	10x	493783.674	1415	347	245.2	702.736883			375.2458
	4	10x	550053.763	1429	307	214.8	558.127261			
	5	10x	614580.587	1412	197	139.5	320.543805			
	6	10x	607085.79	1391	25	18.0	41.1803412			
	7	10x	607085.79	1382	4	2.9	6.5888546			

								Total		
1 Day	Picture #	Mag	Area (um2)	Length	# Cells	cells/mm	cells/mm2	Cells	Length	Cells/mm
slide 3	1	10x	572062.088	1424	51	35.8	89.1511622	532	9720	54.73251
	2	10x	488479.593	1386	73	52.7	149.443295			cells/mm2
	3	10x	507182.622	1369	126	92.0	248.431225			163.7
	4	10x	460011.851	1412	96	68.0	208.690276			
	5	10x	422499.133	1378	60	43.5	142.012126			
	6	10x	398442.016	1379	83	60.2	208.311364			
	7	10x	429432.304	1372	43	31.3	100.132197			
								Total		
2 Day	Picture #	Mag	Area (um2)	Length	# Cells	cells/mm	cells/mm2	Cells	Length	Cells/mm
slide 1	1	20x	280198.549	682	39	57.2	139.187016	607	6831	88.85961
	2	20x	339067.381	679	43	63.3	126.818451			cells/mm2
	3	20x	339067.381	679	72	106.0	212.347174			227.2843
	4	20x	339067.381	679	64	94.3	188.753043			
	5	20x	339067.381	679	64	94.3	188.753043			
	6	20x	270391.58	672	64	95.2	236.693761			
	7	20x	215265.533	682	78	114.4	362.34319			
	8	20x	204517.811	687	73	106.3	356.937128			
	9	20x	232964.152	698	68	97.4	291.890402			
	10	20x	248344.981	694	42	60.5	169.119585			
								Total		
2 Day	Picture #	Mag	Area (um2)	Length	# Cells	cells/mm	cells/mm2	Cells	Length	Cells/mm
slide 2	1	20x	285193.031	690	30	43.5	105.191911	310	5480	56.56934
	2	20x	208625.792	694	30	43.2	143.798136			cells/mm2
	3	20x	229319.899	697	38	54.5	165.707382			176.0828
	5	20x	293787.489	683	46	67.3	156.575762			
	6	20x	144148.724	686	35	51.0	242.804785			
	7	20x	208720.999	680	41	60.3	196.434476			
	8	20x	211169.718	680	46	67.6	217.834264			
	9	20x	244016.382	670	44	65.7	180.315763			
								Total		
2 Day	Picture #	Mag	Area (um2)	Length	# Cells	cells/mm	cells/mm2	Cells	Length	Cells/mm
slide 3	1	10x	455877.847	1399	78	55.8	171.098465	957	11061	86.52021
	2	10x	463226.385	1406	192	136.6	414.484162			cells/mm2
	3	10x	454440.398	1376	170	123.5	374.086461			265.8301
	4	10x	415705.862	1376	161	117.0	387.293071			
	5	10x	473802.752	1376	144	104.7	303.923942			
	6	10x	457658.111	1376	119	86.5	260.019427			
	7	10x	435424.327	1376	67	48.7	153.872891			
	8	10x	420287.316	1376	26	18.9	61.8624427			
								Total		
3 Day	Picture #	Mag	Area (um2)	Length	# Cells	cells/mm	cells/mm2	Cells	Length	Cells/mm
slide 1	0	10x	453695.225	1380	118	85.5	260.086493	2201	9660	227.8468
	1	10x	463917.216	1380	304	220.3	655.289326			cells/mm2
	2	10x	509948.549	1380	449	325.4	880.480984			658.5979
	3	10x	489614.695	1380	467	338.4	953.811241			
	4	10x	464253.671	1380	446	323.2	960.681687			
	5	10x	490734.189	1380	296	214.5	603.177864			
	6	10x	407877.789	1380	121	87.7	296.657487			
								Total		

3 Day	Picture #	Mag	Area (um2)	Length	# Cells	cells/mm	cells/mm2	Cells	Length	Cells/mm
slide 2	0	10x	443907.966	1380	79	57.2	177.964817	2062	11040	186.7754
	1	10x	444348.769	1380	263	190.6	591.877413			Cells/mm2
	2	10x	338906.232	1380	335	242.8	988.474004			700.3155
	3	10x	390678.113	1380	405	293.5	1036.65905			
	4	10x	358381.894	1380	337	244.2	940.337683			
	5	10x	326791.537	1380	325	235.5	994.517799			
	6	10x	366435.426	1380	250	181.2	682.248446			
	7	10x	357059.198	1380	68	49.3	190.444611			
								Total		
3 Day	Picture #	Mag	Area (um2)	Length	# Cells	cells/mm	cells/mm2	Cells	Length	Cells/mm
slide 3	1	10x	440459.591	1386	50	36.1	113.517791	3132	15599	200.7821
	2	10x	525012.14	1393	111	79.7	211.423683			Cells/mm2
	3	10x	432110.649	1386	78	56.3	180.509321			486.0349
	4	10x	508060.758	1455	93	63.9	183.048973			
	5	10x	508894.67	1386	298	215.0	585.582867			
	6	10x	522932.131	1404	409	291.3	782.128264			
	7	10x	615468.84	1450	494	340.7	802.640147			
	8	10x	609031.102	1398	510	364.8	837.395657			
	9	10x	650136.432	1450	503	346.9	773.683761			
	10	10x	676063.707	1450	483	333.1	714.429713			
	11	10x	635709.331	1441	103	71.5	162.023735			
								Total		
4 Day	Picture #	Mag	Area (um2)	Length	# Cells	cells/mm	cells/mm2	Cells	Length	Cells/mm
slide 1	0	10x	520041.045	1380	101	73.2	194.215439	6648	18010	369.1283
old	1	10x	572961.614	1380	287	208.0	500.906157			Cells/mm2
	2	10x	586835.472	1380	502	363.8	855.435678			832.6093
	3	10x	578995.26	1380	647	468.8	1117.45302			
	4	10x	605117.355	1380	759	550.0	1254.30215			
	5	10x	648948.433	1380	872	631.9	1343.71231			
	6	10x	677565.036	1380	855	619.6	1261.87149			
	7	10x	646244.653	1380	800	579.7	1237.92127			
	8	10x	577288.704	1380	633	458.7	1096.50509			
	9	10x	606079.894	1410	456	323.4	752.376056			
	10	10x	668796.971	1420	398	280.3	595.098389			
	11	10x	582931.553	1380	255	184.8	437.444154			
	12	10x	469778.009	1380	83	60.1	176.679194			
								Total		
4 Day	Picture #	Mag	Area (um2)	Length	# Cells	cells/mm	cells/mm2	Cells	Length	Cells/mm
slide 2	0	10x	403379.581	1380	45	32.6	111.557456	2419	16780	144.1597
old	1	10x	425882.761	1380	140	101.4	328.728967			Cells/mm2
	2	10x	398288.82	1380	138	100.0	346.482234			413.1605
	3	10x	399096.427	1380	205	148.6	513.660324			
	4	10x	415787.374	1380	282	204.3	678.231273			
	5	10x	489953.752	1390	292	210.1	595.974618			
	6	10x	513879.061	1430	280	195.8	544.875285			
	7	10x	551923.922	1420	360	253.5	652.26381			
	8	10x	583819.517	1410	316	224.1	541.263166			
	9	10x	560582.437	1420	230	162.0	410.28756			
	10	10x	551621.286	1410	96	68.1	174.032443			
	11	10x	577857.556	1400	35	25.0	60.5685599			
								Total		

4 Day	Picture #	Mag	Area (um2)	Length	# Cells	cells/mm	cells/mm2	Cells	Length	Cells/mm
slide 3	1	10x	600474.043	1397	107	76.6	178.192548	3565	14002	254.6065
18-Jan	2	10x	470249.451	1376	227	165.0	482.72252			Cells/mm2
	3	10x	446011.678	1376	356	258.7	798.185378			717.9605
	4	10x	463998.728	1421	442	311.0	952.588818			
	5	10x	554956.064	1376	725	526.9	1306.40973			
	6	10x	550772.344	1406	716	509.2	1299.99265			
	7	10x	481793.56	1488	524	352.2	1087.60275			
	8	10x	456053.301	1410	284	201.4	622.734227			
	9	10x	409962.423	1376	128	93.0	312.223738			
	10	10x	403014.799	1376	56	40.7	138.952714			
								Total		
5 Day	Picture #	Mag	Area (um2)	Length	# Cells	cells/mm	cells/mm2	Cells	Length	Cells/mm
slide 1	1	10x	398038.791	1557	71	45.6	178.374575	3454	13156	262.5418
	2	10x	406542.953	1427	222	155.6	546.067761			Cells/mm2
	3	10x	425436.467	1444	390	270.1	916.705619			837.8298
	4	10x	509410.915	1503	596	396.5	1169.97886			
	5	10x	526288.299	1514	875	577.9	1662.58684			
	6	10x	430751.243	1389	630	453.6	1462.56107			
	7	10x	410313.331	1417	392	276.6	955.367448			
	8	10x	422855.243	1416	220	155.4	520.272608			
	9	10x	451174.124	1489	58	39.0	128.553472			
								Total		
5 Day	Picture #	Mag	Area (um2)	Length	# Cells	cells/mm	cells/mm2	Cells	Length	Cells/mm
slide 2	1	10x	604019.251	1376	117	85.0	193.702435	1083	9772	110.8269
	2	10x	444570.471	1424	200	140.4	449.872434			Cells/mm2
	3	10x	476818.707	1376	222	161.3	465.58576			297.8002
	4	10x	543339.114	1431	181	126.5	333.12529			
	5	10x	591805.411	1533	178	116.1	300.77454			
	6	10x	544376.228	1256	115	91.6	211.250959			
	7	10x	537264.424	1376	70	50.9	130.289662			
								Total		
5 Day	Picture #	Mag	Area (um2)	Length	# Cells	cells/mm	cells/mm2	Cells	Length	Cells/mm
slide 3	1	10x	397146.491	1413	141	99.8	355.032723	4290	14268	300.6728
	2	10x	407218.754	1443	300	207.9	736.704774			Cells/mm2
	3	10x	374234.015	1376	404	293.6	1079.53843			1002.742
	4	10x	370927.275	1385	488	352.3	1315.62178			
	5	10x	376344.953	1528	674	441.1	1790.91016			
	6	10x	471829.691	1376	774	562.5	1640.42241			
	7	10x	520557.001	1539	673	437.3	1292.84593			
	8	10x	441580.24	1439	421	292.6	953.39411			
	9	10x	482880.102	1393	303	217.5	627.484957			
	10	10x	475656.145	1376	112	81.4	235.464213			

Bundle of 4 EXP2: P7 hMSCs

								Total		
5h	Picture #	Mag	Area (um2)	Length (um)	# Cells	cells/mm	cells/mm2	Cells	Length	Cells/mm
slide 4	1	10x	459756.041	1433	45	31.4	97.87799613	120	7102	16.89665
	2	10x	413210.776	1378	23	16.7	55.66166551			Cells/mm2
	3	10x	448468.32	1394	42	30.1	93.65210011			54.07025
	4	10x	431788.068	1445	5	3.5	11.57975491			
	5	10x	431788.068	1452	5	3.4	11.57975491			
								Total		
5h	Picture #	Mag	Area (um2)	Length	# Cells	cells/mm	cells/mm2	Cells	Length	Cells/mm
slide 5	1	10x	431788.068	1374	1	0.7	2.315950982	170	9821	17.30985
	2	10x	595152.041	1375	9	6.5	15.12218623			Cells/mm2
	3	10x	498598.393	1376	42	30.5	84.2361319			40.40646
	4	10x	638338.536	1382	38	27.5	59.52954092			
	5	10x	661510.579	1405	34	24.2	51.39751514			
	6	10x	660638.802	1437	44	30.6	66.6022036			
	7	10x	549191.236	1472	2	1.4	3.641718711			
								Total		
5h	Picture #	Mag	Area (um2)	Length	# Cells	cells/mm	cells/mm2	Cells	Length	Cells/mm
slide 6	1	10x	594979.766	1493	21	14.1	35.29531793	756	10336	73.14241
	2	10x	841905.134	1454	104	71.5	123.5293572			Cells/mm2
	3	10x	986395.248	1430	242	169.2	245.3377594			118.6572
	4	10x	947011.215	1449	203	140.1	214.3586019			
	5	10x	889429.125	1462	130	88.9	146.1611683			
	6	10x	849019.829	1524	54	35.4	63.6027548			
	7	10x	863730.778	1524	2	1.3	2.315536335			
								Total		
1 Day	Picture #	Mag	Area (um2)	Length	# Cells	cells/mm	cells/mm2	Cells	Length	Cells/mm
slide 4	1	10x	695109.839	1415	106	74.9	152.4938852	602	6957	86.53155
	2	10x	647520.523	1400	157	112.1	242.4633574			Cells/mm2
	3	10x	528463.984	1383	161	116.4	304.6565232			217.9929
	4	10x	416056.191	1381	111	80.4	266.7908864			
	5	10x	542246.792	1378	67	48.6	123.5599749			
								Total		

1 Day	Picture #	Mag	Area (um2)	Length	# Cells	cells/mm	cells/mm2	Cells	Length	Cells/mm
slide 5	1	10x	734105.966	1379	134	97.2	182.5349557	2632	9647	272.8309
	2	10x	803124.061	1377	475	345.0	591.4403802			Cells/mm2
	3	10x	843084.75	1374	427	310.8	506.4734002			455.0261
	4	10x	816049.832	1374	463	337.0	567.3673124			
	5	10x	800555.556	1372	597	435.1	745.7321301			
	6	10x	871938.952	1382	426	308.2	488.5663142			
	7	10x	1067251.127	1389	110	79.2	103.0685255			
								Total		
1 Day	Picture #	Mag	Area (um2)	Length	# Cells	cells/mm	cells/mm2	Cells	Length	Cells/mm
slide 6	1	10x	478798.705	1404	32	22.8	66.83393181	271	8360	32.41627
	2	10x	588892.936	1394	30	21.5	50.94304612			Cells/mm2
	3	10x	642848.306	1395	31	22.2	48.2228851			71.52234
	4	10x	680076.888	1389	43	31.0	63.22814487			
	5	10x	680076.888	1390	114	82.0	167.628105			
	6	10x	650599.491	1388	21	15.1	32.27792258			
								Total		
2 Day	Picture #	Mag	Area (um2)	Length	# Cells	cells/mm	cells/mm2	Cells	Length	Cells/mm
slide 4	1	10x	548981.385	1441	109	75.6	198.5495373	3095	12788	242.0238
	2	10x	620574.055	1447	350	241.9	563.9939298			Cells/mm2
	3	10x	594954.33	1443	620	429.7	1042.096794			569.2331
	4	10x	708530.466	1420	421	296.5	594.1875758			
	5	10x	592675.165	1395	405	290.3	683.3422824			
	6	10x	594150.191	1436	522	363.5	878.5657363			
	7	10x	610188.461	1421	426	299.8	698.1449621			
	8	10x	529928.894	1409	204	144.8	384.9573071			
	9	10x	479433.75	1376	38	27.6	79.2601689			
								Total		
2 Day	Picture #	Mag	Area (um2)	Length	# Cells	cells/mm	cells/mm2	Cells	Length	Cells/mm
slide 5	1	10x	666699.04	1540	56	36.4	83.99592116	278	8434	32.96182
	2	10x	495053.763	1372	136	99.1	274.7176371			Cells/mm2
	3	10x	411688.635	1380	24	17.4	58.29648419			85.92396
	4	10x	577970.286	1391	15	10.8	25.95289129			
	5	10x	680311.019	1377	15	10.9	22.04873886			
	6	10x	633261.36	1374	32	23.3	50.53205836			
								Total		

2 Day	Picture #	Mag	Area (um2)	Length	# Cells	cells/mm	cells/mm2	Cells	Length	Cells/mm
slide 6	1	10x	621383.397	1424	32	22.5	51.49799649	2383	11504	207.1453
	2	10x	620325.471	1402	84	59.9	135.4127856			Cells/mm2
	3	10x	520879.003	1413	238	168.4	456.9199346			570.776
	4	10x	531843.566	1466	1145	781.0	2152.888694			
	5	10x	535886.808	1545	443	286.7	826.6671121			
	6	10x	436822.754	1504	317	210.8	725.6947975			
	7	10x	546841.253	1374	104	75.7	190.1831645			
	8	10x	742286.681	1376	20	14.5	26.94376784			
								Total		
3 Day	Picture #	Mag	Area (um2)	Length	# Cells	cells/mm	cells/mm2	Cells	Length	Cells/mm
slide 4	1	10x	518822.407	1441	178	123.5	343.0846424	3235	13526	239.169
	2	10x	579489.536	1421	494	347.6	852.4744095			Cells/mm2
	3	10x	580459.013	1376	651	473.1	1121.526215			622.6984
	4	10x	592623.425	1547	683	441.5	1152.502536			
	5	10x	570864.84	1630	542	332.5	949.4366477			
	6	10x	579527.402	1528	379	248.0	653.9811555			
	7	10x	574634.64	1437	126	87.7	219.2697607			
	8	10x	558491.733	1456	123	84.5	220.2360263	Total		
	9	10x	642884.148	1690	59	34.9	91.77392254			
3 Day	Picture #	Mag	Area (um2)	Length	# Cells	cells/mm	cells/mm2	Cells	Length	Cells/mm
slide 5	1	10x	548284.195	1397	86	61.6	156.852962	1834	12431	147.5344
	2	10x	440929.009	1375	177	128.7	401.4251646			Cells/mm2
	3	10x	430457.856	1376	393	285.6	912.9813628			447.4031
	4	10x	508272.633	1376	498	361.9	979.7891282			
	5	10x	475250.896	1375	369	268.4	776.4319923			
	6	10x	382837.322	1378	192	139.3	501.5185014			
	7	10x	401199.561	1379	65	47.1	162.0141354			
	8	10x	384120.997	1389	36	25.9	93.72046902			
	9	10x	429650.249	1386	18	13.0	41.89454106			
3 Day	Picture #	Mag	Area (um2)	Length	# Cells	cells/mm	cells/mm2	Cells	Length	Cells/mm
slide 6	1	10x	734089.49	1406	57	40.5	77.64720893	2493	12683	196.5623
	2	10x	750198.578	1412	203	143.8	270.595021			Cells/mm2
	3	10x	719980.923	1408	324	230.1	450.0119234			412.3011
	4	10x	668119.147	1401	445	317.6	666.0488657			
	5	10x	664143.254	1397	473	338.6	712.1957456			
	6	10x	681953.983	1405	292	207.8	428.1813836			
	7	10x	675551.509	1412	216	153.0	319.7387573			
	8	10x	647053.417	1436	318	221.4	491.4586519			
	9	10x	559639.265	1406	165	117.4	294.8327795			

4 Day	Picture #	Mag	Area (um2)	Length	# Cells	cells/mm	cells/mm2	Cells	Length	Cells/mm
slide 4	1	10x	666582.264	1376	55	40.0	82.51044615	5804	16578	350.1025
	2	10x	635588.507	1378	208	150.9	327.2557601			Cells/mm2
	3	10x	662530.061	1385	344	248.4	519.2217233			752.9059
	4	10x	650895.479	1381	482	349.0	740.5182791			
	5	10x	559564.69	1382	562	406.7	1004.352151			
	6	10x	581632.559	1385	667	481.6	1146.772115			
	7	10x	611911.204	1385	667	481.6	1090.027435			
	8	10x	641527.055	1378	759	550.8	1183.114561			
	9	10x	702819.401	1383	826	597.3	1175.266361			
	10	10x	707514.163	1379	787	570.7	1112.345224			
	11	10x	681942.999	1384	355	256.5	520.5713682			
	12	10x	692171.349	1382	92	66.6	132.9150652			
								Total		
4 Day	Picture #	Mag	Area (um2)	Length	# Cells	cells/mm	cells/mm2	Cells	Length	Cells/mm
slide 5	1	10x	573624.118	1408	143	101.6	249.292168	4165	14469	287.8568
	2	10x	588637.415	1615	94	58.2	159.6908345			Cells/mm2
	3	10x	629584.923	1379	386	279.9	613.1023566			657.5484
	4	10x	629450.804	1377	469	340.6	745.0939724			
	5	10x	599387.79	1376	630	457.8	1051.072462			
	6	10x	636400.162	1372	745	543.0	1170.647094			
	7	10x	646372.991	1499	662	441.6	1024.176457			
	8	10x	662409.816	1520	530	348.7	800.1089163			
	9	10x	648021.448	1538	294	191.2	453.6886872			
	10	10x	686949.358	1385	212	153.1	308.6108132			
								Total		
4 Day	Picture #	Mag	Area (um2)	Length	# Cells	cells/mm	cells/mm2	Cells	Length	Cells/mm
slide 6	1	10x	703084.75	1412	63	44.6	89.6051294	1600	11378	140.6223
	2	10x	581179.616	1378	95	68.9	163.4606538			Cells/mm2
	3	10x	498908.544	1407	71	50.5	142.3106516			319.0781
	4	10x	611610.013	1525	138	90.5	225.6339776			
	5	10x	569845.358	1492	308	206.4	540.4975151			
	6	10x	636607.989	1382	406	293.8	637.7551131			
	7	10x	664924.847	1390	329	236.7	494.7927596			
	8	10x	734814.429	1392	190	136.5	258.5686841			
								Total		

5 Day	Picture #	Mag	Area (um2)	Length	# Cells	cells/mm	cells/mm2	Cells	Length	Cells/mm
slide 4	1	10x	734276.217	1589	157	98.8	213.8159951	8070	17767	454.2129
	2	10x	808599.549	1713	525	306.5	649.2707059			Cells/mm2
	3	10x	862291.305	1690	791	468.0	917.3234096			783.4643
	4	10x	964448.202	1494	965	645.9	1000.572139			
	5	10x	910894.612	1393	1142	819.8	1253.712543			
	6	10x	874153.659	1418	1084	764.5	1240.056584			
	7	10x	823701.006	1408	960	681.8	1165.471443			
	8	10x	850135.276	1409	868	616.0	1021.013978			
	9	10x	802706.671	1383	846	611.7	1053.934184			
	10	10x	818347.208	1376	456	331.4	557.220695			
	11	10x	826360.273	1379	232	168.2	280.7492175			
	12	10x	908507.053	1515	44	29.0	48.43110447			
								Total		
5 Day	Picture #	Mag	Area (um2)	Length	# Cells	cells/mm	cells/mm2	Cells	Length	Cells/mm
slide 5	1	10x	754539.542	1376	95	69.0	125.904601	4725	16662	283.5794
	2	10x	699287.779	1383	320	231.4	457.6084548			Cells/mm2
	3	10x	640268.239	1375	458	333.1	715.3251904			602.7357
	4	10x	651579.373	1380	530	384.1	813.4081924			
	5	10x	701004.451	1376	764	555.2	1089.864692			
	6	10x	689902.879	1375	827	601.5	1198.71945			
	7	10x	641115.736	1388	651	469.0	1015.417285			
	8	10x	615337.033	1390	410	295.0	666.3015193			
	9	10x	590108.105	1389	260	187.2	440.597236			
	10	10x	639843.624	1387	182	131.2	284.4445005			
	11	10x	528859.117	1389	174	125.3	329.0101171			
	12	10x	561171.523	1454	54	37.1	96.22726348			
								Total		
5 Day	Picture #	Mag	Area (um2)	Length	# Cells	cells/mm	cells/mm2	Cells	Length	Cells/mm
slide 6	1	10x	645034.397	1487	128	86.1	198.4390299	7667	16088	476.5664
	2	10x	723731.356	1400	295	210.7	407.6098093			Cells/mm2
	3	10x	785506.995	1571	366	233.0	465.9411085			858.9071
	4	10x	831215.747	1401	769	548.9	925.1509043			
	5	10x	907150.827	1642	991	603.5	1092.431347			
	6	10x	1010948.376	2044	1168	571.4	1155.350785			
	7	10x	1059973.985	1865	1608	862.2	1517.018363			
	8	10x	915031.217	1621	1132	698.3	1237.116263			
	9	10x	780989.71	1398	831	594.4	1064.034506			
	10	10x	720561.048	1659	379	228.5	525.9790285			

One Way Analysis of Variance B4 Counts Wednesday, August 13, 2008, 11:20:19 AM

Data source: Data 5 in Thesis statistics

Group Name	N	Missing	Mean	Std Dev	SEM
Row 1	6	0	92.773	50.320	20.543
Row 2	6	0	253.314	140.116	57.202
Row 3	6	0	315.855	205.882	84.051
Row 4	6	0	554.558	120.936	49.372
Row 5	6	0	615.544	203.514	83.084
Row 6	6	0	730.580	248.388	101.404

Source of Variation	DF	SS	MS	F	P
Between Groups	5	1789250.816	357850.163	11.778	<0.001
Residual	30	911458.785	30381.959		
Total	35	2700709.600			

The differences in the mean values among the treatment groups are greater than would be expected by chance; there is a statistically significant difference (P = <0.001).

Power of performed test with alpha = 0.050: 1.000

All Pairwise Multiple Comparison Procedures (Holm-Sidak method):
Overall significance level = 0.05

Comparisons for factor:

Comparison	Diff of Means	t	Unadjusted P	Critical Level	Significant?
Row 6 vs. Row 1	637.807	6.338	0.000000544	0.003	Yes
Row 5 vs. Row 1	522.771	5.195	0.0000134	0.004	Yes
Row 6 vs. Row 2	477.266	4.743	0.0000482	0.004	Yes
Row 4 vs. Row 1	461.786	4.589	0.0000742	0.004	Yes
Row 6 vs. Row 3	414.725	4.121	0.000273	0.005	Yes
Row 5 vs. Row 2	362.229	3.599	0.00113	0.005	Yes
Row 4 vs. Row 2	301.244	2.993	0.00548	0.006	Yes
Row 5 vs. Row 3	299.689	2.978	0.00570	0.006	Yes
Row 4 vs. Row 3	238.703	2.372	0.0243	0.007	No
Row 3 vs. Row 1	223.082	2.217	0.0344	0.009	No
Row 6 vs. Row 4	176.021	1.749	0.0905	0.010	No
Row 2 vs. Row 1	160.542	1.595	0.121	0.013	No
Row 6 vs. Row 5	115.036	1.143	0.262	0.017	No
Row 3 vs. Row 2	62.541	0.621	0.539	0.025	No
Row 5 vs. Row 4	60.985	0.606	0.549	0.050	No

Bundles of 10 Microthreads - summary of attachment counts: average and standard error of mean

Bundles of 10 EXP1				Bundles of 10 EXP2		
5h	Cells/mm	Cells/mm2		5h	Cells/mm	Cells/mm2
slide 1	132.6702	220.5968		slide 1	82.83301	165.2066
slide 2	76.26751	135.7104		slide 2	48.94239	87.95023
slide 3	41.54896	78.06823		slide 3	73.77339	162.9811
SEM	26.55154	41.39426		SEM	10.13034	25.38933
Avg	83.49555	144.7918		Avg	68.51626	138.7126
1 day	Cells/mm	Cells/mm2		1 day	Cells/mm	Cells/mm2
slide 1	52.23113	81.00074		slide 1	92.26643	174.2227
slide 2	106.7422	161.6459		slide 2	66.58383	124.5042
slide 3	132.0042	202.5147		slide 3	83.25549	144.4171
SEM	23.53882	35.69902		SEM	7.523066	14.44689
Avg	96.9925	148.3871		Avg	80.70191	147.7147
2 day	Cells/mm	Cells/mm2		2 day	Cells/mm	Cells/mm2
slide 1	22.89604	38.15615		slide 1	224.8517	276.1997
slide 2	82.6929	117.5841		slide 2	86.08075	116.4557
slide 3	40.98754	84.80531		SEM	69.38546	79.87197
SEM	17.70484	23.04511		Avg	155.4662	196.3277
Avg	52.79447	77.87012		3 day	Cells/mm	Cells/mm2
3 day	Cells/mm	Cells/mm2		slide 1	87.8452	206.3944
slide 1	90.00265	142.5531		slide 2	459.3193	715.4008
slide 2	144.7869	175.9648		slide 3	398.198	461.4668
slide 3	151.617	200.7401		SEM	114.9994	146.9376
SEM	19.49971	16.85869		Avg	273.5822	460.8976
Avg	117.3948	159.2589		4 day	Cells/mm	Cells/mm2
4 day	Cells/mm	Cells/mm2		slide 1	455.8665	560.4823
slide 1	137.9041	249.7453		slide 2	340.9009	792.6499
slide 2	84.21986	163.7797		slide 3	42.06479	57.74781
slide 3	146.365	298.9086		SEM	123.3225	216.8877
SEM	19.4588	39.48766		Avg	398.3837	676.5661
Avg	111.062	206.7625		5 day	Cells/mm	Cells/mm2
5 day	Cells/mm	Cells/mm2		slide 1	725.4319	1095.356
slide 1	322.485	590.6796		slide 2	414.1469	656.3282
slide 2	464.0601	641.0633		slide 3	529.3692	907.0905
slide 3	382.8681	801.1397		SEM	90.86472	127.1638
SEM	41.01611	63.44571		Avg	569.7894	875.8422
Avg	393.2726	615.8714				

Bundle of 10 EXP1: P8 hMSCs								Total		
5h	Picture #	Mag	Area (um2)	Length (um)	# Cells	cells/mm	cells/mm2	Cells	Length	Cells/mm
slide 1	1	10x	573486.241	1376	156	113.4	272.0204756	1107	8344	132.670182
	2	10x	929425.367	1424	289	202.9	310.9448163			
	3	10x	1017985.027	1404	297	211.5	291.7528177			220.596838
	4	10x	852444.213	1379	188	136.3	220.5422914			
	5	10x	778609.666	1385	106	76.5	136.1401028			
	6	10x	770227.772	1376	71	51.6	92.18052449			
								Total		
5h	Picture #	Mag	Area (um2)	Length	# Cells	cells/mm	cells/mm2	Cells	Length	Cells/mm
slide 2	1	10x	820380.68	1386	132	95.2	160.9009125	528	6923	76.2675141
	2	10x	764361.776	1376	163	118.5	213.2498054			
	3	10x	725645.161	1379	85	61.6	117.1371416			135.710414
	4	10x	777068.447	1385	104	75.1	133.836344			
	5	10x	823540.294	1397	44	31.5	53.42786543			
								Total		
5h	Picture #	Mag	Area (um2)	Length	# Cells	cells/mm	cells/mm2	Cells	Length	Cells/mm
slide 3	1	10x	852796.566	1494	36	24.1	42.21405366	353	8496	41.5489642
	2	10x	700265.638	1425	61	42.8	87.10980047			
	3	10x	796109.955	1421	101	71.1	126.8668974			78.0682282
	4	10x	707991.675	1398	97	69.4	137.0072607			
	5	10x	785266.505	1381	32	23.2	40.75049655			
	6	10x	754479.131	1377	26	18.9	34.46086039			
								Total		
1 Day	Picture #	Mag	Area (um2)	Length	# Cells	cells/mm	cells/mm2	Cells	Length	Cells/mm
slide 1	1	10x	805302.058	1414	48	33.9	59.60496378	508	9726	52.231133
	2	10x	822662.736	1388	125	90.1	151.9456206			
	3	10x	885622.037	1405	75	53.4	84.68623958			81.0007363
	4	10x	877651.174	1380	84	60.9	95.71000699			
	5	10x	1054583.478	1381	93	67.3	88.18647546			
	6	10x	986094.057	1381	66	47.8	66.93073499			
	7	10x	852510.117	1377	17	12.3	19.94111232			
								Total		
1 Day	Picture #	Mag	Area (um2)	Length	# Cells	cells/mm	cells/mm2	Cells	Length	Cells/mm
slide 2	1	10x	820781.015	1408	57	40.5	69.44605072	1037	9715	106.742151
	2	10x	724525.09	1376	212	154.1	292.6054638			
	3	10x	826996.763	1376	93	67.6	112.4550955			161.645927
	4	10x	988094.288	1387	188	135.5	190.2652432			
	5	10x	926274.136	1383	147	106.3	158.7003181			
	6	10x	1108703.896	1381	279	202.0	251.6451877			
	7	10x	1081481.096	1404	61	43.4	56.40412969			

								Total		
1 Day	Picture #	Mag	Area (um2)	Length	# Cells	cells/mm	cells/mm2	Cells	Length	Cells/mm
slide 3	1	10x	857060.354	1402	199	141.9	232.1890157	1503	11386	132.004216
	2	10x	941672.448	1392	188	135.1	199.644792			
	3	10x	882962.77	1395	239	171.3	270.6795894			202.514723
	4	10x	951382.241	1423	217	152.5	228.089185			
	5	10x	919565.846	1437	176	122.5	191.3946682			
	6	10x	938080.992	1429	153	107.1	163.0989236			
	7	10x	992365.591	1472	205	139.3	206.577094			
	8	10x	980968.32	1436	126	87.7	128.4445149			
								Total		
2 Day	Picture #	Mag	Area (um2)	Length	# Cells	cells/mm	cells/mm2	Cells	Length	Cells/mm
slide 1	1	10x	722335.53	1399	57	40.7	78.91069681	222	9696	22.8960396
	2	10x	812959.302	1396	54	38.7	66.42398933			
	3	10x	944754.018	1386	31	22.4	32.81277392			38.156151
	4	10x	909443.288	1380	29	21.0	31.88763982			
	5	10x	891746.445	1379	21	15.2	23.54929489			
	6	10x	877188.692	1376	15	10.9	17.10008364			
	7	10x	914155.972	1380	15	10.9	16.40857847			
								Total		
2 Day	Picture #	Mag	Area (um2)	Length	# Cells	cells/mm	cells/mm2	Cells	Length	Cells/mm
slide 2	1	10x	867928.084	1388	29	20.9	33.41290659	807	9759	82.6928989
	2	10x	1001732.57	1383	117	84.6	116.7976399			
	3	10x	1023478.437	1416	183	129.2	178.8020083			117.584092
	5	10x	1026596.716	1409	220	156.1	214.3003154			
	6	10x	877970.864	1385	154	111.2	175.404454			
	7	10x	996721.586	1394	82	58.8	82.26971418			
	8	10x	995402.648	1384	22	15.9	22.10160888			
								Total		
2 Day	Picture #	Mag	Area (um2)	Length	# Cells	cells/mm	cells/mm2	Cells	Length	Cells/mm
slide 3	1	10x	676300.15	1426	31	21.7	45.83763585	342	8344	40.987536
	2	10x	695126.026	1387	54	38.9	77.68375515			
	3	10x	601749.335	1376	67	48.7	111.3420424			84.8053118
	4	10x	724033.414	1380	88	63.8	121.541352			
	5	10x	645905.885	1385	74	53.4	114.5677748			
	6	10x	739580.298	1390	28	20.1	37.85931031			

3 Day	Picture #	Mag	Area (um2)	Length	# Cells	cells/mm	cells/mm2	Total		
slide 1	1	10x	1162373.396	1378	39	28.3	33.55204114	Cells	Length	Cells/mm
	2	10x	950820.615	1380	104	75.4	109.3792019	1020	11333	90.0026471
	3	10x	947007.747	1400	150	107.1	158.3936356			
	4	10x	880867.152	1413	163	115.4	185.0449295			142.553108
	5	10x	822747.716	1434	148	103.2	179.8850329			
	6	10x	832345.936	1445	159	110.0	191.0263427			
	7	10x	881220.083	1443	158	109.5	179.296867			
	8	10x	953327.263	1440	99	68.8	103.8468151			
								Total		
3 Day	Picture #	Mag	Area (um2)	Length	# Cells	cells/mm	cells/mm2	Cells	Length	Cells/mm
slide 2	1	10x	1035238.178	1376	72	52.3	69.54921247	1597	11030	144.786945
	2	10x	1025361.892	1376	142	103.2	138.4876902			
	3	10x	1028874.147	1379	297	215.4	288.6650431			200.740064
	4	10x	942687.016	1381	361	261.4	382.9478861			
	5	10x	981614.059	1389	192	138.2	195.5962206			
	6	10x	994929.472	1376	202	146.8	203.0294666			
	7	10x	1006942.71	1376	245	178.1	243.3107639			
	8	10x	1019751.994	1377	86	62.5	84.33423078			
								Total		
3 Day	Picture #	Mag	Area (um2)	Length	# Cells	cells/mm	cells/mm2	Cells	Length	Cells/mm
slide 4	1		1287654.064	1376	93	67.6	72.22436724	1669	11008	151.617006
	2		1162643.08	1376	174	126.5	149.6589994			
	3		1140030.639	1376	242	175.9	212.2749966			175.964786
	4		1215564.227	1376	316	229.7	259.9615824			
	5		1180943.462	1376	287	208.6	243.026029			
	6		1171556.249	1376	350	254.4	298.7479264			
	7		1196984.044	1376	180	130.8	150.3779444			
	8		1258950.168	1376	27	19.6	21.4464406			
								Total		
4 Day	Picture #	Mag	Area (um2)	Length	# Cells	cells/mm	cells/mm2	Cells	Length	Cells/mm
slide 4	1		882244.479	1457	102	70.0	115.6142117	1941	14075	137.904085
	2		776483.408	1476	225	152.4	289.7679431			
	3		686237.426	1445	300	207.6	437.16648			249.745293
	4		695920.338	1399	206	147.2	296.010892			
	5		868788.299	1378	197	143.0	226.7525935			
	6		873348.942	1380	256	185.5	293.1245321			
	7		826005.608	1383	306	221.3	370.4575333			
	8		772233.206	1396	200	143.3	258.989122			
	9		691669.557	1385	101	72.9	146.0234862			
	10		755356.689	1376	48	34.9	63.54613747			

								Total		
4 Day	Picture #	Mag	Area (um2)	Length	# Cells	cells/mm	cells/mm2	Cells	Length	Cells/mm
slide 5	1		711114.002	1376	51	37.1	71.71845844	1045	12408	84.2198582
	2		686662.909	1378	161	116.8	234.4673025			
	3		693327.552	1376	251	182.4	362.0222495			163.779654
	4		834686.091	1376	227	165.0	271.9585272			
	5		749999.422	1378	139	100.9	185.3334762			
	6		634427.68	1377	50	36.3	78.81118932			
	7		640976.413	1378	82	59.5	127.9298245			
	8		612359.521	1379	59	42.8	96.3486285			
	9		550330.674	1390	25	18.0	45.42723345			
								Total		
4 Day	Picture #	Mag	Area (um2)	Length	# Cells	cells/mm	cells/mm2	Cells	Length	Cells/mm
slide 6	1		650811.944	1449	84	58.0	129.0695427	2271	15516	146.365043
	2		634268.991	1413	170	120.3	268.0250846			
	3		646387.444	1412	253	179.2	391.4061177			298.908597
	4		680924.384	1394	369	264.7	541.9103922			
	5		672099.665	1384	339	244.9	504.3894792			
	6		683183.316	1379	299	216.8	437.6570578			
	7		712095.04	1377	240	174.3	337.0336634			
	8		714936.987	1383	145	104.8	202.8150769			
	9		748172.621	1420	164	115.5	219.2007505			
	10		833872.991	1450	163	112.4	195.4734135			
	11		737535.842	1455	45	30.9	61.01398391			
								Total		
5 Day	Picture #	Mag	Area (um2)	Length	# Cells	cells/mm	cells/mm2	Cells	Length	Cells/mm
slide 4	1		836201.873	1376	310	225.3	370.7238766	4895	15179	322.485012
	2		828125.795	1376	425	308.9	513.2070545			
	3		798590.589	1401	577	411.8	722.5229147			590.679625
	4		753418.314	1382	552	399.4	732.6607142			
	5		703310.209	1376	434	315.4	617.0818999			
	6		685224.303	1376	499	362.6	728.2286951			
	7		685577.523	1376	564	409.9	822.6640768			
	8		770446.294	1386	537	387.4	696.9986152			
	9		827493.352	1382	405	293.1	489.4299139			
	10		752504.914	1376	291	211.5	386.7084382			
	11		721390.623	1372	301	219.4	417.2496708			

								Total		
5 Day	Picture #	Mag	Area (um2)	Length	# Cells	cells/mm	cells/mm2	Cells	Length	Cells/mm
slide 5	1		1017988.207	1391	314	225.7	308.4515104	5804	12507	464.060126
	2		1205187.594	1469	886	603.1	735.1552608			
	3		870039.6	1418	927	653.7	1065.468744			641.063273
	4		1149344.144	1406	1121	797.3	975.3388538			
	5		1139360.62	1585	1109	699.7	973.3529319			
	6		858405.307	1385	791	571.1	921.4761297			
	7		793212.799	1393	440	315.9	554.7061275			
	8		902423.112	1393	164	117.7	181.7329342			
	9		964982.946	1067	52	48.7	53.88696268			
								Total		
5 Day	Picture #	Mag	Area (um2)	Length	# Cells	cells/mm	cells/mm2	Cells	Length	Cells/mm
slide 6	1		594987.86	1376	256	186.0	430.2608796	5815	15188	382.868054
	2		582079.431	1381	279	202.0	479.3160265			
	3		632249.393	1388	396	285.3	626.3351209			801.13975
	4		623344.317	1376	665	483.3	1066.826121			
	5		685505.839	1376	847	615.6	1235.583932			
	6		681261.418	1376	857	622.8	1257.960567			
	7		701696.15	1376	790	574.1	1125.84343			
	8		645911.955	1381	800	579.3	1238.558899			
	9		639114.348	1383	514	371.7	804.2379296			
	10		748979.651	1383	339	245.1	452.6157681			
	11		757906.116	1392	72	51.7	94.99857368			

Bundle of 10 EXP2: P7 hMSCs

								Total		
5h	Picture #	Mag	Area (um2)	Length (um)	# Cells	cells/mm	cells/mm2	Cells	Length	Cells/mm
slide 4	1	10x	705035.264	1408	24	17.0	34.0408505	814	9827	82.83301
	2	10x	705035.264	1424	141	99.0	199.989997			
	3	10x	718884.264	1419	206	145.2	286.555167			165.2066
	4	10x	683346.052	1420	176	123.9	257.556182			
	5	10x	726209.966	1397	117	83.8	161.11043			
	6	10x	670505.261	1382	110	79.6	164.055387			
	7	10x	752755.81	1377	40	29.0	53.1380821			
								Total		
5h	Picture #	Mag	Area (um2)	Length	# Cells	cells/mm	cells/mm2	Cells	Length	Cells/mm
slide 5	1	10x	747590.473	1481	43	29.0	57.518122	435	8888	48.94239
	2	10x	840009.25	1477	87	58.9	103.570288			
	3	10x	868044.861	1477	99	67.0	114.049405			87.95023
	4	10x	783540.872	1522	88	57.8	112.31067			
	5	10x	845541.681	1475	91	61.7	107.623317			
	6	10x	827470.228	1456	27	18.5	32.6295727			
								Total		
5h	Picture #	Mag	Area (um2)	Length	# Cells	cells/mm	cells/mm2	Cells	Length	Cells/mm
slide 6	1	10x	631748.468	1402	31	22.1	49.0701625	627	8499	73.77339
	2	10x	647567.638	1419	99	69.8	152.879783			
	3	10x	703413.978	1432	197	137.6	280.062675			162.9811
	4	10x	635296.566	1443	139	96.3	218.795453			
	5	10x	577743.67	1429	96	67.2	166.163655			
	6	10x	586035.38	1374	65	47.3	110.914805			
								Total		
1 Day	Picture #	Mag	Area (um2)	Length	# Cells	cells/mm	cells/mm2	Cells	Length	Cells/mm
slide 4	1	10x	719110.302	1373	78	56.8	108.467366	1032	11185	92.26643
	2	10x	791743.554	1374	193	140.5	243.765799			
	3	10x	810563.36	1386	100	72.2	123.370985			174.2227
	4	10x	657710.14	1376	86	62.5	130.756689			
	5	10x	663487.686	1376	192	139.5	289.3799			
	6	10x	776806.567	1410	293	207.8	377.185277			
	7	10x	743706.787	1431	72	50.3	96.8123476			
	8	10x	748644.352	1459	18	12.3	24.0434593			

								Total		
1 Day	Picture #	Mag	Area (um2)	Length	# Cells	cells/mm	cells/mm2	Cells	Length	Cells/mm
slide 5	1	10x	726142.329	1381	14	10.1	19.2799668	643	9657	66.58383
	2	10x	751413.458	1376	65	47.2	86.503641			
	3	10x	759849.116	1376	113	82.1	148.713735			124.5042
	4	10x	726000.694	1380	129	93.5	177.685781			
	5	10x	752047.636	1376	158	114.8	210.093074			
	6	10x	721771.881	1376	145	105.4	200.894498			
	7	10x	669984.68	1392	19	13.6	28.3588574			
								Total		
1 Day	Picture #	Mag	Area (um2)	Length	# Cells	cells/mm	cells/mm2	Cells	Length	Cells/mm
slide 6	1	10x	849481.732	1447	96	66.3	113.010082	713	8564	83.25549
	2	10x	861389.756	1451	133	91.7	154.40165			
	3	10x	833967.222	1429	120	84.0	143.890547			144.4171
	4	10x	814666.435	1417	181	127.7	222.176823			
	5	10x	787786.449	1402	136	97.0	172.635617			
	6	10x	778302.983	1418	47	33.1	60.3877937			
								Total		
2 Day	Picture #	Mag	Area (um2)	Length	# Cells	cells/mm	cells/mm2	Cells	Length	Cells/mm
slide 4	1	10x	1273765.75	1376	32	23.3	25.1223586	3411	15170	224.8517
	2	10x	1275572.32	1376	65	47.2	50.9575184			
	3	10x	1095278.07	1376	100	72.7	91.3010157			276.1997
	4	10x	1058494.62	1376	215	156.3	203.118651			
	5	10x	1254062.32	1410	278	197.2	221.679573			
	6	10x	1178662.85	1376	251	182.4	212.953178			
	7	10x	1243384.21	1376	725	526.9	583.086062			
	8	10x	1308792.92	1376	478	347.4	365.222023			
	9	10x	1220331.83	1376	441	320.5	361.377118			
	10	10x	1111685.74	1376	479	348.1	430.877163			
	11	10x	704565.846	1376	347	252.2	492.501875			
								Total		
2 Day	Picture #	Mag	Area (um2)	Length	# Cells	cells/mm	cells/mm2	Cells	Length	Cells/mm
slide 5	1	10x	674355.995	1397	33	23.6	48.9355774	953	11071	86.08075
	2	10x	955764.828	1376	37	26.9	38.712452			
	3	10x	927340.444	1418	121	85.3	130.480667			116.4557
	4	10x	1022203.15	1376	126	91.6	123.26317			
	5	10x	1119011.74	1376	168	122.1	150.132474			
	6	10x	1277288.7	1376	234	170.1	183.200555			
	7	10x	925284.715	1376	178	129.4	192.37322			
	8	10x	867573.13	1376	56	40.7	64.5478728			

								Total		
3 Day	Picture #	Mag	Area (um2)	Length	# Cells	cells/mm	cells/mm2	Cells	Length	Cells/mm
slide 3	1	10x	557182.333	1376	85	61.8	152.553294	967	11008	87.8452
	2	10x	606253.324	1376	91	66.1	150.10227			
	3	10x	680332.986	1376	152	110.5	223.420006			206.3944
	4	10x	568771.534	1376	115	83.6	202.190147			
	5	10x	639597.641	1376	111	80.7	173.546606			
	6	10x	532167.592	1376	170	123.5	319.448239			
	7	10x	581637.183	1376	148	107.6	254.454159			
	8	10x	541495.26	1376	95	69.0	175.440132			
								Total		
3 Day	Picture #	Mag	Area (um2)	Length	# Cells	cells/mm	cells/mm2	Cells	Length	Cells/mm
slide 5	1	10x	895634.177	1376	15	10.9	16.7479093	12307	26794	459.3193
	2	10x	1166156.49	1517	70	46.1	60.026249			
	3	10x	1137993.12	1463	542	370.5	476.277044			715.4008
	4	10x	992255.174	1437	933	649.3	940.282323			
	5	10x	1182993.99	1388	1198	863.1	1012.68477			
	6	10x	1133091.69	1386	1595	1150.8	1407.65308			
	7	10x	1043905.65	1376	1715	1246.4	1642.86877			
	8	10x	1173916.06	1419	1324	933.1	1127.84895			
	9	10x	1145649.79	1452	508	349.9	443.416484			
	10	10x	1183094	1376	31	22.5	26.2024827			
								Total		
3 Day	Picture #	Mag	Area (um2)	Length	# Cells	cells/mm	cells/mm2	Cells	Length	Cells/mm
slide 6	1	10x	951719.563	1445	136	94.1	142.899238	9458	23752	398.198
	2	10x	1050765.99	1417	497	350.7	472.988284			
	3	10x	1093279.86	1376	642	466.6	587.223843			461.4668
	4	10x	1012958.72	1376	691	502.2	682.160076			
	5	10x	1071396.12	1388	715	515.1	667.353549			
	6	10x	1040496.88	1390	625	449.6	600.674556			
	7	10x	1104450.23	1392	559	401.6	506.134172			
	8	10x	1026104.75	1416	378	266.9	368.383442			
	9	10x	1060740.55	1404	133	94.7	125.384101			
								Total		
4 Day	Picture #	Mag	Area (um2)	Length	# Cells	cells/mm	cells/mm2	Cells	Length	Cells/mm
slide 1	1	10x	996385.131	1376	239	173.7	239.867088	5082	11148	455.8665
	2	10x	1176705.4	1406	782	556.2	664.56736			
	3	10x	1174134	1391	931	669.3	792.924825			560.4823
	4	10x	1112743.67	1396	1116	799.4	1002.9264			
	5	10x	1080062.44	1408	837	594.5	774.9552			
	6	10x	1186984.91	1414	715	505.7	602.366545			
	7	10x	1230558.45	1381	389	281.7	316.116639			
	8	10x	809902.59	1376	73	53.1	90.1342963			

								Total		
4 Day	Picture #	Mag	Area (um2)	Length	# Cells	cells/mm	cells/mm2	Cells	Length	Cells/mm
slide 2	1	10x	657344.202	1409	244	173.2	371.190617	3784	11100	340.9009
	2	10x	656931.437	1403	469	334.3	713.925341			
	3	10x	624276.217	1385	569	410.8	911.455514			792.6499
	4	10x	587960.458	1376	721	524.0	1226.27294			
	5	10x	597835.01	1376	732	532.0	1224.41809			
	6	10x	557872.008	1389	611	439.9	1095.2333			
	7	10x	549718.465	1386	354	255.4	643.965998			
	8	10x	542854.087	1376	84	61.0	154.737713			
								Total		
4 Day	Picture #	Mag	Area (um2)	Length	# Cells	cells/mm	cells/mm2	Cells	Length	Cells/mm
slide 3	1		1053118.57	1480	44	29.7	41.7806706	361	8582	42.06479
	2		1055120.53	1501	48	32.0	45.4924328			
	3		1082718.81	1411	83	58.8	76.6588695			57.74781
	4		1075227.77	1404	97	69.1	90.2134436			
	5		990624.35	1379	57	41.3	57.5394699			
	6		919488.38	1407	32	22.7	34.8019624			
								Total		
5 Day	Picture #	Mag	Area (um2)	Length	# Cells	cells/mm	cells/mm2	Cells	Length	Cells/mm
slide 1	1		739875.708	1402	294	209.7	397.364039	9028	12445	725.4319
	2		819817.32	1382	752	544.1	917.277522			
	3		844398.196	1387	1219	878.9	1443.6317			1095.356
	4		929880.911	1385	1398	1009.4	1503.41832			
	5		1023275.52	1378	1572	1140.8	1536.24314			
	6		1014286.05	1377	1469	1066.8	1448.30939			
	7		930631.287	1380	1446	1047.8	1553.784			
	8		834101.052	1378	754	547.2	903.967209			
	9		804090.646	1376	124	90.1	154.211469			
								Total		
5 Day	Picture #	Mag	Area (um2)	Length	# Cells	cells/mm	cells/mm2	Cells	Length	Cells/mm
slide 2	1		791387.444	1376	188	136.6	237.557471	4602	11112	414.1469
	2		844701.7	1378	439	318.6	519.710094			
	3		786546.422	1376	504	366.3	640.775911			656.3282
	4		821723.899	1376	634	460.8	771.548693			
	5		934968.783	1376	668	485.5	714.462357			
	6		994705.457	1404	992	706.6	997.280143			
	7		875953.289	1426	874	612.9	997.770099			
	8		815567.407	1400	303	216.4	371.520487			

								Total		
5 Day	Picture #	Mag	Area (um2)	Length	# Cells	cells/mm	cells/mm2	Cells	Length	Cells/mm
slide 3	1		862444.213	1380	233	168.8	270.162402	5849	11049	529.3692
	2		790865.996	1380	654	473.9	826.94161			
	3		800280.09	1383	935	676.1	1168.34095			907.0905
	4		784104.81	1379	1135	823.1	1447.51057			
	5		783920.684	1386	1168	842.7	1489.94665			
	6		879078.506	1385	895	646.2	1018.11157			
	7		821203.896	1380	655	474.6	797.609465			
	8		730782.749	1376	174	126.5	238.100859			

One Way Analysis of Variance B10 Counts Wednesday, August 13, 2008, 1:37:27 PM

Data source: Data 6 in Thesis statistics

Normality Test: Failed (P < 0.050)

Test execution ended by user request, ANOVA on Ranks begun

Kruskal-Wallis One Way Analysis of Variance on Ranks Wednesday, August 13, 2008, 1:37:27 PM

Data source: Data 6 in Thesis statistics

Group	**N**	**Missing**	**Median**	**25%**	**75%**
5 hour	6	0	149.346	87.950	165.207
1 day	6	0	153.032	124.504	174.223
2 day	5	0	116.456	73.143	157.238
3 day	6	0	203.567	175.965	461.467
4 day	6	0	274.327	163.780	560.482
5 day	6	0	728.734	641.063	907.091

H = 19.094 with 5 degrees of freedom. (P = 0.002)

The differences in the median values among the treatment groups are greater than would be expected by chance; there is a statistically significant difference (P = 0.002)

To isolate the group or groups that differ from the others use a multiple comparison procedure.

All Pairwise Multiple Comparison Procedures (Dunn's Method) :

Comparison	**Diff of Ranks**	**Q**	**P<0.05**
5 day vs 2 day	22.500	3.626	Yes
5 day vs 5 hour	19.667	3.324	Yes
5 day vs 1 day	19.000	3.212	Yes
5 day vs 4 day	10.833	1.831	No
5 day vs 3 day	10.500	1.775	Do Not Test
3 day vs 2 day	12.000	1.934	No
3 day vs 5 hour	9.167	1.549	Do Not Test
3 day vs 1 day	8.500	1.437	Do Not Test
3 day vs 4 day	0.333	0.0563	Do Not Test
4 day vs 2 day	11.667	1.880	Do Not Test

4 day vs 5 hour	8.833	1.493	Do Not Test
4 day vs 1 day	8.167	1.380	Do Not Test
1 day vs 2 day	3.500	0.564	Do Not Test
1 day vs 5 hour	0.667	0.113	Do Not Test
5 hour vs 2 day	2.833	0.457	Do Not Test

Appendix C: Cells per Microthread Calculations

Surface area of microthread bundle was calculated based on bundle circumference estimations

Total thread surface area (B4):	
Individual diameter (um)	100
Circumference of thread (um)	942.477796
Thread length (2cm)	20000
Bundle SA (um^2)	18849555.9
Bundle SA (mm^2)	18.8495559

Unseeded ends were accounted for by measuring the area of several samples, averaging the total unseeded area per thread and multiplying that by two to account for the opposite face.

	area	um2	mm2			area	um2	mm2
5h s1	pic 1	1010797	1.010797		day 1 s1	pic 1	1045188.437	1.04518844
	pic2	1070965	1.070965			pic2	683992.322	0.68399232
	pic3	896036.7	0.896037					1.72918076
			2.977799					
5h s1					day 1 s1	pic 3	1172643.899	1.1726439
	pic 4	1204654	1.204654			pic 4	854020.404	0.8540204
	pic5	1197990	1.19799			pic 5	790495.594	0.79049559
	pic 6	245155.6	0.245156					2.8171599
			2.6478		day 1 s2			
5h s2						pic 1	1205911.302	1.2059113
	pic 1	1305631	1.305631			pic2	681317.028	0.68131703
	pic2	634378.1	0.634378					1.88722833
			1.940009		day 1 s2			
						pic 3	830106.032	0.83010603
						pic4	699114.611	0.69911461
						pic5	488916.308	0.48891631
						pic6	595567.689	0.59556769
								2.61370464
	per end	2.521869						
		avg	stdev			per end	2.261818407	
	per thread	3.782804	2.606106				avg	stdev
	both sides	7.565608	5.212211			per thread	4.523636813	0.03210808
						both sides	9.047273626	0.06421617

	area	um2	mm2				area	um2	mm2
day 2 s1	pic 1	1418447	1.418447			day 3 s1	pic 1	665735.3	0.665735
	pic2	819888.8	0.819889				pic2	1159634	1.159634
			2.238336						1.825369
day 2 s1	pic 3	1272121	1.272121			day 3 s1	pic 3	1339989	1.339989
	pic 4	573456.3	0.573456						
			1.845577						1.339989
day 2 s2	pic 1	1613413	1.613413			day 3 s2	pic 1	606162.7	0.606163
	pic2	635061.5	0.635062				pic2	286125.8	0.286126
			2.248475						0.892289
day 2 s2	pic 3	1337684	1.337684			day 3 s2	pic 3	1504954	1.504954
	pic4	995484.4	0.995484				pic4	602435.5	0.602436
			2.333169						2.10739
day 2 s3	pic 1	617506.5	0.617506			day 3 s3	pic 1	786953.8	0.786954
			0				pic2	286673.9	0.286674
			0.617506						1.073628
day 2 s3	pic2	619024.9	0.619025			day 3 s3	pic 3	392630.2	0.39263
	pic3	372896.7	0.372897						0
			0.991922						0.39263
	per end	1.712497							
		avg	stdev			day 3 s4	pic 1	649832.8	0.649833
	per thread	3.424995	1.5919				pic2	440891.6	0.440892
	both sides	6.849989	3.1838						1.090724
						day 3 s4	pic4	779296.4	0.779296
							pic5	154643.4	0.154643
									0.93394
							per end	1.206995	
								avg	stdev
							per thread	2.413989	0.807745
							both sides	4.827979	1.615489

	area	um2	mm2				area	um2	mm2
day 4 s1	pic 1	1145581	1.145581			day 5 s1	pic 1	928116.9	0.928117
									0
			1.145581						0.928117
						day 5 s1	pic2	1015805	1.015805
day 4 s2	pic 1	936801.7	0.936802						
									1.015805
			0.936802						
						day 5 s2	pic 1	735711.6	0.735712
									0
day 4 s3	pic 1	319533.1	0.319533						0.735712
	pic2	-							
			0.319533			day 5 s2	pic2	441793.1	0.441793
									0
day 4 s3	pic 3	351034.9	0.351035						0.441793
	pic4	310387.7	0.310388						
			0.661423						
							per end	0.780357	
day 4 s3	pic 1	631118.5	0.631119					avg	stdev
			0.631119				per thread	1.560713	0.541939
							both sides	3.121426	1.083877
day 4 s3	pic2	631223.5	0.631223						
	pic 3	283533.3	0.283533						
	pic4	138901.8	0.138902						
			1.053659						
	per end	0.791353							
		avg	stdev						
	per thread	1.187029	0.343779						
	both sides	2.374058	0.687557						

Time Point	Unseeded area Average (mm^2)	Stdev
5 hours	7.565608	5.212211
1 day	9.047274	0.064216
2 day	6.849989	3.1838
3 day	4.827979	1.615489
4 day	2.374058	0.687557
5 day	3.121426	1.083877
Average	5.631056	
SEM	1.071604	

The average unseeded area per microthread bundle is 5.6 $\pm$ 1.1 mm^2. Subtracting this from the total surface area of a microthread bundle (18.8 mm^2) leaves 13.2 mm^2 as the average cell populated surface area of all microthread bundles.

One Way Analysis of Variance B4 Total Cells/Bundle Thursday, August 28, 2008, 1:37:40 PM

Data source: Data 7 in Thesis statistics

Normality Test: Passed (P = 0.847)

Equal Variance Test: Passed (P = 0.446)

Group Name	N	Missing	Mean	Std Dev	SEM
5 hour	6	0	1224.598	664.219	271.166
1 day	6	0	3343.748	1849.528	755.067
2 day	6	0	4169.287	2717.643	1109.473
3 day	6	0	7320.172	1596.351	651.708
4 day	6	0	8125.178	2686.388	1096.713
5 day	6	0	9643.654	3278.715	1338.530

Source of Variation	DF	SS	MS	F	P
Between Groups	5	311759062.104	62351812.421	11.778	<0.001
Residual	30	158812578.661	5293752.622		
Total	35	470571640.765			

The differences in the mean values among the treatment groups are greater than would be expected by chance; there is a statistically significant difference (P = <0.001).

Power of performed test with alpha = 0.050: 1.000

All Pairwise Multiple Comparison Procedures (Holm-Sidak method):
Overall significance level = 0.05

Comparisons for factor:

Comparison	Diff of Means	t	Unadjusted P	Critical Level	Significant?
5 day vs. 5 hour	8419.056	6.338	0.000000544	0.003	Yes
4 day vs. 5 hour	6900.579	5.195	0.0000134	0.004	Yes
5 day vs. 1 day	6299.906	4.743	0.0000482	0.004	Yes
3 day vs. 5 hour	6095.574	4.589	0.0000742	0.004	Yes
5 day vs. 2 day	5474.367	4.121	0.000273	0.005	Yes
4 day vs. 1 day	4781.429	3.599	0.00113	0.005	Yes
3 day vs. 1 day	3976.424	2.993	0.00548	0.006	Yes
4 day vs. 2 day	3955.891	2.978	0.00570	0.006	Yes
3 day vs. 2 day	3150.885	2.372	0.0243	0.007	No
2 day vs. 5 hour	2944.689	2.217	0.0344	0.009	No
5 day vs. 3 day	2323.482	1.749	0.0905	0.010	No
1 day vs. 5 hour	2119.150	1.595	0.121	0.013	No
5 day vs. 4 day	1518.476	1.143	0.262	0.017	No
2 day vs. 1 day	825.538	0.621	0.539	0.025	No
4 day vs. 3 day	805.006	0.606	0.549	0.050	No

Appendix D: CyQuant Standard Curve Data

Fluorescence versus time

50,000 Cells

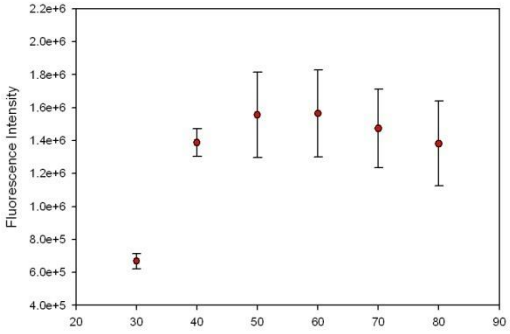

30,000 Cells

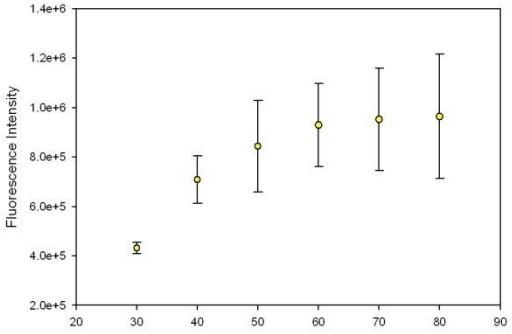

10,000 Cells

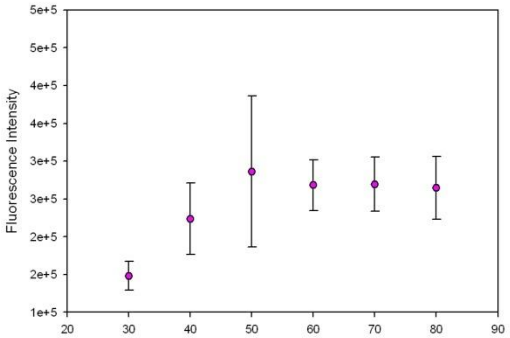

5,000 Cells

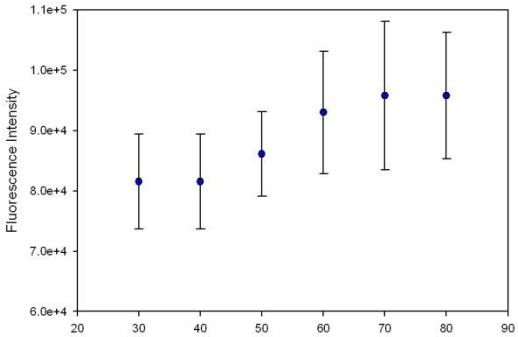

1,000 Cells

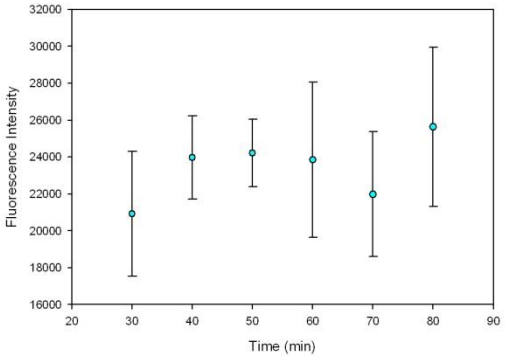

500 Cells

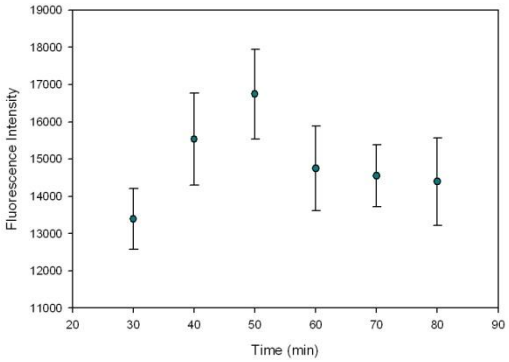

100 Cells

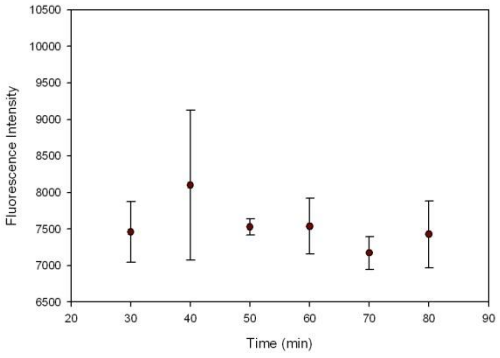

One Way Analysis of Variance 50,000 cells Monday, August 11, 2008, 8:24:05 AM

Data source: Data 3 in Notebook 1

Group Name	N	Missing	Mean	Std Dev	SEM
Row 1(30min)	5	0	668907.200	46237.743	20678.147
Row 2(40min)	5	0	1388193.800	83171.874	37195.593
Row 3(50min)	5	0	1555962.000	258221.828	115480.312
Row 4(60min)	5	0	1564547.800	262671.193	117470.129
Row 5(70min)	5	0	1473916.200	239805.389	107244.230
Row 6(80min)	5	0	1382146.000	257400.936	115113.198

Source of Variation	DF	SS	MS	F	P
Between Groups	5	2.847E+012	569452650616.059	12.726	<0.001
Residual	24	1.074E+012	44748670608.217		
Total	29	3.921E+012			

The differences in the mean values among the treatment groups are greater than would be expected by chance; there is a statistically significant difference (P = <0.001).

Power of performed test with alpha = 0.050: 1.000

All Pairwise Multiple Comparison Procedures (Holm-Sidak method):
Overall significance level = 0.05

Comparisons for factor:

Comparison	Diff of Means	t	Unadjusted P	Critical Level	Significant?
Row 4 vs. Row 1	895640.600	6.694	0.000000634	0.003	Yes
Row 3 vs. Row 1	887054.800	6.630	0.000000739	0.004	Yes
Row 5 vs. Row 1	805009.000	6.017	0.00000327	0.004	Yes
Row 2 vs. Row 1	719286.600	5.376	0.0000161	0.004	Yes
Row 6 vs. Row 1	713238.800	5.331	0.0000180	0.005	Yes
Row 4 vs. Row 6	182401.800	1.363	0.185	0.005	No
Row 4 vs. Row 2	176354.000	1.318	0.200	0.006	No
Row 3 vs. Row 6	173816.000	1.299	0.206	0.006	No
Row 3 vs. Row 2	167768.200	1.254	0.222	0.007	No
Row 5 vs. Row 6	91770.200	0.686	0.499	0.009	No
Row 4 vs. Row 5	90631.600	0.677	0.505	0.010	No
Row 5 vs. Row 2	85722.400	0.641	0.528	0.013	No
Row 3 vs. Row 5	82045.800	0.613	0.545	0.017	No
Row 4 vs. Row 3	8585.800	0.0642	0.949	0.025	No
Row 2 vs. Row 6	6047.800	0.0452	0.964	0.050	No

One Way Analysis of Variance 30,000 cells Monday, August 11, 2008, 8:29:07 AM

Data source: Data 3 in Notebook 1

Group Name	N	Missing	Mean	Std Dev	SEM
Row 1	5	0	431579.800	22976.984	10275.619
Row 2	5	0	708628.600	96896.302	43333.344
Row 3	5	0	843818.400	184638.511	82572.852
Row 4	5	0	929092.200	167858.663	75068.676
Row 5	5	0	951598.400	207141.810	92636.634
Row 6	5	0	964567.400	251472.923	112462.110

Source of Variation	DF	SS	MS	F	P
Between Groups	5	1.063E+012	212588595558.880	7.153	<0.001

Residual	24	713324425166.401	29721851048.600
Total	29	1.776E+012	

The differences in the mean values among the treatment groups are greater than would be expected by chance; there is a statistically significant difference (P = <0.001).

Power of performed test with alpha = 0.050: 0.986

All Pairwise Multiple Comparison Procedures (Holm-Sidak method):
Overall significance level = 0.05

Comparisons for factor:

Comparison	Diff of Means	t	Unadjusted P	Critical Level	Significant?
Row 6 vs. Row 1	532987.600	4.888	0.0000552	0.003	Yes
Row 5 vs. Row 1	520018.600	4.769	0.0000747	0.004	Yes
Row 4 vs. Row 1	497512.400	4.563	0.000126	0.004	Yes
Row 3 vs. Row 1	412238.600	3.781	0.000915	0.004	Yes
Row 2 vs. Row 1	277048.800	2.541	0.0179	0.005	No
Row 6 vs. Row 2	255938.800	2.347	0.0275	0.005	No
Row 5 vs. Row 2	242969.800	2.228	0.0355	0.006	No
Row 4 vs. Row 2	220463.600	2.022	0.0545	0.006	No
Row 3 vs. Row 2	135189.800	1.240	0.227	0.007	No
Row 6 vs. Row 3	120749.000	1.107	0.279	0.009	No
Row 5 vs. Row 3	107780.000	0.988	0.333	0.010	No
Row 4 vs. Row 3	85273.800	0.782	0.442	0.013	No

One Way Analysis of Variance 10,000 cells Monday, August 11, 2008, 8:30:12 AM

Data source: Data 3 in Notebook 1

Group Name	N	Missing	Mean	Std Dev	SEM
Row 1	5	0	148055.000	18920.072	8461.313
Row 2	5	0	223571.600	47322.078	21163.077
Row 3	5	0	286146.600	100081.101	44757.629
Row 4	5	0	268299.800	33668.409	15056.970
Row 5	5	0	269442.600	36049.969	16122.036
Row 6	5	0	264800.600	41615.477	18611.007

Source of Variation	DF	SS	MS	F	P
Between Groups	5	65336539239.366	13067307847.873	4.673	0.004
Residual	24	67114340037.600	2796430834.900		
Total	29	132450879276.967			

The differences in the mean values among the treatment groups are greater than would be expected by chance; there is a statistically significant difference (P = 0.004).

Power of performed test with alpha = 0.050: 0.862

All Pairwise Multiple Comparison Procedures (Holm-Sidak method):
Overall significance level = 0.05

Comparisons for factor:

Comparison	Diff of Means	t	Unadjusted P	Critical Level	Significant?
Row 3 vs. Row 1	138091.600	4.129	0.000380	0.003	Yes
Row 5 vs. Row 1	121387.600	3.629	0.00134	0.004	Yes
Row 4 vs. Row 1	120244.800	3.595	0.00145	0.004	Yes
Row 6 vs. Row 1	116745.600	3.491	0.00189	0.004	Yes

Row 2 vs. Row 1	75516.600	2.258	0.0333	0.005	No
Row 3 vs. Row 2	62575.000	1.871	0.0736	0.005	No
Row 5 vs. Row 2	45871.000	1.372	0.183	0.006	No
Row 4 vs. Row 2	44728.200	1.337	0.194	0.006	No
Row 6 vs. Row 2	41229.000	1.233	0.230	0.007	No
Row 3 vs. Row 6	21346.000	0.638	0.529	0.009	No
Row 3 vs. Row 4	17846.800	0.534	0.599	0.010	No
Row 3 vs. Row 5	16704.000	0.499	0.622	0.013	No
Row 5 vs. Row 6	4642.000	0.139	0.891	0.017	No

One Way Analysis of Variance 5,000 cells Monday, August 11, 2008, 8:31:31 AM

Data source: Data 3 in Notebook 1

Group Name	N	Missing	Mean	Std Dev	SEM
Row 1	5	0	65040.200	5385.951	2408.670
Row 2	5	0	81551.800	7859.450	3514.853
Row 3	5	0	86100.400	7004.436	3132.479
Row 4	5	0	93000.200	10136.731	4533.284
Row 5	5	0	95767.000	12295.574	5498.748
Row 6	5	0	95760.200	10490.365	4691.434

Source of Variation	DF	SS	MS	F	P
Between Groups	5	3492601935.900	698520387.180	8.319	<0.001
Residual	24	2015294958.400	83970623.267		
Total	29	5507896894.300			

The differences in the mean values among the treatment groups are greater than would be expected by chance; there is a statistically significant difference (P = <0.001).

Power of performed test with alpha = 0.050: 0.996

All Pairwise Multiple Comparison Procedures (Holm-Sidak method):
Overall significance level = 0.05

Comparisons for factor:

Comparison	Diff of Means	t	Unadjusted P	Critical Level	Significant?
Row 5 vs. Row 1	30726.800	5.302	0.0000194	0.003	Yes
Row 6 vs. Row 1	30720.000	5.301	0.0000194	0.004	Yes
Row 4 vs. Row 1	27960.000	4.824	0.0000649	0.004	Yes
Row 3 vs. Row 1	21060.200	3.634	0.00132	0.004	Yes
Row 2 vs. Row 1	16511.600	2.849	0.00886	0.005	No
Row 5 vs. Row 2	14215.200	2.453	0.0218	0.005	No
Row 6 vs. Row 2	14208.400	2.452	0.0219	0.006	No
Row 4 vs. Row 2	11448.400	1.975	0.0598	0.006	No
Row 5 vs. Row 3	9666.600	1.668	0.108	0.007	No
Row 6 vs. Row 3	9659.800	1.667	0.109	0.009	No
Row 4 vs. Row 3	6899.800	1.191	0.245	0.010	No
Row 3 vs. Row 2	4548.600	0.785	0.440	0.013	No
Row 5 vs. Row 4	2766.800	0.477	0.637	0.017	No
Row 6 vs. Row 4	2760.000	0.476	0.638	0.025	No
Row 5 vs. Row 6	6.800	0.00117	0.999	0.050	No

One Way Analysis of Variance 1.000 cells Monday, August 11, 2008, 8:32:22 AM

Data source: Data 3 in Notebook 1

Group Name	N	Missing	Mean	Std Dev	SEM
Row 1	5	0	20920.800	3394.390	1518.017
Row 2	5	0	23976.200	2266.069	1013.417
Row 3	5	0	24215.000	1822.671	815.123
Row 4	5	0	23853.200	4213.589	1884.374
Row 5	5	0	21978.200	3389.609	1515.879
Row 6	5	0	25628.400	4316.323	1930.318

Source of Variation	DF	SS	MS	F	P
Between Groups	5	71652084.567	14330416.913	1.267	0.310
Residual	24	271414048.400	11308918.683		
Total	29	343066132.967			

The differences in the mean values among the treatment groups are not great enough to exclude the possibility that the difference is due to random sampling variability; there is not a statistically significant difference (P = 0.310).

Power of performed test with alpha = 0.050: 0.102

The power of the performed test (0.102) is below the desired power of 0.800.
Less than desired power indicates you are more likely to not detect a difference when one actually exists. Be cautious in over-interpreting the lack of difference found here.

One Way Analysis of Variance 500 cells Monday, August 11, 2008, 8:33:29 AM

Data source: Data 3 in Notebook 1

Group Name	N	Missing	Mean	Std Dev	SEM
Row 1	5	0	13394.400	815.016	364.486
Row 2	5	0	15535.600	1236.662	553.052
Row 3	5	0	16742.400	1205.125	538.948
Row 4	5	0	14750.400	1130.662	505.647
Row 5	5	0	14553.400	826.660	369.694
Row 6	5	0	14394.200	1177.491	526.590

Source of Variation	DF	SS	MS	F	P
Between Groups	5	32317279.067	6463455.813	5.545	0.002
Residual	24	27976626.800	1165692.783		
Total	29	60293905.867			

The differences in the mean values among the treatment groups are greater than would be expected by chance; there is a statistically significant difference (P = 0.002).

Power of performed test with alpha = 0.050: 0.934

All Pairwise Multiple Comparison Procedures (Holm-Sidak method):
Overall significance level = 0.05

Comparisons for factor:

Comparison	Diff of Means	t	Unadjusted P	Critical Level	Significant?
Row 3 vs. Row 1	3348.000	4.903	0.0000532	0.003	Yes
Row 3 vs. Row 6	2348.200	3.439	0.00214	0.004	Yes
Row 3 vs. Row 5	2189.000	3.206	0.00379	0.004	Yes
Row 2 vs. Row 1	2141.200	3.136	0.00449	0.004	No
Row 3 vs. Row 4	1992.000	2.917	0.00755	0.005	No
Row 4 vs. Row 1	1356.000	1.986	0.0586	0.005	No
Row 3 vs. Row 2	1206.800	1.767	0.0899	0.006	No
Row 5 vs. Row 1	1159.000	1.697	0.103	0.006	No
Row 2 vs. Row 6	1141.400	1.672	0.108	0.007	No

Row 6 vs. Row 1	999.800	1.464	0.156	0.009	No
Row 2 vs. Row 5	982.200	1.438	0.163	0.010	No
Row 2 vs. Row 4	785.200	1.150	0.262	0.013	No
Row 4 vs. Row 6	356.200	0.522	0.607	0.017	No
Row 4 vs. Row 5	197.000	0.288	0.775	0.025	No
Row 5 vs. Row 6	159.200	0.233	0.818	0.050	No

One Way Analysis of Variance 100 cells Monday, August 11, 2008, 8:35:14 AM

Data source: Data 3 in Notebook 1

Group Name	N	Missing	Mean	Std Dev	SEM
Row 1	5	0	7460.000	413.970	185.133
Row 2	5	0	8099.000	1025.907	458.800
Row 3	5	0	7527.400	110.972	49.628
Row 4	5	0	7537.800	381.481	170.603
Row 5	5	0	7172.600	225.546	100.867
Row 6	5	0	7426.400	456.656	204.223

Source of Variation	DF	SS	MS	F	P
Between Groups	5	2334426.400	466885.280	1.707	0.171
Residual	24	6564416.400	273517.350		
Total	29	8898842.800			

The differences in the mean values among the treatment groups are not great enough to exclude the possibility that the difference is due to random sampling variability; there is not a statistically significant difference (P = 0.171).

Power of performed test with alpha = 0.050: 0.209

The power of the performed test (0.209) is below the desired power of 0.800.
Less than desired power indicates you are more likely to not detect a difference when one actually exists. Be cautious in over-interpreting the lack of difference found here.

Standard Curve: Plated hMSCs

Well	#Cells	60min	corrected	Average	Stdev
A01	50000	1551097	1543993		
A02	50000	1576900	1569796		
A03	50000	1257113	1250009		
A04	50000	1460417	1453313		
A05	50000	1977212	1970108	1557444	262671
B01	30000	800932	793828		
B02	30000	995125	988021		
B03	30000	953864	946760		
B04	30000	734921	727817		
B05	30000	1160619	1153515	921988	167859
C01	10000	271072	263968		
C02	10000	227951	220847		
C03	10000	264324	257220		
C04	10000	320852	313748		
C05	10000	257300	250196	261196	33668
D01	5000	99112	92008		
D02	5000	101169	94065		
D03	5000	83273	76169		
D04	5000	100772	93668		
D05	5000	80675	73571	85896	10137
E01	1000	22911	15807		
E02	1000	29936	22832		
E03	1000	25993	18889		
E04	1000	21225	14121		
E05	1000	19201	12097	16749	4214
F01	500	13821	6717		
F02	500	16721	9617		
F03	500	14462	7358		
F04	500	14372	7268		
F05	500	14376	7272	7646	1131
G01	100	7775	671		
G02	100	8097	993		
G03	100	7304	200		
G04	100	7246	142		
G05	100	7267	163	434	381
H01	0	7192			
H02	0	6914			
H03	0	7105			
H04	0	7152			
H05	0	7157	7104		

Standard Curve: Microthreads (Digested/Re-plated)

Well	#Cells	60min	corrected	Average	Stdev
A01	50000	463496	457672		
A02	50000	449118	449118		
A03	50000	468653	468653		
A04	50000	553448	553448		
A05	50000	372212	372212	460221	64494
B01	30000	282406	282406		
B02	30000	315362	315362		
B03	30000	320586	320586		
B04	30000	311388	311388		
B05	30000	295395	295395	305027	15763
C01	10000	77605	77605		
C02	10000	122547	122547		
C03	10000	122942	122942		
C04	10000	62531	62531		
C05	10000	79186	79186	92962	27954
D01	5000	52654	52654		
D02	5000	32941	32941		
D03	5000	23112	23112		
D04	5000	49452	49452		
D05	5000	37682	37682	39168	12108
E01	1000	8368	8368		
E02	1000	22198	22198		
E03	1000	10944	10944		
E04	1000	11476	11476		
E05	1000	9868	9868	12571	5511
F01	500	7592	7592		
F02	500	7288	7288		
F03	500	9790	9790		
F04	500	7229	7229		
F05	500	8002	8002	7980	1057
G01	100	6048	6048		
G02	100	6019	6019		
G03	100	4848	4848		
G04	100	6215	6215		
G05	100	7477	7477	6121	933
H01	0	5381			
H02	0	5583			
H03	0	5797			
H04	0	5900			
H05	0	6459	5824		

One Way Analysis of Variance (Microthread Std. Curve) Monday, August 11, 2008, 10:29:26 AM

Data source: Data 8 in Notebook 1

Normality Test: Failed (P < 0.050)

Test execution ended by user request, ANOVA on Ranks begun

Kruskal-Wallis One Way Analysis of Variance on Ranks Monday, August 11, 2008, 10:29:26 AM

Data source: Data 8 in Notebook 1

Group	N	Missing	Median	25%	75%
50,000	5	0	463496.000	429891.500	489851.750
30,000	5	0	311388.000	292147.750	316668.000
10,000	5	0	79186.000	73836.500	122645.750
5,000	5	0	37682.000	30483.750	50252.500
1,000	5	0	10944.000	9493.000	14156.500
500	5	0	7592.000	7273.250	8449.000
100	5	0	6048.000	5726.250	6530.500

H = 33.059 with 6 degrees of freedom. (P = <0.001)

The differences in the median values among the treatment groups are greater than would be expected by chance; there is a statistically significant difference (P = <0.001)

To isolate the group or groups that differ from the others use a multiple comparison procedure.

All Pairwise Multiple Comparison Procedures (Student-Newman-Keuls Method) :

Comparison	Diff of Ranks	q	P<0.05
50,000 vs 100	148.000	6.459	Yes
50,000 vs 500	126.000	6.401	Yes
50,000 vs 1,000	101.000	6.137	Yes
50,000 vs 5,000	75.000	5.669	Yes
50,000 vs 10,000	50.000	5.000	Yes
50,000 vs 30,000	25.000	3.693	Yes
30,000 vs 100	123.000	6.248	Yes
30,000 vs 500	101.000	6.137	Yes
30,000 vs 1,000	76.000	5.745	Yes
30,000 vs 5,000	50.000	5.000	Yes
30,000 vs 10,000	25.000	3.693	Yes
10,000 vs 100	98.000	5.955	Yes
10,000 vs 500	76.000	5.745	Yes
10,000 vs 1,000	51.000	5.100	Yes
10,000 vs 5,000	25.000	3.693	Yes
5,000 vs 100	73.000	5.518	Yes
5,000 vs 500	51.000	5.100	Yes
5,000 vs 1,000	26.000	3.840	Yes
1,000 vs 100	47.000	4.700	Yes
1,000 vs 500	25.000	3.693	Yes
500 vs 100	22.000	3.250	Yes

Note: The multiple comparisons on ranks do not include an adjustment for ties.

One Way Analysis of Variance (plated std curve) Monday, August 11, 2008, 11:34:07 AM

Data source: Data 3 in Notebook 1

Normality Test: Failed (P < 0.050)

Test execution ended by user request, ANOVA on Ranks begun

Kruskal-Wallis One Way Analysis of Variance on Ranks Monday, August 11, 2008, 11:34:07 AM

Data source: Data 3 in Notebook 1

Group	N	Missing	Median	25%	75%
50,000	5	0	1551097.000	1409591.000	1676978.000
30,000	5	0	953864.000	784429.250	1036498.500
10,000	5	0	264324.000	249962.750	283517.000
5,000	5	0	99112.000	82623.500	100871.250
1,000	5	0	22911.000	20719.000	26978.750
500	5	0	14376.000	14234.250	15026.750
100	5	0	7304.000	7261.750	7855.500

H = 33.333 with 6 degrees of freedom. (P = <0.001)

The differences in the median values among the treatment groups are greater than would be expected by chance; there is a statistically significant difference (P = <0.001)

To isolate the group or groups that differ from the others use a multiple comparison procedure.

All Pairwise Multiple Comparison Procedures (Student-Newman-Keuls Method) :

Comparison	Diff of Ranks	q	P<0.05
50,000 vs 100	150.000	6.547	Yes
50,000 vs 500	125.000	6.350	Yes
50,000 vs 1,000	100.000	6.076	Yes
50,000 vs 5,000	75.000	5.669	Yes
50,000 vs 10,000	50.000	5.000	Yes
50,000 vs 30,000	25.000	3.693	Yes
30,000 vs 100	125.000	6.350	Yes
30,000 vs 500	100.000	6.076	Yes
30,000 vs 1,000	75.000	5.669	Yes
30,000 vs 5,000	50.000	5.000	Yes
30,000 vs 10,000	25.000	3.693	Yes
10,000 vs 100	100.000	6.076	Yes
10,000 vs 500	75.000	5.669	Yes
10,000 vs 1,000	50.000	5.000	Yes
10,000 vs 5,000	25.000	3.693	Yes
5,000 vs 100	75.000	5.669	Yes
5,000 vs 500	50.000	5.000	Yes
5,000 vs 1,000	25.000	3.693	Yes
1,000 vs 100	50.000	5.000	Yes
1,000 vs 500	25.000	3.693	Yes
500 vs 100	25.000	3.693	Yes

Appendix E: CyQuant Verification Data

With the rinse step in the CyQuant protocol, unseeded threads showed no statistical difference from blank wells with just CyQuant dye.

	Thread control	Blank Well
EXP3	4464	4481
	4306	4410
	4106	4372
	4102	4442
	4171	4328
	4149	4405
	4677	4655
	4470	4498
	4574	4320
	4309	4452
	4201	4314
	4315	4176
	5562	5255
	4824	4791
	4844	4705
	4667	4638
	4840	4849
	4846	4602
EXP4	5057	4996
	4689	4897
	4519	4818
	4425	4617
	4423	4636
		4598
	5548	5173
	5266	4148
	5284	4860
	5422	4991
	4381	4983
	4972	4570
	4913	5323
	5008	4725
	4584	4503
	5385	4856
	5244	4958
	4456	4560

	Thread Control	Blank Well
Average	4714	4664
Stdev	430.6894	290.0652

t-test Monday, August 11, 2008, 8:37:35 AM

Data source: Data 4 in Notebook 1

Normality Test: Passed (P = 0.150)

Equal Variance Test: Failed (P < 0.050)

Test execution ended by user request, Rank Sum Test begun

Mann-Whitney Rank Sum Test Monday, August 11, 2008, 8:37:35 AM

Data source: Data 4 in Notebook 1

Group	N	Missing	Median	25%	75%
Thread Control	36	1	4667.000	4391.500	4999.000
Blank Well	36	0	4626.500	4447.000	4858.000

T = 1272.000 n(small)= 35 n(big)= 36 (P = 0.895)

The difference in the median values between the two groups is not great enough to exclude the possibility that the difference is due to random sampling variability; there is not a statistically significant difference (P = 0.895)

Analysis of the supernatant after centrifugation (left) and the PBS from rinses (right) indicates minimal cell loss and the presence of thread debris.

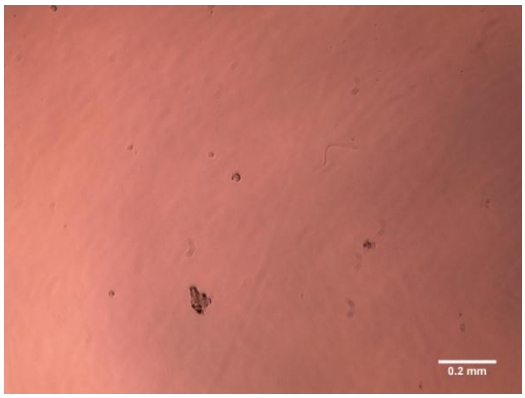

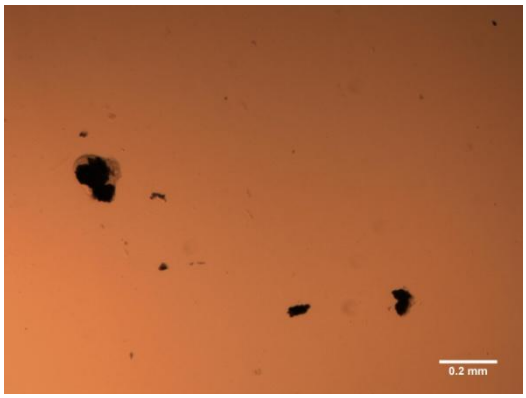

Appendix F: Microthreads CyQuant Data

This appendix contains all of the raw data from the CyQuant assay on microthreads

CyQuant EXP3 Day 1

thread cntr	plate cntr
4464	4481
4306	4410
4106	4372
4102	4442
4171	4328
4149	4405
4216	4406

1d thread	corr.	#cells	avg	stdev
13816	9600	1016.914	1555.985	648.3004
11906	7690	814.5833		
15470	11254	1192.126		
21774	17558	1859.922		
27712	23496	2488.948		
22751	18535	1963.418		

1d plate	corr.	#cells	avg	stdev
43165	38759	1258.807	962.2388	159.3185
30746	26340	855.4617		
32240	27834	903.984		
34356	29950	972.7076		
34421	30015	974.8187		
29274	24868	807.654		

1000 Cels	Thread Control	Thread 1 Day	Blank
43165	4464	13816	4481
30746	4306	11906	4410
32240	4106	15470	4372
34356	4102	21774	4442
34421	4171	27712	4328
29274	4149	22751	4405

CyQuant EXP3 Day 3

thread cntr	plate cntr
4677	4655
4470	4498
4574	4320
4309	4452
4201	4314
4315	4176
4424	4403

3 day thread	corr.	#cells	avg	stdev
15762	11338	1201.024	1861.352	790.1051
22892	18468	1956.321		
35753	31329	3318.715		
22374	17950	1901.448		
15319	10895	1154.096		
19873	15449	1636.511		

3 day plate	corr.	#cells	avg	stdev
56751	52349	1700.179	1495.442	177.3922
56051	51649	1677.444		
52497	48095	1562.017		
46852	42450	1378.678		
43368	38966	1265.525		
47164	42762	1388.811		

1000 Cells	Thread Control	Thread 3 Day	Blank
56751	4677	15762	4655
56051	4470	22892	4498

52497	4574	35753	4320	
46852	4309	22374	4452	
43368	4201	15319	4314	
47164	4315	19873	4176	

CyQuant EXP3 Day 5

thread cntr	plate cntr	5day thread	corr.	#cells	avg	stdev
5562	5255	133460	128530	13615.41	4086.829	4695.578
4824	4791	19673	14743	1561.706		
4844	4705	25132	20202	2139.989		
4667	4638	29119	24189	2562.341		
4840	4849	32502	27572	2920.71		
4846	4602	21175	16245	1720.816		
4931	4807					

5day plate	corr.	#cells	avg	stdev
73295	68488	2224.369	1946.774	251.5261
71725	66918	2173.379		
63589	58782	1909.137		
67286	62479	2029.209		
60004	55197	1792.703		
52588	47781	1551.846		

1000 Cells	Thread Control	Thread 5 Day	Blank
73295	5562	133460	5255
71725	4824	19673	4791
63589	4844	25132	4705
67286	4667	29119	4638
60004	4840	32502	4849
52588	4846	21175	4602

CyQuant EXP4 Day 1

thread cntr	plate cntr	1 day thread	corr.	#cells	avg	stdev
5057	4996	22976	18353	1944.216	1619.181	624.4305
4689	4897	12619	7996	847.0763		
4519	4818	21179	16556	1753.856		
4425	4617	29281	24658	2612.119		
4423	4636	17431	12808	1356.822		
	4598	15960	11337	1200.996		
4623	4760					

1 day plate	corr.	#cells	avg	stdev
24491	19731	640.8141	612.0223	50.29115
24370	19610	636.8843		
21681	16921	549.5507		
24607	19847	644.5816		
24919	20159	654.7147		
21559	16799	545.5884		

1000	Thread	Thread 1	Blank

	Cells	Control	Day	
	24491	5057	22976	4996
	24370	4689	12619	4897
	21681	4519	21179	4818
	24607	4425	29281	4617
	24919	4423	17431	4636
	21559		15960	4598

CyQuant EXP4 Day 3

thread cntr	plate cntr
5548	5173
5266	4148
5284	4860
5422	4991
4381	4983
4972	4570
5146	4788

3 day thread	corr.	#cells	avg	stdev
24220	19075	2020.604	1442.514	600.6925
12961	7816	827.9131		
22658	17513	1855.138		
21892	16747	1773.994		
20426	15281	1618.697		
10420	5275	558.7394		

3 day plate	corr.	#cells	avg	stdev
25196	20409	662.8288	772.3557	71.92165
28406	23619	767.0835		
31658	26871	872.7022		
27950	23163	752.2735		
30246	25459	826.8431		
27954	23167	752.4034		

	1000 Cells	Thread Control	Thread 3 Day	Blank
	25196	5548	24220	5173
	28406	5266	12961	4148
	31658	5284	22658	4860
	27950	5422	21892	4991
	30246	4381	20426	4983
	27954	4972	10420	4570

CyQuant EXP4 Day 5

thread cntr	plate cntr
4913	5323
5008	4725
4584	4503
5385	4856
5244	4958
4456	4560
4932	4821

5 day thread	corr.	#cells	avg	stdev
26739	21807	2310.099	3945.604	1603.839
45403	40471	4287.218		
42357	37425	3964.548		
35115	30183	3197.387		
33492	28560	3025.459		
69963	65031	6888.912		

5 day plate	corr.	#cells	avg	stdev
28497	23676	768.9564	1081.547	224.7985
38702	33881	1100.395		
40883	36062	1171.23		
37507	32686	1061.584		
49146	44325	1439.596		
33995	29174	947.5208		

1000 Cells	Thread Control	Thread 5 Day	Blank
28497	4913	26739	5323
38702	5008	45403	4725
40883	4584	42357	4503
37507	5385	35115	4856
49146	5244	33492	4958
33995	4456	69963	4560

Raw Data Summary: Microthreads

	1 day		3 day		5 day
EXP3	1016.9138		1201.024		13615.413
	814.58333		1956.3206		1561.7055
	1192.1257		3318.7147		2139.9894
	1859.9223		1901.4477		2562.3411
	2488.9477		1154.096		2920.7097
	1963.4181		1636.5113		1720.8157
EXP4	1944.2161		2020.6038		2310.0989
	847.07627		827.91314		4287.2175
	1753.8559		1855.1377		3964.548
	2612.1186		1773.9936		3197.387
	1356.822		1618.697		3025.459
	1200.9958		558.73941		6888.9124
Average	1587.583		1651.9333		4016.2164
Stdev	607.75406		703.99921		3346.1456

One Way Analysis of Variance Microthreads CyQuant Wednesday, August 13, 2008, 11:39:04 AM

Data source: Data 4 in Thesis statistics

Normality Test: Failed (P < 0.050)

Test execution ended by user request, ANOVA on Ranks begun

Kruskal-Wallis One Way Analysis of Variance on Ranks Wednesday, August 13, 2008, 11:39:04 AM

Data source: Data 4 in Thesis statistics

Group	N	Missing	Median	25%	75%
1 day	12	0	1555.339	1104.520	1953.817
3 day	12	0	1705.252	1177.560	1928.884
5 day	12	0	2973.084	2225.044	4125.883

H = 12.911 with 2 degrees of freedom. (P = 0.002)

The differences in the median values among the treatment groups are greater than would be expected by chance; there is a statistically significant difference (P = 0.002)

To isolate the group or groups that differ from the others use a multiple comparison procedure.

All Pairwise Multiple Comparison Procedures (Tukey Test):

Comparison	**Diff of Ranks**	**q**	**P<0.05**
5 day vs 1 day	164.000	4.494	Yes
5 day vs 3 day	157.000	4.302	Yes
3 day vs 1 day	7.000	0.192	No

Note: The multiple comparisons on ranks do not include an adjustment for ties..

Raw Data Summary: plated hMSCs

	day 1		day 3		day 5
EXP3	1258.807		1700.1786		2224.3694
	855.46173		1677.444		2173.3788
	903.98398		1562.0169		1909.1372
	972.70759		1378.6781		2029.2086
	974.81866		1265.5245		1792.7033
	807.654		1388.8113		1551.8458
EXP4	640.81412		662.82884		768.95637
	636.88427		767.08347		1100.3951
	549.55072		872.70218		1171.2298
	644.58157		752.27347		1061.5838
	654.71473		826.84313		1439.5962
	545.58839		752.40338		947.52084
EXP5	1573.3355		559.74884		1306.8854
	652.02988		635.29284		1269.1783
	1085.3849		681.76897		1368.9185
	749.78889		716.71538		1129.4251
	850.04872		611.38898		1372.1988
	644.39753		579.13825		1141.2147
	834.71906		638.021		1371.4193
	638.74635		610.64198		1129.8149
	816.79117		606.74461		1206.723
	731.73108		610.57703		1113.8681
	738.84378		559.61892		995.42059
	745.3394		522.464		962.35791
avg	**812.78012**		**872.45453**		**1355.7229**
stdev	**235.45373**		**385.82977**		**397.82862**

One Way Analysis of Variance: Plated hMSCs CyQuant Tuesday, August 12, 2008, 9:34:06 AM

Data source: Data 8 in Thesis statistics

Normality Test: Failed (P < 0.050)

Test execution ended by user request, ANOVA on Ranks begun

Kruskal-Wallis One Way Analysis of Variance on Ranks Tuesday, August 12, 2008, 9:34:06 AM

Data source: Data 8 in Thesis statistics

Group	N	Missing	Median	25%	75%
1 day	24	0	747.564	644.490	879.723
3 day	24	0	699.242	610.610	1069.113
5 day	24	0	1237.951	1107.132	1495.721

H = 25.533 with 2 degrees of freedom. (P = <0.001)

The differences in the median values among the treatment groups are greater than would be expected by chance; there is a statistically significant difference (P = <0.001)

To isolate the group or groups that differ from the others use a multiple comparison procedure.

All Pairwise Multiple Comparison Procedures (Tukey Test):

Comparison	Diff of Ranks	q	P<0.05
5 day vs 3 day	636.000	6.203	Yes
5 day vs 1 day	633.000	6.174	Yes
1 day vs 3 day	3.000	0.0293	No

Note: The multiple comparisons on ranks do not include an adjustment for ties.

Fibrin Coated Data

CyQuant EXP4 Day 1

1 day fibrin	corr.	#cells	avg	stdev	plate cntr
11030	6270	664.1596	649.0466	213.8303	4996
12588	7828	829.202			4897
14927	10167	1076.977			4818
9004	4244	449.541			4617
8773	4013	425.0706			4636
11186	6426	680.685			4598
12245	7485	792.8672			4760
12933	8173	865.7486			
10870	6110	647.2105			
8483	3723	394.3503			
8729	3969	420.4096			
9880	5120	542.3376			

1000 Cells	Fibrin 3 Day	Fibrin 3 Day	Blank
24491	11030	12245	4996
24370	12588	12933	4897
21681	14927	10870	4818
24607	9004	8483	4617
24919	8773	8729	4636
21559	11186	9880	4598

CyQuant EXP4 Day 3

3 day fibrin	corr.	#cells	avg	stdev	plate cntr
6005	1218	128.9725	157.6801	101.1262	5173
6758	1971	208.7394			4148
8271	3484	369.0148			4860
5735	948	100.3708			4991
6742	1955	207.0445			4983
5518	731	77.38347			4570
6339	1552	164.3538			4788
5680	893	94.54449			
7550	2763	292.6377			
6459	1672	177.0657			
5112	325	34.375			
5143	356	37.6589			

1000 Cells	Fibrin 3 Day	Fibrin 3 Day	Blank
25196	6005	6339	5173
28406	6758	5143	4148
31658	8271	5680	4860
27950	5735	7550	4991
30246	6742	6459	4983
27954	5518	5112	4570

CyQuant EXP4 Day 5

5 day fibrin	corr.	#cells	avg	stdev	plate cntr
23172	18351	1943.98	1235.593	759.2922	5323
21471	16650	1763.789			4725
15055	10234	1084.128			4503
29951	25130	2662.094			4856
24235	19414	2056.585			4958
16548	11727	1242.285			4560
18742	13921	1474.7			4821
8248	3427	363.0473			
9593	4772	505.5261			
7693	2872	304.2549			
9857	5036	533.4922			
13253	8432	893.238			

1000 Cells	Fibrin 5 Day	Fibrin 5 Day	Blank
28497	23172	18742	5323
38702	21471	8248	4725
40883	15055	9593	4503
37507	29951	7693	4856
49146	24235	9857	4958
33995	16548	13253	4560

CyQuant EXP 6 3 and 5 Day

3 day

plate	corr.	#cells	avg	stdev
14189	9392	305.0179	436.3051	151.231
13875	9078	294.8197		
15384	10587	343.8292		
22515	17718	575.4303		
25059	20262	658.0546		
18366	13569	440.6788		

5 day

plate	corr.	#cells	avg	stdev
6344	1547	50.22735	95.41518	25.6801
8418	3621	117.5869		
8191	3394	110.2144		
8348	3551	115.3134		
7360	2563	83.22507		
7751	2954	95.924		

3 day

fibrin	corr.	#cells	avg	stdev
18984	14187	1502.807	1841.278	886.0348
29713	24916	2639.354		
16502	11705	1239.883		
20549	15752	1668.591		
13465	8668	918.1674		
11146	6349	672.5106		
22135	17338	1836.6		
17576	12779	1353.655		
28150	23353	2473.782		
33330	28533	3022.511		
38172	33375	3535.434		
16428	11631	1232.044		

5 day

fibrin	corr.	#cells	avg	stdev
16329	11532	1221.557	1979.908	1038.095
34453	29656	3141.472		
37599	32802	3474.735		
30348	25551	2706.621		
35321	30524	3233.422		
23742	18945	2006.833		
17806	13009	1378.019		
17648	12851	1361.282		
7657	2860	302.9131		
17572	12775	1353.231		
30060	25263	2676.112		
13319	8522	902.7013		

plate cntr	Fibrin 3 Day	Fibrin 3 Day	1000 3 Day	Fibrin 5 Day	Fibrin 5 Day	1000 5 Day	Blank
5061	18984	22135	14189	16329	17806	6344	5061
4637	29713	17576	13875	34453	17648	8418	4637
4538	16502	28150	15384	37599	7657	8191	4538
4898	20549	33330	22515	30348	17572	8348	4898

4772	13465	38172	25059	35321	30060	7360	4772
4879	11146	16428	18366	23742	13319	7751	4879
4798							

Summary Data: Fibrin Coated Plate

	1 day	3 day	5 day
EXP3	664.1596	128.97246	1943.9795
	829.20198	208.73941	1763.7888
	1076.9774	369.01483	1084.1278
	449.54096	100.37076	2662.0939
	425.07062	207.04449	2056.5855
	680.68503	77.383475	1242.2846
	792.86723	164.35381	1474.6999
	865.74859	94.544492	363.04732
	647.21045	292.63771	505.52613
	394.35028	177.06568	304.25494
	420.4096	34.375	533.49223
	542.33757	37.658898	893.23799
EXP6		1502.8072	1221.5572
		2639.3538	3141.4725
		1239.8835	3474.7352
		1668.5911	2706.6208
		918.16737	3233.4216
		672.51059	2006.8326
		1836.5996	1378.0191
		1353.6547	1361.2818
		2473.7818	302.91314
		3022.5106	1353.2309
		3535.4343	2676.1123
		1232.0445	902.70127
Average	**649.04661**	**999.47917**	**1607.7507**
Stdev	**213.83028**	**1058.2008**	**967.28774**

One Way Analysis of Variance: Fibrin coated plate CyQuant Tuesday, August 12, 2008, 9:28:54 AM

Data source: Data 9 in Thesis statistics

Normality Test: Passed (P = 0.175)

Equal Variance Test: Failed (P < 0.050)

Test execution ended by user request, ANOVA on Ranks begun

Kruskal-Wallis One Way Analysis of Variance on Ranks Tuesday, August 12, 2008, 9:28:54 AM

Data source: Data 9 in Thesis statistics

Group	N	Missing	Median	25%	75%
1 day	12	0	655.685	437.306	811.035
3 day	24	0	520.763	146.663	1585.699
5 day	24	0	1369.650	897.970	2359.340

H = 10.121 with 2 degrees of freedom. (P = 0.006)

The differences in the median values among the treatment groups are greater than would be expected by chance; there is a statistically significant difference (P = 0.006)

To isolate the group or groups that differ from the others use a multiple comparison procedure.

All Pairwise Multiple Comparison Procedures (Dunn's Method) :

Comparison	Diff of Ranks	Q	P<0.05
5 day vs 1 day	15.750	2.551	Yes
5 day vs 3 day	14.000	2.777	Yes
3 day vs 1 day	1.750	0.283	No

Note: The multiple comparisons on ranks do not include an adjustment for ties.

Appendix G: Ki-67 Expression

Raw Data from Ki-67 expression counts:

Bundles										
Day 1				**Day 3**				**Day 5**		
Total Cells	Ki-67 positive	Expression Rate		Total Cells	Ki-67 positive	Expression Rate		Total Cells	Ki-67 positive	Expression Rate
66	1	1.515151515		25	8	32		82	4	4.87804878
35	1	2.857142857		142	31	21.83098592		58	4	6.896551724
29	1	3.448275862		112	28	25		84	15	17.85714286
28	0	0		75	10	13.33333333		81	12	14.81481481
6	1	16.66666667		100	23	23		62	4	6.451612903
10	1	10		118	30	25.42372881		60	3	5
91	3	3.296703297		191	34	17.80104712		49	0	0
80	5	6.25		38	10	26.31578947		64	3	4.6875
78	0	0		42	5	11.9047619		53	4	7.547169811
74	2	2.702702703		75	6	8		49	0	0
	average	4.892660022			average	22.6270136			average	6.813284089
	stdev	5.415429201			stdev	5.940549621			stdev	5.68684067

Standard Chamber Slides									
Day 1			**Day 3**			**Day 5**			
Total Cells	Ki-67 positive	Expression Rate	Total Cells	Ki-67 positive	Expression Rate	Total Cells	Ki-67 positive	Expression Rate
18	4	22.22222222	46	7	15.2173913	46	8	17.39130435
19	2	10.52631579	44	19	43.18181818	61	11	18.03278689
16	4	25	44	16	36.36363636	53	14	26.41509434
37	7	18.91891892	40	9	22.5	50	10	20
22	0	0	25	6	24	70	20	28.57142857
21	0	0	14	3	21.42857143	53	17	32.0754717
25	0	0	21	8	38.0952381	12	7	58.33333333
27	0	0	24	1	4.166666667	12	4	33.33333333
10	2	20	23	3	13.04347826	15	3	20
17	1	5.882352941	12	4	33.33333333	14	5	35.71428571
	average	10.25498099		average	26.23474915		average	28.98670382
	stdev	10.38434561		stdev	12.66841689		stdev	12.28218042

Fibrin Coated Chamber Slides										
Day 1				**Day 3**				**Day 5**		
Total Cells	Ki-67 positive	Expression Rate		Total Cells	Ki-67 positive	Expression Rate		Total Cells	Ki-67 positive	Expression Rate
4	1	25		26	7	26.92307692		21	4	19.04761905
12	1	8.333333333		21	6	28.57142857		19	2	10.52631579
16	5	31.25		24	7	29.16666667		28	8	28.57142857
9	2	22.22222222		16	4	25		27	5	18.51851852
8	4	50		22	1	4.545454545		24	5	20.83333333
6	0	0		21	2	9.523809524		27	6	22.22222222
10	1	10		14	7	50		28	3	10.71428571
16	0	0		12	6	50		22	3	13.63636364
25	1	4		8	4	50		17	5	29.41176471
2	1	50		17	10	58.82352941		26	9	34.61538462
	average	20.08055556			average	33.25539656			average	20.80972362
	stdev	18.99867537			stdev	18.34614933			stdev	8.126152771

One Way Analysis of Variance Bundles Ki-67 Wednesday, August 13, 2008, 5:07:41 PM

Data source: Data 13 in Thesis statistics

Normality Test: Passed (P = 0.417)

Equal Variance Test: Passed (P = 0.382)

Group Name	**N**	**Missing**	**Mean**	**Std Dev**	**SEM**
1 day	10	0	4.674	5.152	1.629
3 day	10	0	20.461	7.508	2.374
5 day	10	0	6.813	5.687	1.798

Source of Variation	**DF**	**SS**	**MS**	**F**	**P**
Between Groups	2	1466.920	733.460	19.091	<0.001
Residual	27	1037.339	38.420		
Total	29	2504.259			

The differences in the mean values among the treatment groups are greater than would be expected by chance; there is a statistically significant difference (P = <0.001).

Power of performed test with alpha = 0.050: 1.000

All Pairwise Multiple Comparison Procedures (Holm-Sidak method):
Overall significance level = 0.05

Comparisons for factor:

Comparison	**Diff of Means**	**t**	**Unadjusted P**	**Critical Level**	**Significant?**
3 day vs. 1 day	15.787	5.695	0.00000474	0.017	Yes
3 day vs. 5 day	13.648	4.923	0.0000374	0.025	Yes
5 day vs. 1 day	2.140	0.772	0.447	0.050	No

One Way Analysis of Variance Std Chamber Slide Ki-67 Wednesday, August 13, 2008, 5:12:56 PM

Data source: Data 12 in Thesis statistics

Normality Test: Passed (P = 0.108)

Equal Variance Test: Passed (P = 0.920)

Group Name	N	Missing	Mean	Std Dev	SEM
1 day	10	0	10.255	10.384	3.284
3 day	10	0	25.133	12.442	3.934
5 day	10	0	28.987	12.282	3.884

Source of Variation	DF	SS	MS	F	P
Between Groups	2	1956.947	978.474	7.099	0.003
Residual	27	3721.334	137.827		
Total	29	5678.281			

The differences in the mean values among the treatment groups are greater than would be expected by chance; there is a statistically significant difference (P = 0.003).

Power of performed test with alpha = 0.050: 0.859

All Pairwise Multiple Comparison Procedures (Holm-Sidak method):
Overall significance level = 0.05

Comparisons for factor:

Comparison	Diff of Means	t	Unadjusted P	Critical Level	Significant?
5 day vs. 1 day	18.732	3.568	0.00137	0.017	Yes
3 day vs. 1 day	14.878	2.834	0.00860	0.025	Yes
5 day vs. 3 day	3.854	0.734	0.469	0.050	No

One Way Analysis of Variance Fibrin Coated Ch Slide Wednesday, August 13, 2008, 5:19:24 PM

Data source: Data 11 in Thesis statistics

Normality Test: Passed (P = 0.803)

Equal Variance Test: Passed (P = 0.070)

Group Name	N	Missing	Mean	Std Dev	SEM
1 day	10	0	20.081	18.999	6.008
3 day	10	0	33.255	18.346	5.802
5 day	10	0	20.810	8.126	2.570

Source of Variation	DF	SS	MS	F	P
Between Groups	2	1096.676	548.338	2.154	0.135
Residual	27	6872.087	254.522		
Total	29	7968.763			

The differences in the mean values among the treatment groups are not great enough to exclude the possibility that the difference is due to random sampling variability; there is not a statistically significant difference (P = 0.135).

Power of performed test with alpha = 0.050: 0.223

The power of the performed test (0.223) is below the desired power of 0.800.
Less than desired power indicates you are more likely to not detect a difference when one actually exists. Be cautious in over-interpreting the lack of difference found here.

Comparison of Ki-67 expression on different substrates by day:

One Way Analysis of Variance Wednesday, August 13, 2008, 5:47:16 PM

Data source: Data 14 in Thesis statistics

Normality Test: Passed (P = 0.510)

Equal Variance Test: Failed (P < 0.050)

Test execution ended by user request, ANOVA on Ranks begun

Kruskal-Wallis One Way Analysis of Variance on Ranks Wednesday, August 13, 2008, 5:47:16 PM

Data source: Data 14 in Thesis statistics

Group	N	Missing	Median	25%	75%
1 day M	10	0	3.077	1.515	6.250
1 day Uncoat	10	0	8.204	0.000	20.000
1 day Fibrin coat	10	0	16.111	4.000	31.250

H = 3.973 with 2 degrees of freedom. (P = 0.137)

The differences in the median values among the treatment groups are not great enough to exclude the possibility that the difference is due to random sampling variability; there is not a statistically significant difference (P = 0.137)

One Way Analysis of Variance Wednesday, August 13, 2008, 5:47:41 PM

Data source: Data 14 in Thesis statistics

Normality Test: Passed (P = 0.817)

Equal Variance Test: Passed (P = 0.089)

Group Name	N	Missing	Mean	Std Dev	SEM
3 day microthread	10	0	20.461	7.508	2.374
3 day uncoat	10	0	25.133	12.442	3.934
3 day fibrin coat	10	0	33.255	18.346	5.802

Source of Variation	DF	SS	MS	F	P
Between Groups	2	838.329	419.164	2.296	0.120
Residual	27	4929.731	182.583		
Total	29	5768.060			

The differences in the mean values among the treatment groups are not great enough to exclude the possibility that the difference is due to random sampling variability; there is not a statistically significant difference (P = 0.120).

Power of performed test with alpha = 0.050: 0.247

The power of the performed test (0.247) is below the desired power of 0.800.
Less than desired power indicates you are more likely to not detect a difference when one actually exists. Be cautious in over-interpreting the lack of difference found here.

One Way Analysis of Variance Wednesday, August 13, 2008, 5:48:07 PM

Data source: Data 14 in Thesis statistics

Normality Test: Passed (P = 0.147)

Equal Variance Test: Passed (P = 0.237)

Group Name	N	Missing	Mean	Std Dev	SEM
5 day microthread	10	0	6.813	5.687	1.798
5 day uncoat	10	0	28.987	12.282	3.884
5 day fibrin coat	10	0	20.810	8.126	2.570

Source of Variation	DF	SS	MS	F	P
Between Groups	2	2514.746	1257.373	15.135	<0.001
Residual	27	2243.038	83.075		
Total	29	4757.784			

The differences in the mean values among the treatment groups are greater than would be expected by chance; there is a statistically significant difference (P = <0.001).

Power of performed test with alpha = 0.050: 0.998

All Pairwise Multiple Comparison Procedures (Holm-Sidak method):
Overall significance level = 0.05

Comparisons for factor:

Comparison	Diff of Means	t	Unadjusted P	Critical Level	Significant?
5 day uncoat vs. 5 day microt	22.173	5.440	0.00000937	0.017	Yes
5 day fibrin vs. 5 day microt	13.996	3.434	0.00194	0.025	Yes
5 day uncoat vs. 5 day fibrin	8.177	2.006	0.0550	0.050	No